DEVELOPMENT OF DISTRIBUTION-FREE DOUBLE EXPONENTIALLY AND HOMOGENEOUSLY WEIGHTED MOVING AVERAGE LEPAGE SCHEMES

CHAN KOK MING

MASTER OF SCIENCE

FACULTY OF SCIENCE
UNIVERSITI TUNKU ABDUL RAHMAN

DECEMBER 2021

DEVELOPMENT OF DISTRIBUTION-FREE DOUBLE EXPONENTIALLY AND HOMOGENEOUSLY WEIGHTED MOVING AVERAGE LEPAGE SCHEMES

By

CHAN KOK MING

A dissertation submitted to the Department of Physical and Mathematical Science,
Faculty of Science,
Universiti Tunku Abdul Rahman,
in partial fulfillment of the requirements for the degree of
Master of Science
December 2021

ABSTRACT

DEVELOPMENT OF DISTRIBUTION-FREE DOUBLE EXPONENTIALLY AND HOMOGENEOUSLY WEIGHTED MOVING AVERAGE LEPAGE SCHEMES

CHAN KOK MING

A control scheme is well-known as the most powerful and significant device in statistical process monitoring (SPM). A control scheme no longer only serves the manufacturing sector; instead, it is now playing a remarkable role in the new stage of smart monitoring. Following the current trend, the development of the distribution-free or nonparametric SPM (NSPM)-type scheme is at an active pace. This is because an NSPM-type scheme has a robust in-control (IC) run-length (RL) distribution, regardless of the underlying process distribution. Furthermore, most of the recent research no longer focuses on a single parameter monitoring, but joint monitoring of location-scale parameters attracts researchers' attention. One may notice that most of the available memory-type schemes available in the literature focus on the well-known cumulative sum (CUSUM)- and exponentially weighted moving average (EWMA)-type scheme. Nevertheless, researchers have found that the extension of the EWMA-type scheme, i.e., the double EWMA (DEWMA)-type scheme and the newly proposed homogeneously weighted moving average (HWMA)-type scheme have a better performance in detecting small to moderate shifts in the process compared to the CUSUM- and EWMA-type scheme. In order to capitalise on the strength of the DEWMA- and HWMA-type schemes and the beauty of joint monitoring NSPM-type scheme, two novel NSPM-type joint monitoring schemes based on the popular Lepage statistic are presented in this dissertation. Precisely, they are the DEWMA-Lepage (DL) and HWMA-Lepage (HL) schemes. The proposed schemes are studied and compared with the existing memoryless Shewhart Lepage (SL) and memory-type EWMA-Lepage (EL) schemes through simulation and a real data study regarding e-commerce activity. An upper control limit (UCL) is employed in all the monitoring schemes, such that the SL scheme only has a steady-state UCL, while the EL, DL, and HL schemes have both time-varying and steady-state UCLs. The results show that the HL scheme with the steady-state UCL is not recommended in practice due to its high early false alarm rate (FAR). Generally, from both the simulation and real data studies, the performance of the DL scheme with the time-varying UCL is outstanding, especially in detecting a small to moderate disturbance. Therefore, it is believed that the proposed DL scheme with the time-varying UCL can benefit various industries in this smart monitoring era.

ACKNOWLEDGEMENTS

First and foremost, I would like to grab this opportunity to express my most profound thankfulness to my supervisor, Dr. Lee How Chinh and co-supervisors, Dr. Ng Peh Sang and Dr. Chong Zhi Lin, for their invaluable help and guidance. Under their supervision, I am able to complete my Master’s study successfully and grab a lot of valuable experience and knowledge from them.

Besides, I would like to acknowledge Universiti Tunku Abdul Rahman for awarding me the Research Scholarship Scheme under Fundamental Research Grant Schemes (FRGS), no. FRGS/1/2019/STG06/UTAR/02/2, in conducting my research. I would also like to thank Professor Dr. Amitava Mukherjee from Xavier School of Management, XLRI, India, for his ideas and suggestions to improve the contents of my journal article published in Computers & Industrial Engineering.

Finally, I would like to extend my thanks and gratitude to all my beloved family members for their constant love and moral support. Their utmost wisdom and unconditional faith in me indeed served as a driving force to keep me going in this long and bumpy road journey. Further, I would also like to extend my gratitude to all my friends who have rendered me their assistance, friendship, and moral support — much appreciated to all of you!

APPROVAL SHEET

This dissertation/thesis entitled "**DEVELOPMENT OF DISTRIBUTION-FREE DOUBLE EXPONENTIALLY AND HOMOGENEOUSLY WEIGHTED MOVING AVERAGE LEPAGE SCHEMES**" was prepared by CHAN KOK MING and submitted as partial fulfillment of the requirements for the degree of Master of Science at Universiti Tunku Abdul Rahman.

Approved by:

____
(DR. LEE HOW CHINH)　　　　Date: 23/12/2021
Supervisor
Department of Physical and Mathematical Science
Faculty of Science
Universiti Tunku Abdul Rahman

____
(DR. NG PEH SANG)　　　　Date: 24/12/2021
Co-Supervisor
Department of Physical and Mathematical Science
Faculty of Science
Universiti Tunku Abdul Rahman

____
(DR. CHONG ZHI LIN)　　　　Date: 24/12/2021
Co-Supervisor
Department of Mathematical and Actuarial Sciences
Lee Kong Chian Faculty of Engineering and Science
Universiti Tunku Abdul Rahman

FACULTY OF SCIENCE

UNIVERSITI TUNKU ABDUL RAHMAN

Date: 23 December 2021

SUBMISSION OF DISSERTATION

It is hereby certified that **Chan Kok Ming** (ID No: **20ADM00688**) has completed this dissertation entitled "DEVELOPMENT OF DISTRIBUTION-FREE DOUBLE EXPONENTIALLY AND HOMOGENEOUSLY WEIGHTED MOVING AVERAGE LEPAGE SCHEMES" under the supervision of Dr. Lee How Chinh (Supervisor) and Dr. Ng Peh Sang (Co-Supervisor) from the Department of Physical and Mathematical Science, Faculty of Science, Universiti Tunku Abdul Rahman, and Dr. Chong Zhi Lin (Co-Supervisor) from the Department of Mathematical and Actuarial Sciences, Lee Kong Chian Faculty of Engineering and Science, Universiti Tunku Abdul Rahman.

I understand that University will upload softcopy of my dissertation in pdf format into UTAR Institutional Repository, which may be made accessible to UTAR community and public.

Yours truly,

____

(CHAN KOK MING)

DECLARATION

I CHAN KOK MING hereby declare that the dissertation is based on my original work except for quotations and citations which have been duly acknowledged. I also declare that it has not been previously or concurrently submitted for any other degree at UTAR or other institutions.

(CHAN KOK MING)

Date: 23 December 2021

TABLE OF CONTENTS

LIST OF TABLES

LIST OF FIGURES

LIST OF ABBREVIATIONS / NOTATIONS

The notations and abbreviations used in this dissertation are listed as follows:

AEWMA	Adaptive exponentially weighted moving average
AB	Ansari-Bradley
AB_i	Ansari-Bradley statistic corresponding to the i^{th} test sample
ARL	Average run length
ARL_0	Average run length (in-control)
ARL_1	Average run length (out-of-control)
CvM	Cramér-von Mises
CDF	Cumulative distribution function
F_X	CDF of Phase-I sample X
F_Y	CDF of Phase-II sample Y
υ_1	Conditional mean of the i^{th} Lepage statistic, $E\left(L_i\middle\|\overrightarrow{X_m}, IC\right)$
ξ_2	Conditional mean of υ_2, $E(\upsilon_2\|IC)$
υ_2	Conditional variance of the i^{th} Lepage statistic, $Var\left(L_i\middle\|\overrightarrow{X_m}, IC\right)$
ξ_1	Conditional variance of υ_1, $Var(\upsilon_1\|IC)$
CUSUM	Cumulative sum
CC	CUSUM-Cucconi
CL	CUSUM-Lepage
DEWMA	Double exponentially weighted moving average
DL	DEWMA-Lepage
DL_i	DEWMA-Lepage scheme (the i^{th} plotting statistic)
$EARL$	Expected average run-length
$EWRL$	Expected weighted run-length
EWMA	Exponentially weighted moving average
EC	EWMA-Cucconi
EL	EWMA-Lepage
EL_i	EWMA-Lepage scheme (the i^{th} plotting statistic)
FAR	False alarm rate
FSL	Fuzzy Shewhart-Lepage

GOF	Goodness-of-fit
HWMA	Homogeneously weighted moving average
HL	HWMA-Lepage
HL_i	HWMA-Lepage scheme (the i^{th} plotting statistic)
IC	In-control
IR4.0	Industrial Revolution 4.0
KS	Kolmogorov-Smirnov
L_i	Lepage statistic corresponding to the i^{th} test sample
LCL	Lower control limit
LWL	Lower warning limit
MW	Mann-Whitney
μ_{AB}	Mean of Ansari-Bradley statistic in an IC state
μ_{DL_i}	Mean of DL scheme with time-varying UCL at i^{th} test sample
μ_{EL_i}	Mean of EL scheme with time-varying UCL at i^{th} test sample
μ_{HL_i}	Mean of HL scheme with time-varying UCL at i^{th} test sample
μ_{WRS}	Mean of Wilcoxon rank-sum statistic in an IC state
MRL	Median run-length
NSPM	Nonparametric statistical process monitoring
OC-JM	One-chart joint monitoring
OOC	Out-of-control
PDF	Probability density function
p_A^*	p-value of the AB test for Phase-I and cumulative Phase-II samples
p_A	p-value of the AB test for Phase-I and individual Phase-II samples
p_W^*	p-value of the WRS test for Phase-I and cumulative Phase-II samples
p_W	p-value of the WRS test for Phase-I and individual Phase-II samples
X	Phase-I in-control reference sample
Y	Phase-II test sample
$\overrightarrow{X_m}$	Random sample of an in-control process

$\overrightarrow{Y_{ni}}$	Random sample of the i^{th} test sample
R	Range of sample
RS/P	Recursive segmentation and permutation
RL	Run-length
$\mathbb{Z}^+$	Set of all positive integers
SC	Shewhart-Cucconi
SL	Shewhart-Lepage
N	Size of combined $\overrightarrow{X_m}$ and $\overrightarrow{Y_{ni}}$ samples
m	Size of Phase-I sample
n	Size of Phase-II sample
λ	Smoothing parameter of the EL, DL, and HL schemes
S	Standard deviation of sample
σ_{AB}	Standard deviation of Ansari-Bradley statistic in an IC state
σ_{DL_i}	Standard deviation of DL scheme with time-varying UCL at i^{th} test sample
σ_{EL_i}	Standard deviation of EL scheme with time-varying UCL at i^{th} test sample
σ_{HL_i}	Standard deviation of HL scheme with time-varying UCL at i^{th} test sample
$SDRL$	Standard deviation of run-length
$SDRL_0$	Standard deviation of run-length (in-control)
$SDRL_1$	Standard deviation of run-length (out-of-control)
σ_{WRS}	Standard deviation of Wilcoxon rank-sum statistic in an IC state
SPM	Statistical process monitoring
SS UCL	Steady-state upper control limit
Ψ_{DL}	Steady-state upper control limit of the DL scheme
Ψ_{EL}	Steady-state upper control limit of the EL scheme
Ψ_{HL}	Steady-state upper control limit of the HL scheme
Ψ_{SL}	Steady-state upper control limit of the SL scheme
t	Student's t distribution
TV UCL	Time-varying upper control limit
$\Psi_{DL}(i)$	Time-varying upper control limit of the DL scheme

$\Psi_{EL}(i)$	Time-varying upper control limit of the EL scheme
$\Psi_{HL}(i)$	Time-varying upper control limit of the HL scheme
TEWMA	Triple exponentially weighted moving average
TC-JM	Two-charts joint monitoring
θ	Unknown location parameter
θ_{max}	Unknown location parameter (the maximum that is considered)
θ_{min}	Unknown location parameter (the minimum that is considered)
δ	Unknown scale parameter
δ_{max}	Unknown scale parameter (the maximum that is considered)
δ_{min}	Unknown scale parameter (the minimum that is considered)
UCL	Upper control limit
UWL	Upper warning limit
VSS	Variable sample size
VSI	Variable sampling interval
WRS	Wilcoxon rank-sum
WRS_i	Wilcoxon rank-sum statistic corresponding to the i^{th} test sample
WSR	Wilcoxon signed-rank
WW II	World War II
$\bar{X}$	X-bar, which is the sample mean
$\bar{X}$ & R	X-bar and range
$\bar{X}$ & S	X-bar and standard deviation
ZIP	Zero-inflated Poisson

CHAPTER 1

INTRODUCTION

1.1 Statistical Process Monitoring (SPM)

In this 21^{st} century, customers' satisfaction is of utmost importance to every seller because customers can now easily leave their feedback and review at their fingertips, which will somewhat affect a seller's business. Hence, improving the quality and productivity of a product as well as the quality of service of a seller are crucial that lead to a successful and competitive business. Garvin (1987) proposed eight components or dimensions that can evaluate a product's quality, namely performance, reliability, durability, serviceability, aesthetics, features, perceived quality, and conformance to standards. There are five dimensions to assess service quality on the flip side, i.e., tangibles, reliability, responsiveness, assurance, and empathy (Parasuraman et al., 1985). Generally, there are many definitions of quality from different quality gurus, but one should know that customers are the ones who define quality because "customer is always right".

Consequently, continuous quality improvement or more famously known as Kaizen, is crucial to ensure that a business is thriving and sustainable. To this end, Statistical Process Control (called Statistical Process Monitoring, termed as SPM hereafter) is a collection of powerful analytical tools that can be used to achieve this objective. SPM ensures the performance of a production process can be improved, and higher quality control is sustained by reducing the process variability (Smith, 1998). The statistical strategies in SPM involve real-time analysis by optimising the amount of information required that is used in decision-making for process improvement (Madanhire and Mbohwa, 2016).

The applications of SPM are greatly expanded during and after World War II (WW II). During WW II, quality plays a crucial role in war and safety because it is intolerable with any military equipment that is unsafe for operation. For instance, the War Department of the United States published some guidelines to interpret the process data through a control chart (called control scheme or scheme hereafter) in 1940. Further, from 1940 to 1943, Bell Laboratories consulted the forces to use sampling inspection to ensure the safety of military equipment (Montgomery, 2019).

On the other hand, during the post-WW II era, United States assigned a few quality gurus to Japan to help in rebuilding the country after the war. For instance, W. Edwards Deming was invited to Japan to run some seminars for the management teams of Japanese industries so that they know the importance of quality in helping their business. One of the most significant contributions from Deming is his knowledge and idea influenced a lot of Japan’s homegrown quality experts; one of them is Genichi Taguchi. Other than Deming, Joseph M. Juran became the speaker to the leaders of Japanese industries when Japan started its industrial transformation (Magnier, 1999; Montgomery, 2019).

From the history of the development of SPM, it is undeniable that in the early stage, SPM was employed primarily to monitor the processes in the manufacturing sector. However, in recent years, the role played by SPM is far beyond the manufacturing industries with the emergence of Industrial Revolution 4.0 (IR4.0). As such, SPM is now playing an essential role in multiple sectors. For example, Bersimis et al. (2017) employed SPM in environmental assessment. Besides, Mukherjee and Marozzi (2017a), Mukherjee and Sen (2018), and Song et al. (2020b) capitalised on SPM to monitor the service quality. Further, Chong et al. (2020) and Sanusi et al. (2020) showed that SPM could also be used in monitoring water quality. In addition, Scagliarini et al. (2021) discussed the application of SPM in healthcare monitoring.

A quality practitioner can control, monitor, and improve processes by analysing the process through some simple yet elegant graphical tools. There are seven paramount quality graphical tools in SPM, known as the "Magnificent Seven", which includes check sheet, control scheme, scatter diagram, Pareto chart, cause-and-effect diagram (or Ishikawa diagram), histogram, and defect concentration diagram. (Montgomery, 2019). A quality practitioner can obtain immediate or online information about the production process with the help of these seven simple tools (Lashley, 1995).

1.2 Control Scheme

In general, a control scheme is a time-sequence plot of the statistics used to explain the quality characteristic(s) of a product or service with "decision lines" added, such as the lower and upper warning limits, abbreviated as LWL and UWL, respectively, lower and upper control limits, denoted as LCL and UCL, respectively. With the emergence of advanced and modern computer technology in this era of science and technology, data collection and analysis can be performed in real-time. This strength leads to the continuous development of control schemes, and control schemes are now used utterly in management control.

A control scheme is an excellent and irreplaceable SPM tool among the "Magnificent Seven", keeping a process predictable. This is because a control scheme offers a straightforward graphical display to examine the stability of a process, i.e., whether an underlying process is in-control (IC) or out-of-control (OOC). For instance, a process is deemed to be statistically IC if the plotting statistics are all within the LCL and UCL, where the process variability is due to common or natural causes. On the flip side, a process is OOC if there is any plotting statistic beyond the LCL or UCL, such that the observed variability is relatively larger than expected, and it is due to the occurrence of assignable or special causes.

Shewhart (1926) mentioned that it is impracticable for a manufacturer to produce every single unit of a product identically due to non-assignable causes of variation in the quality of the product. Thus, as a manufacturer, the aim is to produce uniform and controlled products. To achieve this objective, the manufacturer needs to identify the assignable cause by applying the control scheme and rectify it without changing the whole process. In particular, a good control scheme should have the ability to differentiate between chance causes of variation or "background noise" and abnormal variation. This can ensure that actions are only taken when the process is OOC, in order to avoid any unnecessary process adjustment when the process is IC.

There are two main types of control schemes, i.e., variable control schemes and attribute control schemes. Gitlow et al. (1995) elucidated that a variable control scheme is employed to monitor quality characteristics that are expressed as continuous data. The scheme helps to achieve a continuous reduction in process variations and a never-ending process improvement. In contrast, an attribute control scheme is used to monitor characteristics that are in the form of categorical data, i.e., the inspected items are categorised into conforming or nonconforming units. The scheme is used to achieve a zero-defect process by preventing defects.

Furthermore, control schemes also can be categorised into two big families, i.e., the memoryless- and memory-type schemes. The traditional Shewhart-type control scheme is known as the memoryless-type control scheme. This is because the scheme only considers the observation collected at the current time point, while all the historical data are ignored in detecting process variation. Hence, this type of control scheme only effectively detects a large shift in the process (Qiu, 2014; Montgomery, 2019). To overcome this weakness, memory-type control schemes are proposed. A memory-type control scheme incorporates all the observations available from the beginning until the current time points. Hence, memory-type control schemes have a better performance in detecting small to moderate disturbances in the process.

The two major memory-type control schemes practically used are the cumulative sum (CUSUM)- and exponentially weighted moving average (EWMA)-type schemes, which were proposed by Page (1954) and Roberts (1959), respectively. Although these two schemes take past observations into account, the way they account for the observations is distinct. For instance, the EWMA-type scheme assigns a specific weight to the current observation, and the weight to the previous observations geometrically decreases. In other words, the weight decreases as the observation became older. Some other famous memory-type control scheme includes the extension of the EWMA-type scheme, i.e., the double EWMA (DEWMA)-type scheme developed by Shamma and Shamma (1992), and homogenously weighted moving average (HWMA)-type scheme proposed by Abbas (2018) recently.

In the 20th century, and even for the past twenty years, the majority of the monitoring schemes developed are known as parametric SPM-type control schemes. This is because, in order to employ those schemes, certain assumptions related to the underlying process distribution need to be made, such as the normality assumption. However, those assumptions are easily infringed, which causes by the convolutions of the current era. Further, the performance of the parametric SPM-type schemes is often unreliable if the normality assumption is violated (Qiu and Li, 2011). For instance, the IC-average run-length (ARL), abbreviated as ARL_0, for a CUSUM-type scheme will be smaller than the nominal ARL_0. This is because there are many false alarms caused by skewed process distribution and a small number of degrees of freedom.

Besides, if the underlying process distribution is not known, the sufficiency of the subgroup size will significantly affect the reliability of the estimation of the process parameters. Quesenberry (1993) proposed that there should be at least 100 subgroups with a subgroup size of 5 for the traditional $\bar{X}$ scheme or the equivalent $Q(\bar{X})$ scheme with a known mean and standard deviation presented by Quesenberry (1991) to perform as well as a scheme with known parameters. Also, at least 2000 observations, which are equivalent to 400 subgroups with a size of 5, are required to estimate the parameters of the EWMA-type scheme with a smoothing constant of $\lambda = 0.1$, where this is quite impractical in the industrial sector (Jones et al., 2001).

Further, it is strenuous to identify the actual underlying parametric distribution of a process due to insufficient prior knowledge. Therefore, in recent years, the distribution-free or nonparametric SPM (NSPM)-type scheme attracts the attention of researchers. The main advantage of the NSPM-type scheme over the parametric SPM-type scheme is its robustness towards different distributions. For instance, Chapters 8 and 9 of the book by Qiu (2014) have a brief introduction to the NSPM-type scheme. On the other hand, Qiu (2018) discussed some more recent and newfangled NSPM-type schemes.

In the early stage of the development of control schemes, regardless of the parametric SPM- or NSPM-type schemes, a control scheme is employed primarily to monitor a single parameter of a process, particularly the location parameter. For instance, the $\bar{X}$ statistic is famously used to monitor the location parameter of a normally distributed process for a parametric SPM-type scheme. On the other hand, the nonparametric Wilcoxon signed-rank (WSR) statistic that is capable in monitoring the location parameter of any distribution is employed in the NSPM-type scheme. However, researchers know that all these schemes are not perfect and have the main limitation, i.e., it is insufficient to justify the stability of a process by solely monitoring the process location parameter.

To this end, two-parameter joint monitoring schemes draw attention from researchers in more recent times. For instance, $\bar{X}$ & R and $\bar{X}$ & S schemes are the two famous parametric SPM-type schemes used to monitor the location and scale parameters of a normally distributed process. On the flip side, the development of the NSPM-type joint monitoring scheme only blossoms in recent decades. Among the NSPM-type joint monitoring schemes, the Lepage- and Cucconi-type schemes are the most well-known. A Lepage-type scheme employs the statistic of Lepage (1971) and it was initiated by Mukherjee and Chakraborti (2012). On the flip side, Chowdhury et al. (2014) initiated the Cucconi-type scheme by employing the Cucconi (1968) statistic. These two statistics can jointly monitor both the location and scale parameters of any continuous process under a single statistic.

Until here, one may notice that there are different kinds of control schemes available for quality practitioners. Also, more advanced and sophisticated control schemes are proposed as time goes. However, the typical steps in constructing any control scheme, in practice, can be illustrated as follows (Xie et al., 2002):

Step I. Collect a sequence of plotting statistics representing a quality characteristic of interest.

Step II. Compute the mean and standard deviation of the plotting statistics, where the mean is set as the centre line of the scheme.

Step III. Establish the LCL and UCL. For instance, if an SPM-type scheme is considered, the LCL and UCL are 3-standard deviations from the centre line.

Step IV. Plot and connect all the plotting statistics with a straight line.

Step V. If any plotting statistic beyond the LCL or UCL, find and eliminate the assignable cause(s). Then, revise the centre line, LCL, and UCL.

Step VI. Continue plotting whenever a new plotting statistic is obtained.

In practice, there are two phases in employing a control scheme, namely Phase-I and Phase-II. The production process is properly set up during Phase-I so that it can run stably due to the fact that the process is not known much at the beginning. However, it is not always the case when primary data is obtained, and it is hard to guarantee that the dataset obtained is collected from a correctly set up process. Hence, a control scheme is used retrospectively to analyse the Phase-I dataset. Once the Phase-I dataset is found to be IC, and is suitable to be treated as a reference sample, the data points here are used to estimate the IC run-length (RL) distribution of the quality characteristics. See Chakraborti et al. (2009) and Jones-Farmer et al. (2014) for a more comprehensive description of Phase-I control schemes.

In contrast, in Phase-II or better known as the monitoring phase, the IC process will be monitored online to ensure that it can still run stably. Here, a control scheme is adopted prospectively to detect any disturbances in the process being monitored. In SPM, Phase-II monitoring is the primary goal because it is crucial that an OOC process needs to be rectified into statistically IC (Jensen et al., 2006). This is why most of the SPM control schemes available in the literature are designed for Phase-II monitoring.

1.3 Problem Statement

The world nowadays is more complicated and advanced as compared to the old-time. This undeniably increases the difficulty of fitting any data with statistical probability distributions. To this end, the reliability and suitability of the parametric SPM-type schemes significantly deteriorate due to the violation of assumption(s) (Qiu and Li, 2011). This indirectly increases the demand for the NSPM-type scheme, which acts as complementary to the weakness of the SPM-type scheme. However, one may notice that the development of the NSPM-type schemes, especially the two-parameter joint monitoring schemes, only active since twenty-tens, which causes the available literature to be very limited.

Further, one may notice that the available literature in modifying and improving memory-type schemes mainly focused on the traditional CUSUM- and EWMA-type. However, some researchers, such as Zhang and Chen (2005), Abbas (2018), among others, found that the DEWMA- and HWMA-type schemes have a better performance than the well-known CUSUM- and EWMA-type schemes, especially in detecting a small to moderate shift. Nevertheless, the literature on the development of the DEWMA- and the newly-born HWMA-type schemes, especially the NSPM-type joint monitoring of these schemes, are bounded. This indirectly indicates that there are still many research opportunities that have not been explored in modifying and improving the DEWMA- and HWMA-type schemes.

1.4 Objectives of the Research

The main objective of this dissertation is to develop two new Phase-II distribution-free memory-type control schemes that can jointly monitor both the location and scale parameters of a process based on the Lepage statistic, namely the DEWMA-Lepage (DL) and HWMA-Lepage (HL) schemes.

Then, the specific objectives are shown in the following:

1. To derive the time-varying UCL for the proposed DL and HL schemes, and provide some charting constants of the schemes in order to ease quality practitioners when implementing the schemes.
2. To compare the IC performances of the two proposed control schemes with the existing memoryless Shewhart-Lepage (SL) schemes and

memory-type EWMA-Lepage (EL), in terms of ARL_0, IC-standard deviation of RL ($SDRL$), denoted as $SDRL_0$, some IC-percentiles (5^{th}, 25^{th}, 50^{th}, 75^{th}, and 95^{th} percentiles) of the RL, and the false alarm rate (FAR).

3. To compare the OOC performance of the two proposed control schemes with the existing SL and EL schemes, in terms of OOC-ARL (ARL_1) and OOC-$SDRL$ ($SDRL_1$).
4. To evaluate the performance of the two proposed control schemes with the existing SL and EL schemes in a specific range of shift sizes by assessing their expected ARL ($EARL$) values.
5. To apply the existing SL, EL, and the two proposed schemes using e-commerce real data in detecting OOC signal(s).

1.5 Significance of the Research

The majority of the existing NSPM-type joint monitoring schemes, especially the Lepage-type schemes, are memoryless Shewhart type, which has a weaker ability to detect a small to moderate shift in a process. Although more research is done recently on the memory-type Lepage scheme, only the well-known CUSUM- and EWMA-type schemes are being considered. However, one should admit the fact that the development of memory-type control schemes is vigorous and never-ending. Prior to this dissertation, there is no other memory-type Lepage scheme, except the CUSUM- and EWMA-type, in the literature. Hence, this dissertation attempts to fill this research gap by developing two new memory-type Lepage schemes by capitalising on the beauty of DEWMA- and HWMA-type schemes. To this end, the novel DL and HL schemes are proposed.

The best selling point of the proposed schemes in this research is the ability in detecting a small to moderate OOC disturbance of a process that appears as faster than the existing memoryless SL scheme as well as the memory-type EL scheme. Hence, a hastier detection of an OOC process leads to minimising scraps and reworks, yielding high-quality products. In turn, cost and time are saved, and most importantly, consumers feel more confident with the quality of products or services purchased. In other words, the proposed schemes can help maintain and sustain the success of an organisation.

One of the main differences between memory- and memoryless-type control schemes is the types of control limit. For instance, a memoryless Shewhart-type scheme only has a steady-state control limit. On the other hand, any memory-type scheme can have either steady-state or actual time-varying control limits. To this end, in this dissertation, the time-varying UCL of the proposed DL and HL schemes are derived using a theoretical approach. Further, the estimated value of the two important components in obtaining the time-varying control limit, i.e., the conditional mean and conditional variance of the Lepage statistic, are included in this dissertation. This enables quality practitioners to develop other memory-type Lepage schemes more conveniently, which will significantly enhance the development of the NSPM-type schemes in the future.

Furthermore, a step-by-step charting procedure for the proposed schemes is also included in order to ease quality practitioners to employ these schemes. Thereafter, some charting constants to implement the schemes for some common nominal ARL_0 are also tabulated to grant quality practitioners to execute these schemes efficiently. Next, the effects of selection of different parameters, such as the size of the Phase-I sample (m), size of the Phase-II sample (n), and smoothing parameter for the memory-type EL, DL, and HL schemes (λ) are examined, in terms of their IC and OOC performances. Also, the proposed DL and HL are compared with the existing SL and EL schemes. From the Monte-Carlo simulation study, the results showed that the proposed schemes, particularly the DL scheme, outperforms and superior to both the SL and EL schemes, especially in detecting a small to moderate shift in the process. Finally, the implementation of the proposed schemes is illustrated on a real dataset; precisely, the schemes are used in monitoring the e-commerce activity, i.e., online shoppers' intentions.

1.6 Flowchart of the Research Methodology

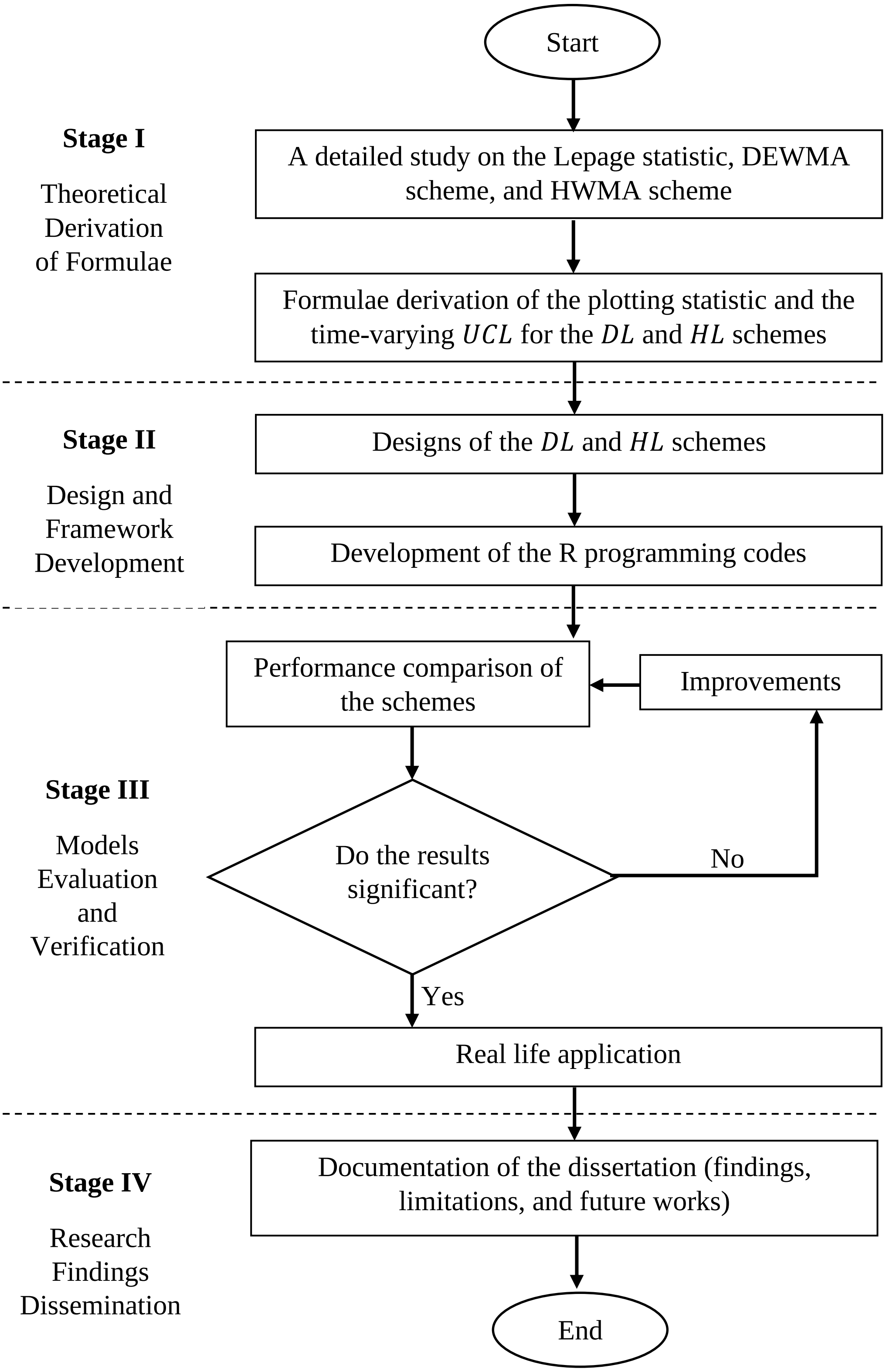

1.7 Organisation of the Dissertation

The basic idea of SPM and the control scheme are briefly presented in Chapter 1. Also, this chapter discusses the problem statement, objectives, significance, and the research methodology of this research. In Chapter 2, the literature review of the development of the parametric SPM- and NSPM-type schemes are discussed in detail. For instance, the development of the parametric SPM-type scheme from monitoring a single parameter to joint monitoring two parameters is firstly introduced in this chapter. Then, the literature review on EWMA-, DEWMA-, and HWMA-type schemes are also explored. It follows with the discussion on the development of the NSPM-type schemes, ranging from single-parameter monitoring schemes to two-parameter joint monitoring schemes. Lastly, this chapter reveals the development of the distribution-free Lepage-type scheme, which is able to joint monitor both the location and scale parameters of a process, particularly the existing SL and EL schemes.

Chapter 3 illustrates the step-by-step charting procedure to implement the proposed DL and HL schemes. In addition, the derivation of their time-varying UCLs is also scrutinised. Next, the method of determination of both the time-varying and steady-state UCLs for all the schemes, i.e., the standard searching algorithm to ensure that the nominal ARL_0 is attained, is explained. With this, the Monte-Carlo simulation is also explained. Lastly, all the RL metrics used to evaluate the performance of a scheme are also studied.

In Chapter 4, the IC performance of the proposed DL and HL schemes are studied and compared with the existing memoryless SL and memory-type EL schemes. Here, ARL_0, $SDRL_0$, and some IC-percentiles (5^{th}, 25^{th}, 50^{th}, 75^{th}, and 95^{th}) of the RL are employed as the indicators for the comparison study. Next, all the schemes are also compared by their OOC performance at micro and macro levels under three different underlying statistical distributions, i.e., Normal, Laplace, and Shifted Exponential distributions. For instance, ARL_1 and $SDRL_1$ are used for the OOC comparison study at the micro level, while the $EARL$ is the indicator for OOC comparison study when a specific range of shift sizes is considered at the macro level. Lastly, this chapter presents an illustrative example of implementing the proposed schemes using actual data obtained from the Kaggle website. Precisely, the dataset explained the online shoppers' intentions, where the schemes are employed to monitor e-commerce activity.

Last but not least, the foremost contributions of this research are summarised in Chapter 5. Further, Chapter 5 also presents the limitations of this research along with some ideas, recommendations, and directions for future research. Some important lemma for the derivation of the time-varying UCL for the DL scheme and numerous programs written in the R programming software are provided in Appendix A and Appendix B, respectively.

CHAPTER 2

LITERATURE REVIEW

2.1 Introduction

In this chapter, the relevant literature that is essential for this research is reviewed. Yang et al. (2012) mentioned that there exists a big gap between the research field and the actual industrial application of SPM. For instance, the most fundamental and traditional Shewhart $\bar{X}$ scheme is still broadly used in the manufacturing industries nowadays to monitor the process mean, even though more advanced computer systems and more efficient control schemes are available. Although the application of SPM in the industrial sector appears to be not up-to-date, at least this indicates that SPM is still widely used in the industrial field to help improve the quality of a product. However, it is insufficient only to monitor the process mean of a process to determine the process stability. Hence, the development of the parametric SPM-type joint monitoring schemes is discussed in Section 2.2.

Besides, one knows that the Shewhart $\bar{X}$ scheme is comparatively insensitive than the memory-type schemes towards small to moderate shifts in the process mean. To this end, some significant researches on selected memory-type parametric SPM-type schemes are discussed in this chapter. This includes the EWMA-, DEWMA-, and HWMA-type schemes, respectively, studied in Sections 2.3, 2.4, and 2.5.

The major weakness of those parametric SPM-type schemes is the underlying process distribution is assumed to follow some theoretical probability distribution, such as the normal distribution. However, this assumption is not always valid in real life. As mentioned in the previous chapter, the parametric SPM-type scheme is unreliable if any assumptions are breached. Therefore, Section 2.6 reveals the development of the NSPM-type schemes from single-parameter monitoring to two-parameter joint monitoring.

In recent decades, the joint monitoring NSPM-type schemes receive growing attention among researchers. Among them, the Lepage-type scheme is the most famous. Therefore, the development of the Lepage-type scheme and the fundamental of the Lepage statistic are reviewed in Sections 2.7 and 2.8, respectively. Lastly, some existing Lepage-type schemes, i.e., the SL and EL schemes, are discussed in Section 2.9.

2.2 Development of the Parametric SPM-Type Joint Monitoring Scheme

Researchers and quality practitioners knew that it is not convincing to conclude that a particular process is statistically IC or OOC by just monitoring the process location, i.e., the mean under a parametric set-up. Therefore, in the early days of SPM, practitioners used two individual and separate schemes (called two-charts joint monitoring scheme, abbreviated as TC-JM scheme hereafter). For instance, when the underlying process distribution is normally distributed, $\bar{X}$ scheme is used to monitor the process mean, while S or R scheme monitors the process variance. With such, the Shewhart $\bar{X}$ & R and $\bar{X}$ & S are the two most well-known TC-JM schemes. Nevertheless, a TC-JM scheme may be a combination of any Shewhart-, EWMA-, or CUSUM-type. For example, one may use EWMA-$\bar{X}$ and Shewhart-S to monitor the mean and variance of a process, respectively.

The TC-JM scheme has been popular in the industry for many years because it seems intrinsic to some quality practitioners. Further, the $\bar{X}$ and S statistics are stochastically independent. However, the TC-JM scheme costs more time, personnel, and resource than a single charting scheme (Cheng and Thaga, 2006). Hawkins and Deng (2009) mentioned that the control limits of the $\bar{X}$ scheme are functions of $SDRL_0$. Hence, a false signal may be seen on the $\bar{X}$ scheme when the variability increases, and vice versa. Also, a TC-JM scheme, such as the $\bar{X}$ & R and $\bar{X}$ & S schemes ignore the relationship between the process mean and process variance. Moreover, the fact is, one can never neglect the tendency that a bi-aspect phenomenon, i.e., a simultaneous shift in the mean and variance, occur. It is discriminatory to deal with a bivariate case by using two marginals.

To this end, a combined charting method (called one-chart joint monitoring scheme, termed as OC-JM scheme hereafter) is proposed in the 20^{th} century, in order to deal with this weakness. The two prominent OC-JM schemes are the max- and distance-type schemes, respectively, introduced by Chen and Cheng (1998) and Ramzy (2005). Again, both of these schemes assume that the process follows a normal distribution. For instance, the plotting statistic of a max-type scheme is the maximum value of the absolute values of two normalised statistics, where one for the mean and one for the variance, i.e., the i^{th} plotting statistic of a max-type scheme, M_i, is defined as

$$M_i = \max\left(\left|\frac{\bar{X}_i-\mu}{\sigma/\sqrt{n_i}}\right| \quad , \quad \left|\Phi^{-1}\left\{F\left[\frac{(n_i-1)S_i^2}{\sigma^2};\ n_i-1\right]\right\}\right|\right), \qquad (2.1)$$

where $F(w;v)$ is the cumulative distribution function (CDF) of a chi-square distribution with v degrees of freedom, n_i is the size of the i^{th} sample, and $\Phi^{-1}\{.\}$ is the inverse CDF of a standard normal distribution.

The main strength of the OC-JM scheme is it is more straightforward than the TC-JM scheme because only a single plotting statistic is required. Most of these schemes available in the literature are categorised as the "Case K" schemes because all the relevant process parameters are standard known. Nevertheless, the assumption of "Case K" is not practical because there exist some parameters that are unknown and unspecified. To this end, "Case U" schemes, where the relevant parameters are standard unknown, are developed.

For the "Case U" scheme, even the underlying process distribution is known, the estimation of the parameters, such as the mean and variance, depends statistically on the data. On top of that, the construction of the trial control limits also depends on the data. All these factors leading a "Case U" scheme is more challenging (see, for example, Chakraborti et al., 2009). There are a few "Case U" schemes for joint monitoring that are available in the literature. For instance, McCracken et al. (2013) revised the previous works in order to monitor a normally distributed process when both the mean and variance are unknown. Besides, Yeh et al. (2004) considered a pair of CUSUM mean and variance statistics, which is computed from some suitable functions of $\bar{X}$ and S, then probability integral transformation is applied.

Besides the normal distribution, parametric SPM-type joint monitoring for the shifted exponential distribution also received growing attention among researchers. This is because the shifted exponential distribution plays an essential role in time-to-event modelling for reliability and life testing. For instance, this distribution is very functional in predicting light bulbs' life span or cancer patients' life expectancy (Basu, 1971). Noting the importance of this distribution, Mukherjee et al. (2015) developed Case K control schemes to jointly monitor a shifted exponential distribution parameters. Then, a Case U joint monitoring scheme for the two unknown parameters was introduced by Chong et al. (2021) recently.

2.3 Development of the Parametric Exponentially Weighted Moving Average (EWMA)-Type Scheme

For most cases, particularly in practical applications, the memory-type schemes have a better performance than the memoryless Shewhart-type scheme, especially in detecting small to moderate shifts in a process. To this end, an EWMA-type scheme was proposed by Roberts (1959), which can be used to monitor and control a statistical process. An EWMA-type scheme assigns a weight to the current observation, while the weight decreases exponentially as the observation becomes older. For instance, the i^{th} plotting statistic of an EWMA $\bar{X}$ scheme, E_i, is defined as

$$E_i = \lambda \bar{X}_i + (1 - \lambda) E_{i-1}, \quad (2.2)$$

where $\lambda \in (0, 1]$ is the smoothing parameter of an EWMA-type scheme. A small value of λ is preferred for the EWMA-type scheme to monitor a small disturbance in the process and vice versa.

Since then, a bundle of extension works on the EWMA-type scheme was done. For instance, Crowder (1987) employed the integral equation to evaluate the statistical properties of an EWMA-type scheme in monitoring the shift of the process mean. Unlike Crowder (1987), Lucas and Saccucci (1990) used the Markov Chain method to evaluate the performance of the EWMA-type scheme. On top of that, Lucas and Saccucci (1990) did a comparison study between EWMA- and CUSUM-type schemes. They concluded that both schemes have nearly the same performance.

The traditional EWMA-type scheme is a two-sided scheme because it has two control limits, i.e., LCL and UCL, where this type of EWMA-type scheme is studied extensively in the literature. However, the weakness of this scheme is it might suffer from the inertial effect if the EWMA plotting statistic is distant from the centre line and it is in the opposite direction just before there is a process mean shift (Woodall and Mahmoud, 2005). The inertial effect happens as the EWMA-type scheme takes several periods to react to the process shift (Montgomery, 2019). The consequence of this problem is an OOC signal may be delayed if the value of λ is small. This is because a small value of λ indicates that the current observation has a small weight. Therefore, the performance of an EWMA-type scheme deteriorates caused by the inertial issue. To this end, Lucas and Saccucci (1990) recommended a combined Shewhart-EWMA-type scheme, i.e., the Shewhart-type control limit is added to the EWMA-type scheme, in order to curb the inertial effect.

Except for the combined Shewhart-EWMA-type scheme, many more schemes are developed to alleviate the inertial effect of an EWMA-type scheme. For instance, Capizzi and Masarotto (2003) designed an adaptive EWMA (AEWMA)-type scheme, i.e., a combined Shewhart-EWMA-type scheme with a variable smoothing parameter. Therefore, the AEWMA-type scheme can detect all types of shifts in the process, ranging from small to large, and the impact of the inertial issue is reduced. Besides, an improved one-sided EWMA $\bar{X}$ scheme was proposed by Shu et al. (2007), which is beneficial for the industrial sector, such as milling operations or hole-finishing. The proposed scheme is useful when the cost of quality incurred is distinct, such as the cost of oversized quality characteristics is different from that of undersized.

Since then, more adaptive strategies, such as the variable sampling interval (VSI) and variable sample size (VSS) are adopted in the EWMA-type scheme. These adaptive features can improve the sensitivity and effectiveness of an EWMA-type scheme in detecting a process shift. For example, Saccucci et al. (1992) developed a VSI-EWMA $\bar{X}$ scheme, where the sampling interval is varied and depends on the present plotting statistic. They showed that the proposed scheme is better and more efficient than the traditional EWMA-type scheme with a fixed sampling interval. On the other hand, Amiri et al. (2014) designed a novel VSS-EWMA $\bar{X}$ scheme to monitor the process mean, where the sample size is determined using an integer linear function. They showed that this proposed scheme is superior to the traditional EWMA- and VSS-EWMA-type schemes. Besides, an optimal VSS-EWMA S^2 scheme to monitor the process dispersion was developed by Castagliola et al. (2008). They found that the proposed scheme outperforms the EWMA S^2 scheme with a fixed sample size.

2.4 Development of the Parametric Double EWMA (DEWMA)-Type Scheme

Shamma and Shamma (1992) first conceptualised the DEWMA-type scheme, which is an extension of the ideas of the fundamental EWMA-type scheme. With such, the i^{th} DEWMA $\bar{X}$ plotting statistic, termed as D_i, is defined as

$$D_i = \lambda E_i + (1-\lambda)D_{i-1}, \tag{2.3}$$

where $0 < \lambda \leq 1$ is the smoothing parameter of the DEWMA-type scheme and E_i statistic is computed by using Equation (2.2). They showed that the DEWMA-type scheme is able to predict a disturbance in the process mean, which is as good as the EWMA-type scheme. Besides, in terms of detecting a small to moderate shift in the process mean, the DEWMA-type scheme is superior to the Shewhart-type scheme.

Different from Shamma and Shamma (1992), a variant of the DEWMA-type scheme with distinct smoothing parameters is designed by Zhang and Chen (2005). For instance, the i^{th} EWMA and DEWMA $\bar{X}$ plotting statistics, y_i and z_i, respectively, defined by Zhang and Chen (2005) are

$$y_i = \lambda_1 \bar{X}_i + (1 - \lambda_1) y_{i-1} \quad (2.4)$$

and

$$z_i = \lambda_2 y_i + (1 - \lambda_2) z_{i-1}, \quad (2.5)$$

where $\lambda_1 \in (0, 1]$ and $\lambda_2 \in (0, 1]$ are, respectively, the smoothing parameters of the EWMA $\bar{X}$ and DEWMA $\bar{X}$ schemes. Therefore, it is evident that the DEWMA-type scheme proposed by Shamma and Shamma (1992) is a special case of the DEWMA-type scheme proposed by Zhang and Chen (2005), i.e., when $\lambda_1 = \lambda_2 = \lambda$. It is worth mentioning that Zhang and Chen (2005) concluded that the performance of the DEWMA-type scheme in detecting a small shift in the process mean is better than the EWMA-type scheme.

Thenceforth, a host of researches were done to improve the DEWMA-type scheme, especially the DEWMA-type scheme developed by Shamma and Shamma (1992) due to its simplicity compared to the scheme presented by Zhang and Chen (2005). Most of the new DEWMA-type schemes proposed are also compared with their counterpart of the EWMA-type scheme. For instance, Khoo et al. (2010) presented a single Max-DEWMA scheme, where the plotting statistic of the scheme is the maximum of the absolute values of two DEWMA statistics (one for the mean and variance, respectively). They showed that the Max-DEWMA scheme has a better performance than its counterpart, i.e., the Max-EWMA scheme, in terms of small to moderate shifts in the location and/or scale parameters of a process.

Most of the researches done on the EWMA- and DEWMA-type schemes have a normality assumption, where it is not always true. Hence, Borror et al.

(1999) studied the performance of an EWMA-type scheme under some skewed distributions. They concluded that the ARL performance of an EWMA-type scheme is robust towards non-normality. This finding motivated Alkahtani (2013) to study the robustness of a DEWMA-type scheme towards non-normality. Alkahtani (2013) showed that a DEWMA-type scheme outperforms, i.e., has a lower ARL_1, compared to the EWMA-type scheme if the underlying process distribution is skewed. Further, the author also found that the robustness of the DEWMA-type scheme towards non-normality has a positive relationship with the value of the smoothing parameter.

Similar to parametric SPM-type schemes, the development of the parametric DEWMA-type scheme is not only limited to the normal distribution, but different kinds of the statistical probability distribution are explored. This includes the DEWMA-type scheme to monitor Poisson data presented by Zhang et al. (2003). The results showed that the Poisson-DEWMA scheme detects an OOC signal faster than the Poisson-EWMA scheme. Particularly, the Poisson-DEWMA scheme is more sensitive than the Poisson-EWMA scheme in terms of identifying a small downward shift in the process mean.

Recently, a DEWMA-type scheme to monitor a process that follows a zero-inflated Poisson (ZIP) distribution, abbreviated as the ZIP-DEWMA scheme, was proposed by Alevizakos and Koukouvinos (2020). Similarly, the proposed scheme was then compared with its counterpart, i.e., the ZIP-EWMA scheme. The results found that the ZIP-DEWMA scheme performs better in detecting a small shift in the process, while the ZIP-EWMA scheme is superior in detecting a moderate to large shift in the process.

Further, Haq et al. (2020) proposed a novel DEWMA-type scheme to monitor the process mean. The proposed scheme is named the DEWMA-t scheme because the plotting statistic of the scheme follows a Student's t distribution. They found that the proposed scheme is uniformly and substantially outperforms the EWMA-t scheme counterpart, regardless of the types of shifts in the process mean.

2.5 Development of the Parametric Homogeneously Weighted Moving Average (HWMA)-Type Scheme

With a different weighting design as the traditional EWMA- and DEWMA-type schemes, Abbas (2018) originated a new process monitoring scheme named the HWMA-type scheme recently. To be precise, the HWMA-type scheme assigns a predetermined weight to the current observation, and then all the previous observations are equally important, such that the remaining weight is divided fairly to them. For instance, the HWMA $\bar{X}$ scheme has the i^{th} plotting statistic, H_i, which is defined as

$$H_i = \lambda \bar{X}_i + \left(\frac{1-\lambda}{i-1}\right)[\bar{X}_{i-1} + \bar{X}_{i-2} + \cdots + \bar{X}_2 + \bar{X}_1], \tag{2.6}$$

where $\lambda \in (0, 1]$ is the smoothing parameter of the HWMA-type scheme. For the special case, when $i = 1$, the plotting statistic of the HWMA $\bar{X}$ scheme is $H_1 = \lambda \bar{X}_1 + (1 - \lambda)\bar{X}_0$. The author proved that the latest HWMA-type scheme is superior to other memory-type schemes in most kinds of shifts in the process mean, including the well-known EWMA-type scheme.

Thenceforward, some researchers turn their focus to this novel and interesting idea. To this end, there are a few advanced HWMA-type schemes available in the literature. For instance, an auxiliary HWMA-type scheme to monitor the process mean was presented by Adegoke et al. (2019). The proposed scheme employs both the quality characteristic monitored and its auxiliary variables under a regression estimator. The estimate of the process mean obtained by this method is more efficient and unbiased. The results showed that the proposed scheme has an outstanding performance in detecting a small shift in the process mean compared to some existing memory-type schemes, including the HWMA-type scheme. However, they found that the proposed scheme is less sensitive to non-normality.

Besides, Adeoti and Koleoso (2020) proposed a new hybrid HWMA-type scheme, where the hybrid HWMA-type scheme is obtained by implementing the HWMA concept on the HWMA statistic. Precisely, let the i^{th} plotting statistics of the HWMA $\bar{X}$ and hybrid HWMA $\bar{X}$, denoted as y_i and z_i be defined as

$$y_i = \lambda_1 \bar{X}_i + \left(\frac{1-\lambda_1}{i-1}\right)[\bar{X}_{i-1} + \bar{X}_{i-2} + \cdots + \bar{X}_2 + \bar{X}_1] \qquad (2.7)$$

and

$$z_i = \lambda_2 y_i + \left(\frac{1-\lambda_2}{i-1}\right)[y_{i-1} + y_{i-2} + \cdots + y_2 + y_1], \qquad (2.8)$$

where $\lambda_1 \in (0, 1]$ and $\lambda_2 \in (0, 1]$, are respectively, the smoothing parameters of the HWMA $\bar{X}$ and hybrid HWMA $\bar{X}$ schemes. The results proved that the proposed hybrid HWMA-type scheme is superior to some existing memory-type schemes in most situations.

Slightly different from Adeoti and Koleoso (2020), a double HWMA-type scheme was proposed by Abid et al. (2020), with the i^{th} plotting statistic, DH_i, is defined as

$$DH_i = \lambda^2 \bar{X}_i + \left(\frac{1-\lambda^2}{i-1}\right)[\bar{X}_{i-1} + \bar{X}_{i-2} + \cdots + \bar{X}_2 + \bar{X}_1], \tag{2.9}$$

where $0 < \lambda \leq 1$ is the smoothing parameter of the double HWMA $\bar{X}$ scheme. The results showed that the proposed scheme performs efficiently for various shifts and dominates some well-known memory-type schemes. Other than monitor the process mean, monitoring the process dispersion is also of utmost importance. To this end, Riaz et al. (2020) developed an HWMA-type scheme to monitor a small shift in the process dispersion. From the results, it is concluded that the proposed scheme outperforms its competitors.

2.6 Development of the Nonparametric SPM (NSPM)-Type Scheme

All of the schemes discussed earlier in this chapter, and the majority of the available literature, are focused on the parametric SPM-type scheme. The selling point of a parametric SPM-type scheme is that the underlying process distribution is known, and therefore it is easy to develop. At the same time, this is also the main weakness of a parametric SPM-type scheme. This is because a parametric SPM-type scheme is no longer reliable and convincible if the underlying process distribution does not follow the assumption. Hence, an NSPM-type scheme acts as a remedy to overcome this issue because the underlying process needs not follow a specific probability distribution for an NSPM-type scheme.

2.6.1 Single-Parameter NSPM-Type Scheme

In the early stage of the development of the NSPM-type scheme, research is done on developing NSPM-type schemes that can only monitor a single parameter of a process, especially the location parameter. For instance, the WSR statistic, which is one of the famous nonparametric statistics used to monitor the location parameter, is embedded in the NSPM-type schemes. Some of the WSR statistic related NSPM-type schemes include the CUSUM-, EWMA-, and Shewhart-type, presented by Bakir and Reynolds (1979), Amin and Searcy (1991), and Bakir (2004), respectively. Other than the WSR statistic, the sign statistic was also embedded in the NSPM-type schemes, such as the Shewhart- and CUSUM-type schemes proposed by Amin et al. (1995).

The research field of NSPM-type schemes continues to grow rapidly, especially in the twenty-tens. Hence, more new and advanced NSPM-type schemes have been added to the literature. These include the distribution-free CUSUM- and EWMA-type schemes based on the Wilcoxon rank-sum (WRS) statistic developed by Li et al. (2010). Besides, a nonparametric change-point scheme based on the Mann-Whitney (MW) statistic was introduced by Hawkins and Deng (2010). Further, Mukherjee et al. (2013) designed a distribution-free CUSUM-type scheme based on the exceedance statistic. To this end, there are a few works of literature that present the overall review of the distribution-free

Shewhart-, CUSUM-, and EWMA-type schemes that are used to monitor a single parameter, such as Chakraborti et al. (2001; 2011).

One may notice that most of the literature regarding the NSPM-type scheme is the famous memoryless Shewhart-type or memory-type CUSUM- and EWMA-type schemes. Therefore, the literature on the NSPM DEWMA- and especially the HWMA-type schemes are currently very limited. Some of the available NSPM DEWMA-type schemes include the nonparametric DEWMA scheme using a transformed random variable to monitor the location parameter proposed by Riaz and Abbasi (2016). Recently, NSPM DEWMA-type schemes to monitor the process location using the WSR and WRS statistics were, respectively, presented by Raza et al. (2020a) and Malela-Majika (2020). Apart from the NSPM DEWMA-type scheme, two NSPM HWMA-type schemes based on the sign and WSR statistics were proposed by Raza et al. (2020b).

2.6.2 Two-Parameter Joint NSPM-Type Scheme

Similar to the SPM-type scheme, it is also insufficient to conclude the stability of a process by just monitoring the process location using an NSPM-type scheme. To this end, the two-parameter joint NSPM-type scheme attracts the researchers' attention. For instance, an NSPM EWMA-type scheme based on the goodness-of-fit (GOF) test was proposed by Zou and Tsung (2010). The results showed that the scheme effectively detects shifts in the location, scale, and shape parameters of a process.

Apart from the GOF test, Mukherjee and Chakraborti (2012) employed the famous nonparametric statistic for the location-scale test, i.e., the Lepage (1971) statistic in the Shewhart-type scheme, termed as the SL scheme. Two years later, Chowdhury et al. (2014) embedded another well-known distribution-free statistic that can jointly monitor the location and scale parameters, but with a simpler expression, i.e., the Cucconi (1968) statistic in the Shewhart-type scheme, named as the Shewhart-Cucconi (SC) scheme. Since then, the two-parameter joint NSPM-type schemes, particularly the Lepage- and Cucconi-type schemes, continue to grow at a rapid pace.

Comparatively, the Lepage-type schemes receive more attention from researchers than the Cucconi-type schemes. Moreover, two novel Lepage-type schemes will be proposed in this dissertation. To this end, the development of some related Lepage-type schemes will be discussed in-depth in the next few sections. On the other hand, since the SC scheme proposed by Chowdhury et al. (2014), there are a few Phase-II Cucconi-type schemes introduced and available in the literature. For instance, Mukherjee and Marozzi (2017a) presented a CUSUM-type scheme based on the Cucconi statistic, termed as the CUSUM-Cucconi (CC) scheme. Further, an EWMA-type scheme by employing the Cucconi statistic, i.e., the EWMA-Cucconi (EC) scheme, was developed by Xiang et al. (2019). Recently, Song et al. (2020b) modified the SC scheme proposed by Chowdhury et al. (2014), and they presented a one-sided SC scheme. Other than the Phase-II Cucconi-type schemes, Li et al. (2020) developed a Phase-I scheme using multi-sample Cucconi statistic.

Other than the Lepage- and Cucconi-type distribution-free schemes, Zhang et al. (2017) developed a novel NSPM-type scheme based on the Cramér-von Mises (CvM) test. Precisely, they embedded the test in the EWMA-type scheme so that the proposed scheme can be used to monitor the location and scale parameters of a process jointly. Recently, Song et al. (2020a) studied and compared the performance of various kinds of two-parameter joint NSPM EWMA-type schemes, which include the Lepage-, Cucconi-, CvM-, and Kolmogorov-Smirnov (KS)-type schemes. Further, they also proposed the component-wise Lepage- and Cucconi-type schemes, i.e., the Lepage and Cucconi statistics are decomposed into two individual statistics, one for the location and one for the scale. For the up-to-date overall review of the single-parameter and two-parameter joint NSPM-type schemes, one may refer to Chakraborti and Graham (2019).

2.7 Development of the Lepage-Type Scheme

The first nonparametric Lepage-type scheme available in the literature is coined by Mukherjee and Chakraborti (2012), i.e., the SL scheme. Precisely, they embedded the Lepage (1971) statistic, which is a quadratic combination of the standardised WRS and standardised Ansari-Bradley (AB) statistics, i.e., to test the location and scale parameters, respectively, in the traditional Shewhart-type scheme. Further, the SL scheme has a post-signal diagnostic process, which can determine the nature of the shift easily.

Since then, various explorations on the NSPM Lepage-type scheme are introduced in the literature. For instance, the memoryless SL scheme is extended to various memory-type schemes, such as the CUSUM- and EWMA-type, i.e., the CUSUM-Lepage (CL) and EL schemes, proposed by Chowdhury et al. (2015) and Mukherjee (2017), respectively. The CL scheme presented by Chowdhury et al. (2015) uses a steady-state UCL, and it is shown that the proposed scheme is superior to the memoryless SL scheme and memory-type CUSUM-CvM and CUSUM-KS schemes. Unlike Chowdhury et al. (2015), Mukherjee (2017) studied EL scheme with both steady-state and time-varying UCLs. The results indicated that the EL scheme performs significantly better than the SL and CL schemes in most cases.

Moreover, Mukherjee and Marozzi (2017b) extended the SL scheme, i.e., from a standard control scheme to a novel circular grid control scheme by modifying the Lepage statistic. For instance, the traditional SL scheme uses an UCL to identify the stability of a process. As depicted in Figure 2.1, the process is considered OOC if the plotting statistic is beyond the UCL, and vice versa. If an OOC signal is generated, a follow-up procedure is conducted to identify the nature of the shift. Comparatively, it is much convenient to identify a shift and its nature using the circular-grid modified SL scheme. This is because the nature of an OOC signal can be identified easily from the plotting statistic belongs to, without performing any follow-up procedure.

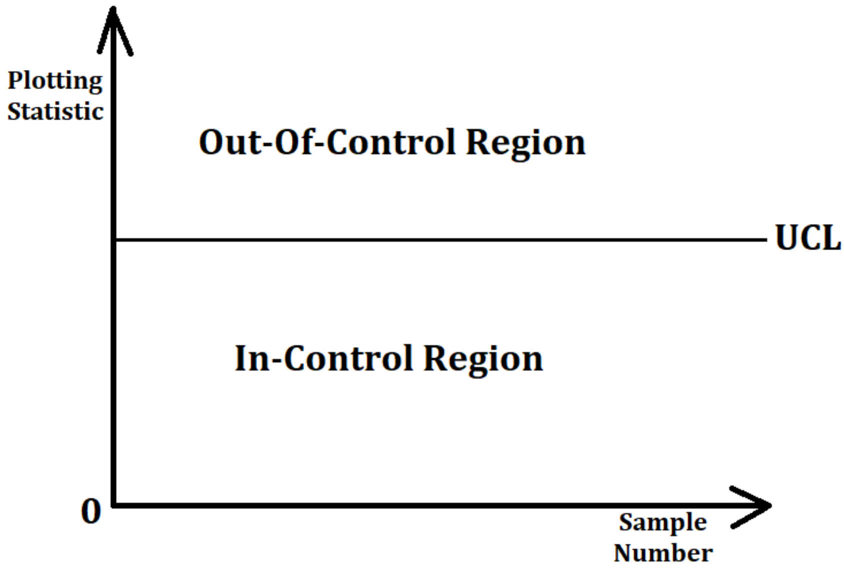

Figure 2.1: Graphical Description of A Standard SL Scheme

Furthermore, Chong et al. (2017) presented a premier SL scheme, and precisely it is a Fuzzy SL (FSL) scheme, i.e., both the max- and distance-type schemes are used simultaneously. The results showed that the FSL scheme outperforms the SL scheme and other competing schemes. Besides, Mukerjee and Sen (2018) presented some generalised SL schemes using an adaptive approach. To be exact, they employed some percentile modifications of ranks, or better known as the adaptive Gastwirth Score in their proposed schemes.

One may note that all the aforementioned Lepage-type schemes are known as Phase-II schemes. Researchers are also aware that the Phase-I type scheme is important in process monitoring. To this end, the first distribution-free location-scale joint monitoring Phase-I scheme with a single statistic, i.e., the multi-sample Lepage statistic, was proposed by Li et al. (2019). The authors compared the proposed scheme with some existing Phase-I schemes, and the results revealed that the proposed scheme is superior in various cases.

2.8 Statistical Framework and Preliminaries of the Lepage Statistic

Assume that the CDFs of the Phase-I reference sample X and Phase-II test sample Y be F_X and F_Y, respectively. Then, it can be expressed that $F_Y(y) = F_X\left(\frac{x-\theta}{\delta}\right)$, where $\theta \in (-\infty, \infty)$ is the unknown location parameter of a process and $\delta \in (0, \infty)$ is the unknown scale parameter of the process. Hence, it is very obvious that when the process is IC, the unknown location and scale parameters are 0 and 1, respectively, i.e., $(\theta, \delta) = (0, 1)$. Otherwise, a process is OOC if $(\theta, \delta) \neq (0, 1)$.

Suppose that $\overrightarrow{X_m} = \{X_1, X_2, X_3, \ldots, X_m\}$ is a random sample collected from an IC process with size m, where it is suitable to be employed as a reference sample. Then, $\overrightarrow{Y_{ni}} = \{Y_{1i}, Y_{2i}, Y_{3i}, \ldots, Y_{ni}\}$ is the i^{th} test sample, where $i \in \mathbb{Z}^+$, assembled during the Phase-II monitoring of a process. Next, the samples $\overrightarrow{X_m}$ and $\overrightarrow{Y_{ni}}$ are combined with size $N = m + n$, and all the observations in the combined samples are ranked. To this end, let the n sample ranks of the Y observations corresponding to $\overrightarrow{Y_{ni}}$ in the combined samples, be $R_{1i} \leq R_{2i} \leq R_{3i} \leq \cdots \leq R_{ni}$.

Hence, the WRS and AB statistics corresponding to the i^{th} test sample are defined as

$$WRS_i = \sum_{j=1}^{n} R_{ji} \tag{2.10}$$

and

$$AB_i = \sum_{j=1}^{n} \left| R_{ji} - \frac{N+1}{2} \right|, \tag{2.11}$$

respectively. When the process is IC, the mean of the WRS_i and AB_i are, respectively, defined as

$$\mu_{WRS} = E(WRS_i|IC) = \frac{n(N+1)}{2} \tag{2.12}$$

and

$$\mu_{AB} = E(AB_i|IC) = \begin{cases} \frac{n(N^2-1)}{4N} & \text{if } N \text{ is odd} \\ \frac{nN}{4} & \text{if } N \text{ is even} \end{cases}. \tag{2.13}$$

In addition, the standard deviations of the WRS_i and AB_i in an IC state are

$$\sigma_{WRS} = \sqrt{Var(WRS_i|IC)} = \sqrt{\frac{mn(N+1)}{12}} \tag{2.14}$$

and

$$\sigma_{AB} = \sqrt{Var(AB_i|IC)} = \begin{cases} \sqrt{\frac{mn(N+1)(N^2+3)}{48N^2}} & \text{if } N \text{ is odd} \\ \sqrt{\frac{mn(N^2-4)}{48(N-1)}} & \text{if } N \text{ is even} \end{cases}, \tag{2.15}$$

respectively. Therefore, the i^{th} Lepage statistic, termed as L_i, which is defined as the Euclidean distance-based quadratic combination of the standardised WRS_i and standardised AB_i, can be expressed as

$$L_i = \left(\frac{WRS_i - \mu_{WRS}}{\sigma_{WRS}}\right)^2 + \left(\frac{AB_i - \mu_{AB}}{\sigma_{AB}}\right)^2. \tag{2.16}$$

2.9 Related Lepage-Type Schemes

In this section, a brief discussion on the implementation procedure of two competing Lepage-type scheme is presented. These two existing Lepage-type schemes will also be studied and compared with the two proposed Lepage-type schemes in Chapter 4. The two competing Lepage-type schemes include the memoryless SL and memory-type EL schemes.

2.9.1 The Shewhart-Lepage (SL) Scheme and Its Implementation

The SL scheme is developed with only a single control limit. This is because $L_i \geq 0$ by definition. Further, it is known that $E(L_i|IC) = 2$, where a shift in the process might lead to $E(L_i|IC) > 2$. Thus, an OOC signal is suspected if the value of L_i is high. To this end, the SL scheme employes an upper one-sided monitoring procedure, i.e., an upper control limit (UCL) is employed.

The implementing steps of the SL scheme are described below.

Step I. A reference sample with size m, $\overrightarrow{X_m} = \{X_1, X_2, X_3, \dots, X_m\}$ from a process that is assumed to be IC, is collected.

Step II. The i^{th} test sample with size n, $\overrightarrow{Y_{ni}} = \{Y_{1i}, Y_{2i}, Y_{3i}, \dots, Y_{ni}\}$ is collected.

Step III. The i^{th} plotting statistic, i.e., the L_i is computed using Equation (2.16).

Step IV. The L_i is plotted against the steady-state UCL, denoted as Ψ_{SL}. Note that the determination of Ψ_{SL} will be discussed in Section 3.4.

Step V. The process is declared IC if $L_i < \Psi_{SL}$ and the next test sample is examined. Otherwise, the process is OOC at the i^{th} test sample and assignable cause(s) are investigated.

Step VI. When the process is OOC at the i^{th} test sample, a follow-up procedure is conducted. Here, all the observations in $\overrightarrow{X_m}$ are treated as the first sample, while all the observations in $\overrightarrow{Y_{ni}}$ are treated as the second sample. Then, the p-values for the two-tailed WRS test (p_W) for location and two-tailed AB test (p_A) for scale are computed.

a. If p_W is significant but p_A is insignificant, it indicates a pure location shift in the process.

b. If p_W is insignificant but p_A is significant, it indicates a pure scale shift is in the process.

c. If p_W and p_A are both significant, it indicates a mixed shift in the location and scale parameters of the process.

d. If p_W and p_A are both insignificant, it indicates a complicated simultaneous shift in the location and scale parameters, or it is just a false alarm.

2.9.2 The EWMA-Lepage (EL) Scheme and Its Implementation

The EL scheme presented by Mukherjee (2017) employed the max-approach, which has a better performance in reducing the inertial effect compared to the traditional set-up. However, the inertial effect is not considered in this dissertation since the main objective of this dissertation is to propose two new control schemes, and it usually starts from a basic scheme without many adaptive features. Thus, the EL scheme studied here is not exactly the one presented by Mukherjee (2017). On the other hand, the basic and traditional EL scheme, which has a weaker performance if an inertial issue occurred, as presented by Chakraborti and Graham (2019) and Song et al. (2020a), is considered here. To this end, the i^{th} plotting statistic of the EL scheme is defined as

$$EL_i = \lambda L_i + (1 - \lambda)EL_{i-1}, \tag{2.17}$$

where $\lambda \in (0, 1]$ is the smoothing parameter of the EL scheme.

Using the same argument discussed in Section 2.9.1, the EL scheme studied in this research is also considered as an upper one-sided monitoring scheme, i.e., an UCL is used to monitor a process. However, there are two types of UCLs which will be considered for the EL scheme, i.e., the time-varying UCL, $\Psi_{EL}(i)$ and the steady-state UCL, Ψ_{EL}. Again, the determination of two types of UCLs will be covered in Section 3.4. Further, it is assumed that $L_0 = EL_0 = 2$ (Mukherjee, 2017; Song et al., 2020a).

Mukherjee (2017) defined that the time-varying UCL for the EL scheme, $\Psi_{EL}(i)$ can be expressed as

$$\Psi_{EL}(i) = \mu_{EL_i} + L_{EL}\sigma_{EL_i}, \tag{2.18}$$

where μ_{EL_i} and σ_{EL_i} are the i^{th} mean and standard deviation of the EL scheme with time-varying UCL, respectively, while L_{EL} is the charting constant of the EL scheme with time-varying UCL. With the notation of $E\left(L_i|\overrightarrow{X_m}, IC\right) = \upsilon_1$ and $Var\left(L_i|\overrightarrow{X_m}, IC\right) = \upsilon_2$, Mukherjee (2017) proved that

$$\mu_{EL_i} = 2 \tag{2.19}$$

and

$$\sigma_{EL_i} = \sqrt{\frac{\lambda}{2-\lambda}[1-(1-\lambda)^{2i}]\xi_2 + [1-(1-\lambda)^i]^2\xi_1}, \tag{2.20}$$

where $\xi_1 = Var(\upsilon_1|IC)$ and $\xi_2 = E(\upsilon_2|IC)$.

Then, the step-by-step implementing procedure of the EL scheme is described below.

Step I. A reference sample with size m, $\overrightarrow{X_m} = \{X_1, X_2, X_3, \dots, X_m\}$ from a process that is assumed to be IC, is collected.

Step II. The i^{th} test sample with size n, $\overrightarrow{Y_{ni}} = \{Y_{1i}, Y_{2i}, Y_{3i}, \dots, Y_{ni}\}$ is collected.

Step III. The i^{th} plotting statistic, i.e., the EL_i is computed using Equation (2.17).

Step IV. The EL_i is plotted against the UCLs, either $\Psi_{EL}(i)$ or Ψ_{EL}.

Step V. The process is declared IC if $EL_i < \Psi_{EL}(i)$ (or Ψ_{EL}) and the following test sample is examined. Otherwise, the process is OOC at the i^{th} test sample and assignable cause(s) are investigated.

Step VI. When the process is OOC at the i^{th} test sample, a follow-up procedure is done. Here, all the observations in $\overrightarrow{X_m}$ is treated as the first sample, while all the observations in the 1^{st} until i^{th} test samples, with a total of size ni is treated as the second sample. Then, the p-values for the two-tailed WRS test (p_W^*) for location and two-tailed AB test (p_A^*) for scale are computed.

a. If p_W^* is significant but p_A^* is insignificant, it indicates a pure location shift in the process.

b. If p_W^* is insignificant but p_A^* is significant, it indicates a pure scale shift is in the process.

c. If p_W^* and p_A^* are both significant, it indicates a mixed shift in the location and scale parameters of the process.

d. If p_W^* and p_A^* are both insignificant, it indicates a complicated simultaneous shift in the location and scale parameters, or it is just a false alarm.

CHAPTER 3

RESEARCH METHODOLOGY

3.1 Introduction

The proposed DL and HL schemes and their implementations are firstly presented in Section 3.2. This includes the explanation of the plotting statistics for these two novel schemes. Then, in Section 3.3, the time-varying UCLs for the two proposed schemes are derived theoretically. Next, the determination of UCLs for the two proposed schemes and two competing schemes, i.e., the SL and EL schemes, are discussed in Section 3.4. Further, the Monte-Carlo simulation is also explained here. Lastly, Section 3.5 presents the various types of RL metrics that will be employed in this dissertation for the performance evaluation of a control scheme.

3.2 The Proposed DEWMA-Lepage (DL) and HWMA-Lepage (HL) Schemes and Their Implementations

The i^{th} plotting statistic of the EL scheme as depicted in Equation (2.17) is extended to the proposed DL scheme with the idea of Shamma and Shamma (1992). To this end, the i^{th} plotting statistic of the DL scheme is defined as

$$DL_i = \lambda EL_i + (1 - \lambda) DL_{i-1}, \tag{3.1}$$

where $\lambda \in (0, 1]$ is the smoothing parameter of the DL scheme and EL_i is computed with Equation (2.17).

Similar to the discussion for the implementation of the SL and EL schemes, the DL scheme proposed is used to monitor the process with an UCL, either the time-varying UCL, $\Psi_{DL}(i)$ or the steady-state UCL, Ψ_{DL}. The expression of $\Psi_{DL}(i)$ will be derived in the next section, whereas the determination of $\Psi_{DL}(i)$ and Ψ_{DL} will be covered in Section 3.4. Then, it is assumed that $L_0 = EL_0 = DL_0 = 2$.

Next, the charting procedures for the implementation of the DL scheme are delineated below.

Step I. A reference sample with size m, $\overrightarrow{X_m} = \{X_1, X_2, X_3, \dots, X_m\}$ from a process that is assumed to be IC, is collected.

Step II. The i^{th} test sample with size n, $\overrightarrow{Y_{ni}} = \{Y_{1i}, Y_{2i}, Y_{3i}, \dots, Y_{ni}\}$ is collected.

Step III. The i^{th} plotting statistic, i.e., the DL_i is computed using Equation (3.1).

Step IV. The DL_i is plotted against the UCLs, either $\Psi_{DL}(i)$ or Ψ_{DL}.

Step V. The process is declared IC if $DL_i < \Psi_{DL}(i)$ (or Ψ_{DL}) and the following test sample is examined. Otherwise, the process is OOC at the i^{th} test sample and assignable cause(s) are investigated.

Step VI. When the process is OOC at the i^{th} test sample, a follow-up procedure is done. Here, all the observations in $\overrightarrow{X_m}$ is treated as the first sample, while all the observations in the 1^{st} until i^{th} test samples, with a total of size ni is treated as the second sample.

Then, the p-values for the two-tailed WRS test (p_W^*) for location and two-tailed AB test (p_A^*) for scale are computed.

a. If p_W^* is significant but p_A^* is insignificant, it indicates a pure location shift in the process.

b. If p_W^* is insignificant but p_A^* is significant, it indicates a pure scale shift is in the process.

c. If p_W^* and p_A^* are both significant, it indicates a mixed shift in the location and scale parameters of the process.

d. If p_W^* and p_A^* are both insignificant, it indicates a complicated simultaneous shift in the location and scale parameters, or it is just a false alarm.

On the flip side, adopting the idea of the HWMA-type scheme proposed by Abbas (2018), the i^{th} plotting statistic of the HL scheme is defined as

$$HL_i = \begin{cases} \lambda L_1 + (1-\lambda)L_0 & \text{if } i = 1 \\ \lambda L_i + \left(\frac{1-\lambda}{i-1}\right)(L_{i-1} + L_{i-2} + \cdots + L_2 + L_1) & \text{if } i > 1 \end{cases}, \tag{3.2}$$

where $\lambda \in (0, 1]$ is the smoothing parameter of the HL scheme, while Equation (2.16) is used to compute L_i.

Similarly, an UCL, either the time-varying UCL, $\Psi_{HL}(i)$ or the steady-state UCL, Ψ_{HL} is employed in the HL scheme. Note that in Section 3.3, the derivation of $\Psi_{HL}(i)$ is discussed, while Section 3.4 presents the determination of $\Psi_{HL}(i)$ and Ψ_{HL}. Further, the assumption of $L_0 = 2$ is still upheld in the HL scheme.

To this end, the implementation steps of the HL scheme are demonstrated below.

Step I. A reference sample with size m, $\overrightarrow{X_m} = \{X_1, X_2, X_3, \dots, X_m\}$ from a process that is assumed to be IC, is collected.

Step II. The i^{th} test sample with size n, $\overrightarrow{Y_{ni}} = \{Y_{1i}, Y_{2i}, Y_{3i}, \dots, Y_{ni}\}$ is collected.

Step III. The i^{th} plotting statistic, i.e., the HL_i is computed using Equation (3.2).

Step IV. The HL_i is plotted against the UCLs, either $\Psi_{HL}(i)$ or Ψ_{HL}.

Step V. The process is declared IC if $HL_i < \Psi_{HL}(i)$ (or Ψ_{HL}) and the next test sample is examined. Otherwise, the process is OOC at the i^{th} test sample and assignable cause(s) are investigated.

Step VI. When the process is OOC at the i^{th} test sample, a follow-up procedure is done. Here, all the observations in $\overrightarrow{X_m}$ is treated as the first sample, while all the observations in the 1^{st} until i^{th} test samples, with a total of size ni is treated as the second sample. Then, the p-values for the two-tailed WRS test (p_W^*) for location and two-tailed AB test (p_A^*) for scale are computed.

a. If p_W^* is significant but p_A^* is insignificant, it indicates a pure location shift in the process.

b. If p_W^* is insignificant but p_A^* is significant, it indicates a pure scale shift is in the process.

c. If p_W^* and p_A^* are both significant, it indicates a mixed shift in the location and scale parameters of the process.

d. If p_W^* and p_A^* are both insignificant, it indicates a complicated simultaneous shift in the location and scale parameters, or it is just a false alarm.

3.3 The Time-Varying UCLs for the DL and HL Schemes

Similar to the time-varying UCL of the EL scheme, the time-varying UCLs of the DL and HL schemes can be expressed, respectively, as

$$\Psi_{DL}(i) = \mu_{DL_i} + L_{DL}\sigma_{DL_i} \tag{3.3}$$

and

$$\Psi_{HL}(i) = \mu_{HL_i} + L_{HL}\sigma_{HL_i}, \tag{3.4}$$

where μ_{DL_i}, σ_{DL_i}, μ_{HL_i}, and σ_{HL_i} are the mean and standard deviation of the DL and HL schemes with time-varying UCLs corresponding to the i^{th} test sample, respectively. On the other hand, L_{DL} and L_{HL} are, respectively, the charting constants of the DL and HL schemes with time-varying UCLs.

Using the same notation explained before, i.e., $\upsilon_1 = E\left(L_i|\overrightarrow{X_m}, IC\right)$ and $\upsilon_2 = Var\left(L_i|\overrightarrow{X_m}, IC\right)$ with $\xi_1 = Var(\upsilon_1|IC)$ and $\xi_2 = E(\upsilon_2|IC)$, the derivations of μ_{DL_i} and σ_{DL_i} for the DL scheme will be discussed in Section 3.3.1, while the derivation of μ_{HL_i} and σ_{HL_i} for the HL scheme will be explained in Section 3.3.2.

3.3.1 Derivations of $\boldsymbol{\mu_{DL_i}}$ and $\boldsymbol{\sigma_{DL_i}}$ for the $\boldsymbol{DL}$ Scheme

Using the idea discussed in Riaz and Abbasi (2016), the i^{th} plotting statistic of the DL scheme, i.e., DL_i, as displayed in Equation (3.1) can also be expressed as

$$DL_i = \lambda \sum_{j=0}^{i-1} (1-\lambda)^j \left[\lambda \sum_{k=0}^{i-j-1} (1-\lambda)^k L_{i-j-k} + (1-\lambda)^{i-j} EL_0\right] + (1-\lambda)^i DL_0. \tag{3.5}$$

Since it is assumed that $EL_0 = DL_0 = 2$, Equation (3.5) can be further expressed as

$$DL_i = \lambda^2 \left[L_i + 2(1-\lambda)L_{i-1} + 3(1-\lambda)^2 L_{i-2} + \cdots + i(1-\lambda)^{i-1} L_1\right] + 2(1+i\lambda)(1-\lambda)^i. \tag{3.6}$$

It is straightforward to show that $\mu_{DL_i} = 2$, as shown below.

(i) $E\left(DL_i|\overrightarrow{X_m}, IC\right) = E\{\lambda^2 [L_i + 2(1-\lambda)L_{i-1} + 3(1-\lambda)^2 L_{i-2} + \cdots + i(1-\lambda)^{i-1} L_1] + 2(1+i\lambda)(1-\lambda)^i |\overrightarrow{X_m}, IC\}$

(ii) $E\left(DL_i|\overrightarrow{X_m}, IC\right) = \lambda^2 [1 + 2(1-\lambda) + 3(1-\lambda)^2 + \cdots + i(1-\lambda)^{i-1}] \upsilon_1 + 2(1+i\lambda)(1-\lambda)^i$

From Equation (A.1) derived in Lemma 1, which is shown in Appendix A, it is obvious that when $r = 1-\lambda$ or equivalent to $1 - r = \lambda$, the equation can be expressed as

(iii) $E\left(DL_i|\overrightarrow{X_m}, IC\right) = \lambda^2 \left[\frac{1-(1-\lambda)^i}{\lambda^2} - \frac{i(1-\lambda)^i}{\lambda}\right] \upsilon_1 + 2(1+i\lambda)(1-\lambda)^i$

(iv) $E\left(DL_i|\overrightarrow{X_m}, IC\right) = [1 - (1-\lambda)^i - i\lambda(1-\lambda)^i] \upsilon_1 + 2(1+i\lambda)(1-\lambda)^i$

(v) $E\left(DL_i|\overrightarrow{X_m}, IC\right) = [1 - (1+i\lambda)(1-\lambda)^i] \upsilon_1 + 2(1+i\lambda)(1-\lambda)^i$

Then, since $\upsilon_1 = E\left(L_i|\overrightarrow{X_m}, IC\right)$, it is reasonable that $E(\upsilon_1|IC) = 2$. Hence,

$$\mu_{DL_i} \tag{3.7}$$

$= E\left[E\left(DL_i|\overrightarrow{X_m}, IC\right)\right] = 2\left[1 - (1 + i\lambda)(1 - \lambda)^i\right] + 2(1 + i\lambda)(1 - \lambda)^i$

$= 2$

On the flip side, the derivation of σ_{DL_i} is slightly more complicated, which can be done as below.

(i) $Var\left(DL_i|\overrightarrow{X_m}, IC\right) = Var\{\lambda^2\left[L_i + 2(1 - \lambda)L_{i-1} + 3(1 - \lambda)^2 L_{i-2} + \cdots + i(1 - \lambda)^{i-1}L_1\right] + 2(1 + i\lambda)(1 - \lambda)^i|\overrightarrow{X_m}, IC\}$

(ii) $Var\left(DL_i|\overrightarrow{X_m}, IC\right) = \lambda^4\left[1 + 2^2(1 - \lambda)^2 + 3^2(1 - \lambda)^4 + \cdots + i^2(1 - \lambda)^{2(i-1)}\right]\upsilon_2$

Then, refers to Equation (A.2) derived in Lemma 2, which is available in Appendix A, it is obtained that $r = 1 - \lambda$, which implies that $1 - r^2 = \lambda(2 - \lambda)$, the equation is now expressed as

(iii) $Var\left(DL_i|\overrightarrow{X_m}, IC\right) = \lambda^4\left\{\frac{2\left[1-(1-\lambda)^{2i}\right]}{[\lambda(2-\lambda)]^3} + \frac{i^2(1-\lambda)^{2(i+1)}+\left(1-2i-i^2\right)(1-\lambda)^{2i}-1}{[\lambda(2-\lambda)]^2}\right\}\upsilon_2$

(iv) $Var\left(DL_i|\overrightarrow{X_m}, IC\right) = \left\{\frac{2\lambda\left[1-(1-\lambda)^{2i}\right]}{(2-\lambda)^3} + \frac{\lambda^2\left[i^2(1-\lambda)^{2(i+1)}+\left(1-2i-i^2\right)(1-\lambda)^{2i}-1\right]}{(2-\lambda)^2}\right\}\upsilon_2$

(v) $\left(\sigma_{DL_i}\right)^2 = E\left[Var\left(DL_i|\overrightarrow{X_m}, IC\right)\right] + Var\left[E\left(DL_i|\overrightarrow{X_m}, IC\right)\right]$

(vi) $\left(\sigma_{DL_i}\right)^2 = \left\{\frac{2\lambda\left[1-(1-\lambda)^{2i}\right]}{(2-\lambda)^3} + \frac{\lambda^2\left[i^2(1-\lambda)^{2(i+1)}+\left(1-2i-i^2\right)(1-\lambda)^{2i}-1\right]}{(2-\lambda)^2}\right\}\xi_2$

$+\left[1 - (1 + i\lambda)(1 - \lambda)^i\right]^2\xi_1$

To this end, σ_{DL_i} is expressed as

$$\sigma_{DL_i} = \sqrt{\left(\sigma_{DL_i}\right)^2}. \tag{3.8}$$

3.3.2 Derivations of $\boldsymbol{\mu_{HL_i}}$ and $\boldsymbol{\sigma_{HL_i}}$ for the $\boldsymbol{HL}$ Scheme

For the derivations of μ_{HL_i} and σ_{HL_i}, it is essential to divide the proof into two cases, i.e., $i = 1$ and $i > 1$. Easily, it can be shown that $\mu_{HL_i} = 2$, i.e.,

1. When $i = 1$,

(i) $E\left(HL_1|\overrightarrow{X_m}, IC\right) = E\left[\lambda L_1 + (1-\lambda)L_0|\overrightarrow{X_m}, IC\right]$

(ii) $E\left(HL_1|\overrightarrow{X_m}, IC\right) = \lambda \upsilon_1 + 2(1-\lambda)$

Then, $\mu_{HL_1} = E\left[E\left(HL_1|\overrightarrow{X_m}, IC\right)\right] = \lambda(2) + 2(1-\lambda) = 2.$

2. When $i > 1$,

(i) $E\left(HL_i|\overrightarrow{X_m}, IC\right) = E\left[\lambda L_i + \left(\frac{1-\lambda}{i-1}\right)(L_{i-1} + L_{i-2} + \cdots + L_1)|\overrightarrow{X_m}, IC\right]$

(ii) $E\left(HL_i|\overrightarrow{X_m}, IC\right) = \lambda \upsilon_1 + \left(\frac{1-\lambda}{i-1}\right)(i-1)\upsilon_1 = \upsilon_1$

Then, $\mu_{HL_i} = E\left[E\left(HL_i|\overrightarrow{X_m}, IC\right)\right] = 2.$

On the other hand, the standard deviation of the HL scheme with time-varying UCL corresponding to the i^{th} test sample can be derived as below.

1. When $i = 1$,

(i) $Var\left(HL_1|\overrightarrow{X_m}, IC\right) = Var\left[\lambda L_1 + (1-\lambda)L_0|\overrightarrow{X_m}, IC\right]$

(ii) $Var\left(HL_1|\overrightarrow{X_m}, IC\right) = \lambda^2 \upsilon_2$

(iii) $\left(\sigma_{HL_1}\right)^2 = E\left[Var\left(HL_1|\overrightarrow{X_m}, IC\right)\right] + Var\left[E\left(HL_1|\overrightarrow{X_m}, IC\right)\right]$

(iv) $\left(\sigma_{HL_1}\right)^2 = \lambda^2\xi_2 + \lambda^2\xi_1 = \lambda^2(\xi_1 + \xi_2)$

Therefore, it is obtained that

$$\sigma_{HL_1} = \sqrt{\lambda^2(\xi_1 + \xi_2)}. \tag{3.9}$$

2. When $i > 1$,

(i) $Var(HL_i|\overrightarrow{X_m}, IC) = Var\left[\lambda L_i + \left(\frac{1-\lambda}{i-1}\right)(L_{i-1} + L_{i-2} + \cdots + L_1)|\overrightarrow{X_m}, IC\right]$

(ii) $Var(HL_i|\overrightarrow{X_m}, IC) = \lambda^2 \upsilon_2 + \left(\frac{1-\lambda}{i-1}\right)^2 (i-1)\upsilon_2$

(iii) $Var(HL_i|\overrightarrow{X_m}, IC) = \left[\lambda^2 + \frac{(1-\lambda)^2}{i-1}\right]\upsilon_2$

(iv) $\left(\sigma_{HL_i}\right)^2 = E\left[Var(HL_i|\overrightarrow{X_m}, IC)\right] + Var\left[E(HL_i|\overrightarrow{X_m}, IC)\right]$

(v) $\left(\sigma_{HL_i}\right)^2 = \left[\lambda^2 + \frac{(1-\lambda)^2}{i-1}\right]\xi_2 + \xi_1$

Thus, it is shown that

$$\sigma_{HL_i} = \sqrt{\left[\lambda^2 + \frac{(1-\lambda)^2}{i-1}\right]\xi_2 + \xi_1}. \tag{3.10}$$

To this end, it is summarised that

$$\sigma_{HL_i} = \begin{cases} \sqrt{\lambda^2(\xi_1 + \xi_2)} & \text{if } i = 1 \\ \sqrt{\left[\lambda^2 + \frac{(1-\lambda)^2}{i-1}\right]\xi_2 + \xi_1} & \text{if } i > 1 \end{cases}. \tag{3.11}$$

3.4 Determination of UCLs

One may notice that in order to obtain the time-varying UCLs for the memory-type EL, DL, and HL schemes, it is of utmost importance to have the values of ξ_1 and ξ_2. Since ξ_1 and ξ_2 depend on the Phase-I reference sample, $\overrightarrow{X_m}$, then it is hard to obtain their exact forms. To this end, the Monte-Carlo simulation can be employed to estimate the values of ξ_1 and ξ_2 for some selected pairs of (m, n).

Then, the time-varying UCLs for EL, DL, and HL schemes, i.e., $\Psi_{EL}(i)$, $\Psi_{DL}(i)$, and $\Psi_{HL}(i)$ are now depending on the value of the charting constants, L_{EL}, L_{DL}, and L_{HL}, respectively. To this end, all the charting constants L_{EL}, L_{DL}, and L_{HL} (time-varying UCLs) and Ψ_{SL}, Ψ_{EL}, Ψ_{DL}, and Ψ_{HL} (steady-state UCLs) are determined by using a standard searching algorithm under a targeted ARL_0 through Monte-Carlo simulation. The standard searching algorithm is described below.

Step I. A reference sample with size m, $\overrightarrow{X_m} = \{X_1, X_2, X_3, \ldots, X_m\}$ is simulated from a standard normal distribution.

Step II. Then, the i^{th} test sample with size n, $\overrightarrow{Y_{ni}} = \{Y_{1i}, Y_{2i}, Y_{3i}, \ldots, Y_{ni}\}$ is also simulated from a standard normal distribution.

Step III. All the i^{th} plotting statistics are then computed, and compared with the trial UCL inputted.

Step IV.
- i. If the ARL_0 obtained at the end of the simulation is nearly the same as the nominal value, then the trial UCL is the desired UCL.
- ii. If the ARL_0 obtained at the end of the simulation is less than the nominal value, repeat the steps with a larger value of trial UCL.
- iii. If the ARL_0 obtained at the end of the simulation is more than the nominal value, repeat the steps with a smaller value of trial UCL.

It is worth mentioning that it is not compulsory to use a standard normal distribution, but other continuous statistical probability distributions can also be used. This is because the schemes studied here are distribution-free, so all the continuous distributions would output almost the same IC result. Again, the rationale of employing the Monte-Carlo simulation here is because there is no closed-form expression for the RL distribution of the schemes. Further, it is not suitable to use the asymptotic theory in SPM due to the size of the test sample, n is habitually small.

3.5 RL Metrics for Performance Evaluation of A Scheme

The most commonly used RL metric in evaluating the performance of a scheme is ARL. For instance, when the process is IC, the desired ARL_0 should be large so that the FAR is reduced. On the flip side, if the process is OOC, the ARL_1 should be small so that the OOC signal can be detected hastily (Montgomery, 2019). However, it is known that the RL distribution of a control scheme is not symmetric, but it is highly positively (right) skewed, such that the distribution of RL has a long tail on the right side. Therefore, it is inconvincible that interpretation solely based on the ARL is sufficient to measure the performance of a control scheme. To this end, other RL properties, such as the $SDRL$, and percentiles of the RL, such as 5^{th}, 25^{th}, 50^{th}, 75^{th}, and 95^{th} percentiles are also utilised to evaluate the performance of a control scheme.

As discussed in Section 3.4, it is hard to obtain the exact- or closed-form expressions of all the RL metrics of the schemes. Hence, all the RL metrics will only be obtained from the Monte-Carlo simulation study. Further, all these RL metrics are only meaningful if the exact shift size of the parameter(s) in the process is known. Nevertheless, the exact shift size is commonly unknown in real life applications. To this end, a scheme with better overall performance, i.e., the scheme performs well within a specific predefined range of shift sizes, is more fancied by quality practitioners.

Ryu et al. (2010) employed the expected weighted RL ($EWRL$), which is an index used to evaluate the overall performance of a scheme. Among the various expressions of the $EWRL$ index, the expected ARL, termed as $EARL$ is the most straightforward index, which leads to the vast usage of $EARL$. Recently, Mukherjee and Marozzi (2017a), Mukherjee and Sen (2018), and Song et al. (2020a) considered this index to assess the performance of the control schemes proposed. For instance, when a scheme is only used to monitor a single parameter, says the location parameter θ, then the $EARL$ of a scheme when the possible shift in the location considered $[\theta_{\min}, \theta_{\max}]$ is defined as

$$EARL = \frac{1}{\theta_{\max} - \theta_{\min}} \int_{\theta_{\min}}^{\theta_{\max}} ARL(\theta)\ d\theta. \tag{3.12}$$

Then, extending the idea of $EARL$ to a two-parameter joint monitoring scheme. The $EARL$ of a scheme when the possible location-scale parameters shift considered is $[\theta_{\min}, \theta_{\max}] \times [\delta_{\min}, \delta_{\max}]$, will be defined as

$$EARL = \frac{1}{(\theta_{\max} - \theta_{\min})(\delta_{\max} - \delta_{\min})} \int_{\delta_{\min}}^{\delta_{\max}} \int_{\theta_{\min}}^{\theta_{\max}} ARL(\theta, \delta)\ d\theta\ d\delta. \tag{3.13}$$

CHAPTER 4

RESULTS AND DISCUSSION

4.1 Introduction

This chapter firstly present the charting constants for all the Lepage-type schemes studied here, i.e., the SL, EL, DL, and HL schemes under some chosen m, n, λ, and ARL_0. Also, the IC performance comparison among all the schemes is then studied. Some of the RL metrics used are ARL_0, $SDRL_0$, and IC-percentiles of the RL. Further, the FAR of all the schemes is also determined by assessing the IC-percentiles of the RL. Next, Sections 4.3 and 4.4 reveal the OOC performance comparison among all the schemes at the micro and macro levels, respectively. Three probability distributions are considered here, namely the Normal, Laplace, and Shifted Exponential distributions. Note that ARL_1, $SDRL_1$, and $EARL$ are employed to evaluate the performance of each scheme in the OOC case. Lastly, an illustrative example using a real dataset regarding the online shoppers' intention is given in Section 4.5.

4.2 IC Performance Analysis of the SL, EL, DL, and HL Schemes

Note that as in Song et al. (2020a), the essential parameters for the NSPM-type schemes considered in this dissertation are $m \in \{100, 300, 500\}$, $n \in \{5, 10, 15\}$, and the smoothing parameter for the memory-type EL, DL, and

HL schemes is $\lambda \in \{0.05, 0.10, 0.20\}$. Before employing any control scheme, it is of utmost importance to obtain the control limits first, where it is the UCL here. The UCLs for all the schemes are obtained through the Monte-Carlo simulation with 50,000 replicates and a winsorisation limit of 5,000, as employed by Mukherjee and Marozzi (2017b), such that the nominal value of ARL_0 is approximately equal to some standard values, i.e., 250, 370, and 500. The two important components in the time-varying UCLs, i.e., ξ_1 and ξ_2 for nine pairs of (m, n) are estimated from the Monte-Carlo simulation of 25,000 replicates, then tabulated in Table 4.1.

Table 4.1: The Estimated Values of ξ_1 and ξ_2 for Some Selected (m, n)

m	n	ξ_1	ξ_2
	5	0.02665	3.5257
100	10	0.04685	3.6909
	15	0.07875	3.7288
	5	0.00755	3.5758
300	10	0.01052	3.7673
	15	0.01474	3.8306
	5	0.00447	3.5867
500	10	0.00553	3.7811
	15	0.00719	3.8482

Mukherjee (2017) argued that using the large sample theory, ξ_1 and ξ_2 are approximately 0 and 4, respectively. From Table 4.1, one may notice that the estimation of ξ_1 and ξ_2 are reasonably accurate because when the value of m and/or n increases, the estimated values of ξ_1 and ξ_2 appear to be converging to the estimated values with the large sample theory. However, due to the natural selection of the small sample size in industrial applications, the asymptotic theory is not effectively applicable in SPM. Therefore, it is more accurate and appropriate to use the estimations of ξ_1 and ξ_2 as displayed in Table 4.1.

4.2.1 The Charting Constants

The charting constants L_{EL}, L_{DL}, and L_{HL} for the time-varying UCLs of the EL, DL, and HL schemes, respectively, when $ARL_0 \approx 250$, for different triplets (m, n, λ) are juxtaposed in Table 4.2. On the other hand, the charting constants for the steady-state UCLs of the EL, DL, and HL schemes, i.e., Ψ_{EL}, Ψ_{DL}, and Ψ_{HL}, respectively, for the same (m, n, λ), when $ARL_0 \approx 250$ are tabulated in Table 4.3. Besides, Ψ_{SL}, i.e., the charting constant for the SL scheme with the steady-state UCL, for the same pairs of (m, n) is also included in Table 4.3.

Then, when $ARL_0 \approx 370$, the charting constants for the schemes with time-varying and steady-state UCLs are, respectively, tabulated in Tables 4.4 and 4.5. Lastly, Tables 4.6 and 4.7 presents the charting constants of the schemes with time-varying and steady-state UCLs, respectively, when $ARL_0 \approx 500$.

Table 4.2: The Charting Constants of Various Schemes with Time-Varying UCLs when $ARL_0 \approx 250$

m	n	EL (L_{EL})			DL (L_{DL})			HL (L_{HL})		
		λ			λ			λ		
		0.05	0.10	0.20	0.05	0.10	0.20	0.05	0.10	0.20
100	5	1.585	2.180	2.811	0.701	1.249	1.876	1.211	2.395	3.451
	10	1.407	2.022	2.682	0.545	1.094	1.751	0.902	2.004	3.134
	15	1.167	1.811	2.515	0.369	0.897	1.557	0.612	1.617	2.818
300	5	1.982	2.505	3.084	1.093	1.589	2.153	1.973	3.129	3.959
	10	1.946	2.466	3.042	1.047	1.559	2.125	1.837	2.979	3.841
	15	1.886	2.425	3.007	0.980	1.504	2.090	1.686	2.835	3.737
500	5	2.071	2.567	3.145	1.179	1.665	2.211	2.163	3.285	4.071
	10	2.051	2.549	3.112	1.166	1.654	2.197	2.081	3.183	3.966
	15	2.031	2.533	3.092	1.139	1.629	2.183	2.011	3.112	3.921

Table 4.3: The Charting Constants of Various Schemes with Steady-State UCLs when $ARL_0 \approx 250$

m	n	EL (Ψ_{EL})			DL (Ψ_{DL})			HL (Ψ_{HL})			SL (Ψ_{SL})
		λ			λ			λ			
		0.05	0.10	0.20	0.05	0.10	0.20	0.05	0.10	0.20	
100	5	2.512	2.984	3.809	2.141	2.400	2.866	2.335	2.755	3.548	9.999
	10	2.492	2.971	3.798	2.115	2.375	2.855	2.293	2.711	3.513	9.910
	15	2.445	2.922	3.751	2.076	2.331	2.807	2.236	2.651	3.453	9.818
300	5	2.600	3.089	3.952	2.213	2.480	2.962	2.433	2.871	3.705	10.504
	10	2.608	3.110	3.981	2.214	2.486	2.980	2.425	2.869	3.715	10.527
	15	2.604	3.107	3.981	2.205	2.483	2.979	2.415	2.856	3.694	10.481
500	5	2.617	3.114	3.987	2.228	2.495	2.985	2.459	2.898	3.739	10.608
	10	2.632	3.134	4.020	2.232	2.506	3.004	2.457	2.901	3.752	10.673
	15	2.634	3.142	4.029	2.231	2.509	3.012	2.449	2.895	3.748	10.662

Table 4.4: The Charting Constants of Various Schemes with Time-Varying UCLs when $ARL_0 \approx 370$

m	n	EL (L_{EL})			DL (L_{DL})			HL (L_{HL})		
		λ			λ			λ		
		0.05	0.10	0.20	0.05	0.10	0.20	0.05	0.10	0.20
100	5	1.779	2.394	3.067	0.869	1.438	2.087	1.451	2.743	3.836
	10	1.584	2.226	2.917	0.695	1.265	1.943	1.088	2.287	3.489
	15	1.329	2.001	2.738	0.499	1.047	1.738	0.763	1.840	3.116
300	5	2.211	2.754	3.377	1.292	1.810	2.392	2.368	3.616	4.426
	10	2.169	2.711	3.318	1.247	1.769	2.355	2.194	3.441	4.286
	15	2.100	2.661	3.269	1.171	1.710	2.313	1.991	3.256	4.161
500	5	2.307	2.829	3.442	1.395	1.892	2.449	2.619	3.818	4.547
	10	2.285	2.803	3.399	1.377	1.874	2.435	2.515	3.703	4.449
	15	2.261	2.786	3.374	1.345	1.851	2.415	2.407	3.602	4.359

Table 4.5: The Charting Constants of Various Schemes with Steady-State UCLs when $ARL_0 \approx 370$

m	n	EL (Ψ_{EL})			DL (Ψ_{DL})			HL (Ψ_{HL})			SL (Ψ_{SL})
		λ			λ			λ			
		0.05	0.10	0.20	0.05	0.10	0.20	0.05	0.10	0.20	
100	5	2.584	3.089	3.976	2.192	2.470	2.969	2.391	2.835	3.689	10.678
	10	2.562	3.075	3.963	2.166	2.449	2.959	2.349	2.789	3.652	10.603
	15	2.515	3.026	3.912	2.121	2.401	2.909	2.294	2.730	3.585	10.455
300	5	2.677	3.205	4.139	2.269	2.556	3.076	2.485	2.956	3.863	11.275
	10	2.688	3.224	4.165	2.270	2.564	3.095	2.475	2.953	3.869	11.308
	15	2.683	3.223	4.162	2.262	2.558	3.093	2.465	2.936	3.847	11.230
500	5	2.696	3.230	4.177	2.285	2.574	3.099	2.509	2.983	3.901	11.399
	10	2.712	3.253	4.210	2.290	2.586	3.121	2.506	2.985	3.915	11.477
	15	2.715	3.262	4.217	2.289	2.589	3.130	2.499	2.977	3.903	11.434

Table 4.6: The Charting Constants of Various Schemes with Time-Varying UCLs when $ARL_0 \approx 500$

m	n	EL (L_{EL})			DL (L_{DL})			HL (L_{HL})		
		λ			λ			λ		
		0.05	0.10	0.20	0.05	0.10	0.20	0.05	0.10	0.20
100	5	1.945	2.582	3.278	1.011	1.588	2.255	1.652	3.031	4.158
	10	1.729	2.393	3.112	0.818	1.407	2.097	1.249	2.518	3.758
	15	1.462	2.159	2.918	0.608	1.169	1.882	0.897	2.028	3.358
300	5	2.387	2.947	3.602	1.445	1.976	2.573	2.684	4.004	4.791
	10	2.344	2.901	3.533	1.398	1.935	2.530	2.473	3.796	4.628
	15	2.272	2.853	3.492	1.317	1.869	2.485	2.248	3.599	4.502
500	5	2.487	3.026	3.671	1.565	2.066	2.636	2.988	4.233	4.919
	10	2.464	2.997	3.615	1.541	2.047	2.617	2.863	4.098	4.802
	15	2.435	2.971	3.591	1.503	2.021	2.596	2.723	3.981	4.708

Table 4.7: The Charting Constants of Various Schemes with Steady-State UCLs when $ARL_0 \approx 500$

m	n	EL (Ψ_{EL})			DL (Ψ_{DL})			HL (Ψ_{HL})			SL (Ψ_{SL})
		λ			λ			λ			
		0.05	0.10	0.20	0.05	0.10	0.20	0.05	0.10	0.20	
100	5	2.642	3.172	4.113	2.234	2.527	3.057	2.436	2.901	3.810	11.247
	10	2.620	3.158	4.093	2.208	2.508	3.042	2.392	2.853	3.764	11.106
	15	2.573	3.109	4.038	2.162	2.457	2.993	2.341	2.792	3.689	10.947
300	5	2.735	3.294	4.281	2.311	2.614	3.162	2.525	3.022	3.988	11.889
	10	2.747	3.315	4.307	2.313	2.624	3.185	2.519	3.019	3.985	11.915
	15	2.741	3.311	4.308	2.303	2.618	3.183	2.504	2.999	3.966	11.824
500	5	2.757	3.321	4.321	2.328	2.634	3.184	2.548	3.048	4.027	12.040
	10	2.773	3.345	4.355	2.335	2.648	3.210	2.546	3.051	4.038	12.098
	15	2.775	3.350	4.360	2.333	2.649	3.218	2.538	3.043	4.023	12.048

4.2.2 IC Performance Comparative Study

For brevity, the IC performance of all the schemes are studied and compared by only considering $ARL_0 \approx 500$. By using the charting constants tabulated in Tables 4.6 and 4.7, the obtained ARL_0, $SDRL_0$, and IC-RL percentiles (5^{th}, 25^{th}, 50^{th}, 75^{th}, and 95^{th}) from the Monte-Carlo simulation are tabulated in Tables 4.8, 4.9, and 4.10, respectively, when $\lambda = 0.05$, $\lambda = 0.10$, and $\lambda = 0.20$. Due to the space constraints, the time-varying and steady-state UCLs, are abbreviated as TV UCL and SS UCL, respectively. Note that each cell contains ARL_0, $SDRL_0$ in a bracket, and followed by the five IC percentiles of the RL.

Table 4.8: The IC Performance of Various Schemes when $ARL_0 \approx 500$ and $\lambda = 0.05$ for the Memory-Type Schemes

m	n	Memory-Type Schemes ($\lambda = 0.05$)						SL (SS UCL)
		EL		DL		HL		
		TV UCL	SS UCL	TV UCL	SS UCL	TV UCL	SS UCL	
100	5	499.06 (899.70) 2,33,160, 517,2293	505.15 (853.38) 15,70,198, 531,2119	502.14 (1013.94) 1,9,107, 448,2724	501.67 (899.61) 20,63,175, 483,2246	498.37 (936.46) 1,31,156, 483,2362	496.35 (1198.58) 2,2,6, 229,4195	503.62 (670.35) 18,104,271, 629,1771
	10	500.08 (944.82) 1,19,131, 496,2462	500.91 (875.39) 12,57,176, 513,2216	499.70 (1051.99) 1,4,72, 408,2959	500.38 (934.48) 16,49,151, 464,2391	500.82 (1048.52) 1,8,87, 415,2942	501.68 (1232.86) 2,2,6, 186,4730	499.57 (667.38) 17,99,266, 624,1786
	15	499.96 (1004.00) 1,10,94, 448,2748	502.27 (923.55) 10,44,151, 486,2381	500.51 (1121.42) 1,2,37, 346,3444	500.46 (992.70) 12,35,118, 431,2677	502.09 (1143.16) 1,4,38, 316,3652	503.50 (1266.65) 2,2,5, 135,5000	499.16 (684.73) 15,94,258, 620,1797
300	5	499.87 (704.01) 3,79,256, 629,1834	496.38 (640.82) 23,110,277, 625,1705	498.36 (781.34) 1,43,218, 603,1991	499.42 (684.45) 30,107,266, 604,1774	499.79 (581.50) 7,153,326, 633,1537	502.84 (1081.38) 2,2,8, 411,3107	503.69 (570.81) 23,129,319, 669,1606
	10	500.97 (709.74) 2,73,253, 626,1876	501.14 (661.11) 23,106,274, 624,1752	498.55 (791.87) 1,37,207, 599,2052	499.55 (693.97) 29,102,258, 602,1790	499.30 (623.61) 4,129,308, 627,1641	504.78 (1098.80) 2,2,8, 394,3182	499.63 (565.50) 22,126,315, 664,1607
	15	502.18 (737.20) 2,65,239, 622,1918	498.35 (672.45) 21,98,262, 622,1783	498.67 (822.93) 1,27,187, 581,2126	499.31 (710.06) 27,95,249, 594,1822	502.27 (698.56) 3,100,274, 616,1785	502.58 (1125.66) 2,2,7, 337,3401	499.66 (567.74) 22,123,311, 667,1619
500	5	498.59 (636.11) 3,92,285, 656,1717	500.27 (595.49) 26,123,303, 647,1629	502.04 (714.80) 1,59,254, 641,1865	499.63 (610.83) 34,124,295, 631,1657	499.21 (480.05) 26,192,368, 651,1391	498.99 (1028.47) 2,2,9, 477,2828	498.70 (538.41) 24,133,328, 674,1546
	10	499.07 (641.30) 3,89,281, 655,1741	502.34 (600.04) 26,121,301 651,1654	500.71 (715.43) 1,53,247, 645,1902	500.89 (611.85) 34,121,293, 639,1680	498.68 (499.07) 15,180,359, 653,1430	499.18 (1043.59) 2,2,9, 455,2895	500.71 (545.47) 23,132,327, 676,1560
	15	501.81 (660.11) 3,86,277, 656,1765	500.90 (610.40) 25,117,295, 649,1668	498.33 (729.64) 1,47,236, 636,1904	500.75 (623.70) 32,116,286, 634,1712	500.38 (528.10) 8,164,346, 658,1487	500.44 (1065.78) 2,2,8, 428,3027	501.70 (555.54) 22,130,322, 675,1586

Table 4.9: The IC Performance of Various Schemes when $ARL_0 \approx 500$ and $\lambda = 0.10$ for the Memory-Type Schemes

m	n	Memory-Type Schemes ($\lambda = 0.10$)						SL (SS UCL)
		EL		DL		HL		
		TV UCL	SS UCL	TV UCL	SS UCL	TV UCL	SS UCL	
100	5	498.64 (795.55) 4,64,212, 570,2008	498.80 (771.88) 16,79,223, 564,1961	499.01 (884.60) 1,40,172, 526,2227	499.66 (830.08) 18,74,203, 527,2079	498.01 (726.58) 18,107,253, 568,1828	504.52 (1010.85) 2,3,72, 482,2753	503.62 (670.35) 18,104,271, 629,1771
	10	499.47 (833.67) 2,50,189, 553,2115	499.49 (796.47) 13,69,209, 557,2028	502.12 (926.23) 1,26,146, 510,2398	504.00 (867.43) 16,62,185, 521,2197	500.92 (805.22) 4,76,214, 551,2008	498.89 (1036.01) 2,3,51, 440,2865	499.57 (667.38) 17,99,266, 624,1786
	15	502.93 (887.12) 2,37,166, 531,2289	500.90 (849.62) 11,57,183, 535,2152	498.67 (978.62) 1,12,108, 470,2596	499.69 (901.13) 13,50,157, 493,2313	499.32 (889.44) 2,45,166, 514,2258	504.02 (1079.43) 2,3,39, 400,3113	499.16 (684.73) 15,94,258, 620,1797
300	5	500.49 (643.14) 8,103,283, 646,1714	501.64 (625.87) 24,116,292, 638,1694	499.44 (688.18) 2,83,264, 632,1793	500.49 (644.55) 27,113,281, 626,1713	500.45 (508.68) 60,180,348, 641,1440	498.11 (847.27) 2,3,140, 614,2200	503.69 (570.81) 23,129,319, 669,1606
	10	500.46 (644.32) 7,100,280, 643,1746	502.73 (629.31) 21,113,287, 640,1722	499.87 (699.02) 1,77,256, 631,1876	500.55 (650.85) 26,109,278, 621,1750	499.42 (529.68) 52,169,338, 637,1488	502.85 (875.91) 2,3,125, 605,2316	499.63 (565.50) 22,126,315, 664,1607
	15	499.00 (661.86) 6,93,271, 640,1776	499.75 (644.23) 21,106,279, 634,1739	499.66 (722.54) 1,68,241, 619,1915	504.07 (675.06) 25,104,268, 623,1774	501.62 (565.07) 43,156,324, 633,1574	501.43 (893.15) 2,3,110, 587,2360	499.66 (567.74) 22,123,311, 667,1619
500	5	498.86 (591.19) 9,113,304, 665,1636	502.23 (576.60) 25,128,314, 663,1606	501.86 (642.72) 2,96,287, 656,1723	499.92 (582.95) 30,128,308, 648,1623	502.38 (460.92) 69,199,369, 654,1379	499.82 (800.44) 2,3,160, 659,2100	498.70 (538.41) 24,133,328, 674,1546
	10	498.29 (591.66) 9,111,301, 665,1649	500.40 (575.47) 25,124,309, 662,1623	501.80 (646.52) 2,90,282, 658,1756	501.76 (587.02) 30,126,305, 652,1641	499.69 (469.00) 66,193,363, 650,1387	501.69 (830.43) 2,3,147, 642,2197	500.71 (545.47) 23,132,327, 676,1560
	15	499.38 (603.16) 9,109,298, 663,1667	499.21 (581.16) 24,123,306, 658,1623	498.12 (652.00) 2,86,277, 648,1750	501.78 (601.49) 28,122,298, 653,1657	502.16 (480.51) 62,187,359, 655,1420	499.38 (834.58) 2,3,139, 639,2197	501.70 (555.54) 22,130,322, 675,1586

Table 4.10: The IC Performance of Various Schemes when $ARL_0 \approx 500$ and $\lambda = 0.20$ for the Memory-Type Schemes

m	n	Memory-Type Schemes ($\lambda = 0.20$)						SL (SS UCL)
		EL		DL		HL		
		TV UCL	SS UCL	TV UCL	SS UCL	TV UCL	SS UCL	
100	5	499.44 (731.46) 9,84,242, 596,1882	500.27 (723.02) 16,90,247, 596,1861	501.50 (793.33) 3,69,215, 573,2006	501.54 (764.68) 17,83,228, 577,1927	501.26 (678.37) 32,116,270, 598,1771	501.52 (816.19) 2,39,199, 584,2120	503.62 (670.35) 18,104,271, 629,1771
	10	501.54 (762.24) 8,74,228, 585,1954	498.96 (747.45) 14,79,232, 582,1923	500.50 (816.79) 2,56,197, 565,2098	501.81 (793.35) 15,73,215, 563,2006	499.38 (711.47) 23,100,250, 589,1831	502.57 (846.74) 2,27,175, 574,2192	499.57 (667.38) 17,99,266, 624,1786
	15	500.57 (791.06) 5,62,209, 576,2024	499.07 (777.42) 11,69,214, 573,1982	498.28 (860.97) 1,41,167, 541,2191	498.00 (829.00) 12,60,190, 538,2124	499.24 (749.99) 16,84,228, 578,1946	499.08 (873.74) 2,21,155, 548,2283	499.16 (684.73) 15,94,258, 620,1797
300	5	502.42 (604.68) 16,116,302, 659,1648	498.79 (591.58) 22,121,303, 653,1618	500.28 (632.85) 8,105,290, 650,1689	497.23 (607.88) 24,118,294, 636,1661	499.78 (534.35) 46,157,331, 650,1519	500.40 (679.78) 2,65,265, 662,1816	503.69 (570.81) 23,129,319, 669,1606
	10	501.47 (608.80) 15,113,298, 654,1674	500.17 (599.43) 21,118,300, 649,1657	501.74 (645.85) 6,100,281, 648,1757	500.44 (613.07) 23,117,295, 645,1669	499.17 (545.35) 43,149,326, 649,1547	498.74 (690.67) 2,56,253, 656,1854	499.63 (565.50) 22,126,315, 664,1607
	15	500.74 (620.36) 14,108,291, 651,1712	498.54 (608.60) 21,113,293, 646,1687	500.52 (655.13) 5,94,275, 644,1768	499.29 (629.42) 22,111,285, 638,1717	500.12 (563.78) 41,145,318, 641,1587	498.49 (703.85) 2,53,243, 653,1886	499.66 (567.74) 22,123,311, 667,1619
500	5	502.14 (568.19) 17,124,317, 672,1617	500.27 (559.22) 24,129,318, 666,1594	498.15 (590.72) 9,113,306, 664,1646	500.74 (572.68) 27,128,313, 659,1619	500.48 (502.55) 49,167,346, 661,1471	499.44 (627.22) 2,74,287, 682,1730	498.70 (538.41) 24,133,328, 674,1546
	10	498.32 (567.99) 18,123,312, 666,1606	502.18 (564.67) 24,128,317, 670,1608	502.54 (601.82) 8,112,303, 669,1665	499.93 (567.92) 26,127,311, 665,1602	499.31 (508.34) 48,162,342, 658,1473	499.18 (651.30) 2,65,275, 675,1787	500.71 (545.47) 23,132,327, 676,1560
	15	500.28 (572.52) 16,122,312, 672,1609	499.19 (563.07) 23,127,314, 669,1590	499.43 (603.94) 7,108,300, 661,1671	501.46 (574.62) 25,126,312, 667,1617	499.64 (514.14) 47,159,338, 659,1493	500.50 (663.67) 2,62,268, 674,1813	501.70 (555.54) 22,130,322, 675,1586

The first inception that can be made from Tables 4.8 – 4.10 is the IC RL distributions of all the schemes are positively skewed. One may easily observe that the RL distribution of all the schemes has a long right tail. On top of that, the ARL_0 value is higher than the 50^{th} percentile (median) of the RL. Further, the difference between the 75^{th} and 50^{th} percentiles is bigger than that of the 50^{th} and 25^{th} percentiles. All these indications suggest that it is insufficient to study the IC performance of all the schemes purely based on ARL_0 due to the

RL distribution is asymmetric. To this end, it is also vital to evaluate other IC RL metrics, such as $SDRL_0$ and IC percentiles.

4.2.2.1 IC Performance of the EL and DL Schemes

Refers to Tables 4.8 – 4.10, one can see that the IC performance of the EL scheme with the steady-state UCL is slightly better than its counterpart with the time-varying UCL. By evaluating the 5^{th} and 25^{th} of the IC percentiles of the RL distributions, it is noticed that the scheme is apparently weaker if the time-varying UCL is considered. This is because the 5^{th} and 25^{th} of the IC percentiles of the scheme with the time-varying UCL are lower than those of the steady-state UCL, which indicates the EL scheme with the time-varying UCL has a higher FAR at the early monitoring stage. The same conclusion can also be made for the DL scheme.

However, if one ignores the performance of the 5^{th} and 25^{th} percentiles, the performance of the time-varying and steady-state UCLs for these two schemes are almost the same. For instance, the ARL_0 is located between the 50^{th} and 75^{th} percentiles for these two schemes, regardless of the types of UCLs, with some exceptions. These include $(m, n, \lambda) = (100, 15, 0.05)$ for the EL scheme and additionally $(100, 10, 0.05)$ for the EL scheme with the time-varying UCL. On the flip side, the exception for the DL schemes are $(m, \lambda) = (100, 0.05)$ and $(m, n, \lambda) = (100, 15, 0.10)$. Note that the ARL_0 is located between the 75^{th} and 95^{th} percentiles for all these exceptions.

Besides, regardless of the types of UCL, when the value of m increases, most of the percentiles of these two schemes also increase, except the 95^{th} percentile, which has a negative relationship with m. However, the effect of m on the 5^{th} percentile of these two schemes with time-varying UCLs is minimal. This is because the 5^{th} percentile remains almost constant when $\lambda = 0.05$ for the two schemes with the time-varying UCLs, and additionally $\lambda = 0.10$ for the DL scheme with the time-varying UCL. Further, the $SDRL_0$ decreases as m increases.

When the value of λ increases, one may notice almost the same pattern as m increases. On the contrary, the increment in n yields a totally contradicting effect as the increment in m or λ. For example, as n increases, all the percentiles decrease, except the 95^{th} percentile and $SDRL_0$.

To this end, the IC performance of these two schemes can be improved if one uses a larger m and λ, but with a smaller n. Both time-varying and steady-state UCLs of these two schemes are acceptably employable. However, comparatively, it will be much better to use these schemes with steady-state UCLs due to the lower early FAR than their time-varying UCLs counterparts.

4.2.2.2 IC Performance of the HL Scheme

The HL scheme displays an opposite pattern compared to the EL and DL schemes, as observed in Tables 4.8 – 4.10. This is because the HL scheme with the time-varying UCL has a better IC performance than its counterpart with the steady-state UCL. Notably, the 5^{th} and 25^{th} percentiles of the scheme with the steady-state UCL are significantly lower than that of the time-varying UCL, except $(m, \lambda) = (100, 0.05)$. It is worth mentioning that the 5^{th} percentile of the HL scheme with the steady-state UCL is fixed at 2, for every (m, n, λ).

Further, the 25^{th} percentile of the HL scheme with the steady-state UCL when $\lambda = 0.05$ and $\lambda = 0.10$ are very unsatisfactory, i.e., 2 and 3, respectively. This indicates the scheme with the steady-state UCL has a high tendency of signalling a false alarm at the beginning of process monitoring, i.e., by the 3^{rd} test sample, in 25% of the time. However, when $\lambda = 0.20$, the 25^{th} percentile of the HL scheme with the steady-state UCL is more acceptable. In addition, the 50^{th} percentile of the RL when $\lambda = 0.05$ is very unsatisfactory, i.e., less than 10. Nevertheless, the value of 50^{th} percentile appears to improve as the value of λ increases.

In general, the ARL_0 is located between the 50^{th} and 75^{th} percentiles for the HL scheme with the time-varying UCL, except $(m, \lambda) = (100, 0.05)$. Comparatively, the ARL_0 of the HL scheme with the steady-state UCL is located between the 75^{th} and 95^{th} percentiles when $\lambda = 0.05$, which indicates that the RL distribution is extremely right-skewed. However, when $\lambda \geq 0.10$, the ARL_0 is situated between the 50^{th} and 75^{th} percentiles, except $(m, \lambda) = (100, 0.10)$. As usual, the IC percentiles, except 95^{th} percentile of the HL scheme, tend to increase as m or λ increases. The opposite trend is observed for the IC percentiles and $SDRL_0$ as n changing. On the flip side, when m or λ decreases, the 95^{th} percentile and $SDRL_0$ tend to increase.

To this end, one can conclude that the HL scheme with the time-varying UCL is a better choice. This is because the HL scheme with the steady-state UCL has a very high probability of giving false alarms at the early stage of monitoring, especially $\lambda = 0.05$. However, the IC performance of the HL scheme with the steady-state UCL gets better as the value of λ increases. Therefore, in order to employ HL scheme with the steady-state UCL, it is better to choose $\lambda \geq 0.20$.

4.2.2.3 IC Performance of the SL Scheme

The IC performance of the SL scheme is almost the same as that of the EL and DL schemes with steady-state UCLs. Refers to Tables 4.8 – 4.10, one can see that the ARL_0 is positioned between the 50^{th} and 75^{th} percentiles. Similarly, in order to have a better IC performance, one should use a larger m and a smaller n when employing the SL scheme.

4.2.2.4 Summary

Some of the remarks on the IC performance of all the schemes are listed down below.

1. When the EL or DL scheme is used to monitor a process, both time-varying and steady-state UCLs are acceptable. However, the scheme with the steady-state UCL is preferable due to the two facts below.
    i. The IC performance of the scheme with the steady-state UCL is comparatively better than its time-varying UCL counterpart.

ii. It is easier to implement the scheme with a steady-state UCL.

2. When the HL scheme is used for process monitoring, the time-varying UCL is preferable due to its lower early FAR. However, if one wishes to use the HL scheme with the steady-state UCL due to easier implementation, it is suggestible that one should choose $\lambda \geq 0.20$.
3. A larger value of m and a smaller value of n is preferable to implement all of the SL, EL, DL, or HL schemes.

4.3 $\boldsymbol{OOC}$ Performance Analysis of the $\boldsymbol{SL}$, $\boldsymbol{EL}$, $\boldsymbol{DL}$, and $\boldsymbol{HL}$ Schemes at Micro Level

Again, the Monte-Carlo simulation is employed to evaluate the OOC performance of each scheme, but with 25,000 replicates and a winsorisation limit of 5,000. Note that ARL_1 and $SDRL_1$ are used to compare the OOC RL properties of various schemes. There are three famous probability distributions considered in this dissertation, where two of them follow symmetric distribution, and the other follows an asymmetric distribution. The distributions considered are

1. Symmetric thin-tailed Normal distribution with a probability density function (PDF) of $f(x) = \frac{1}{\delta\sqrt{2\pi}} \exp\left[-\frac{(x-\theta)^2}{2\delta^2}\right]$, $x \in (-\infty, \infty)$, where θ and δ are the location and scale parameters, respectively.
2. Symmetric heavy-tailed Laplace distribution with a PDF of $f(x) = \frac{1}{2\delta} \exp\left[-\frac{|x-\theta|}{\delta}\right]$, $x \in (-\infty, \infty)$.
3. Asymmetric Shifted Exponential distribution with a PDF of $f(x) = \frac{1}{\delta} \exp\left(\frac{x-\theta}{\delta}\right)$, $x \in [\theta, \infty)$.

In the simulation study, $\overrightarrow{X_m}$ is simulated from the corresponding distribution under the setting of $\theta = 0$ and $\delta = 1$. Then, there are a total of 34 OOC cases considered for comparison, such that $\overrightarrow{Y_{ni}}$ is simulated from the same distribution with $\theta \in \{0, 0.1, 0.25, 0.5, 1, 1.5, 2\}$ and $\delta \in \{1, 1.25, 1.5, 1.75, 2\}$. In this dissertation, the OOC performance of all the schemes are studied and compared under the setting of $(m, n) = (100, 5)$ and $ARL_0 \approx 500$.

For each shift size, the corresponding ARL_1 and $SDRL_1$ for the Normal, Laplace, and Shifted Exponential distributions are reported in Tables 4.11 – 4.13, 4.14 – 4.16, and 4.17 – 4.19, respectively. As discussed previously, the early FAR of the HL scheme with the steady-state UCL is very high if $\lambda < 0.20$. Therefore, when $\lambda = 0.05$ and $\lambda = 0.10$, only six approaches will be studied and compared, i.e., EL and DL scheme (two types of UCLs), HL scheme (time-varying UCL only), and SL scheme (steady-state UCL). On the other hand, when $\lambda = 0.20$, all the seven approaches will be studied.

To this end, in Tables 4.11 – 4.13, 4.14 – 4.16, and 4.17 – 4.19, the cell that is filled with grey colour indicates that it appears to have the best performance. For instance, when $\lambda = 0.05$ and $\lambda = 0.10$, the grey coloured cell has the lowest ARL_1 among the six approaches. On the flip side, the grey coloured cell in these tables with $\lambda = 0.20$ indicates that its ARL_1 is the least among the seven approaches.

4.3.1 OOC Performance of the Schemes under the Normal Distribution

Tables 4.11, 4.12, and 4.13 present the OOC RL properties of various schemes when the underlying process is normally distributed such that the smoothing parameter for the memory-type schemes (EL, DL, and HL) are $\lambda = 0.05$, $\lambda = 0.10$, and $\lambda = 0.20$, respectively. Refers to Tables 4.11 – 4.13, some of the conclusions that can be made if the process follows a Normal distribution are as below:

1. One can easily notice that in none of the case the SL scheme performs the best if compared with the memory-type EL, DL, and HL schemes, even in terms of detecting a large disturbance in the process.

2. Comparatively, both the EL and DL schemes seem to perform better with their time-varying UCLs, if compared with their steady-state UCLs. The opposite pattern is observed for the HL scheme.

3. When the value of λ increases, excluding the DL scheme with the steady-state UCL, the memory-type schemes' performance appears to deteriorate, especially in terms of detecting a small to moderate pure or mixed shift. Their performance in detecting a large shift is almost constant or slightly worsen. For instance,
    a. The performance of the EL and DL schemes with time-varying UCLs, and HL scheme with the steady-state UCL significantly deteriorates in detecting pure or mixed shifts with $\theta < 1.5$.

b. The EL scheme with the steady-state UCL performs significantly worse in detecting a shift with $\theta < 1$ and/or $\delta < 2$.

c. The performance of the HL scheme with the time-varying UCL substantially worsens in detecting shifts with $\theta < 2$.

4. In terms of detecting a small to moderate shift, the performance of the DL scheme with the steady-state UCL also seems to deteriorate when λ value increases. However, its performance in detecting a moderate to large shift, says $\theta \geq 1$ and/or $\delta \geq 1.75$, significantly improves.

5. Generally, when $\lambda = 0.05$ and excluding the HL scheme with the steady-state UCL due to its high early FAR, it is observed that

    a. The EL, DL, and HL schemes with time-varying UCLs are performing almost equally good in detecting a large pure or mixed shift with $\theta \geq 1.5$ in the process.

    b. The DL scheme with the time-varying UCL appears to have the best performance in general, except in detecting a small and pure location shift, i.e., $(\theta, \delta) = (0.1, 1)$ where the HL scheme with the time-varying UCL able to detect it the fastest.

6. When $\lambda = 0.10$ and excluding the HL scheme with the steady-state UCL, again, the DL scheme with the time-varying UCL seems to have the best overall performance in detecting all shift sizes in the process. This is true except for a very small shift in the location, i.e., $(\theta, \delta) =$

$(0.1, 1)$, such that the DL scheme with the steady-state UCL is apparently better.

7. The DL scheme with the time-varying UCL and the HL scheme with the steady-state UCL perform equally good when $\lambda = 0.20$, such that
    a. The DL scheme with the time-varying UCL seems better in detecting a pure location shift, except for $(\theta, \delta) = (1, 1)$. Also, it is good in detecting a large mixed shift with $\theta \geq 1.5$.
    b. For the rest of the cases, the HL scheme with the steady-state UCL appears to superior

Table 4.11: The OOC Performance of Various Schemes when $(m, n) = (100, 5)$ and $\lambda = 0.05$ for the Memory-Type Schemes when $ARL_0 \approx 500$ under the Normal Distribution

Case	θ	δ	Memory-Type Schemes ($\lambda = 0.05$)						SL (SS UCL)
			EL		DL		HL		
			TV UCL	SS UCL	TV UCL	SS UCL	TV UCL	SS UCL	
Pure Shift in θ	0.1	1	419.3 (810.4)	414.7 (742.6)	411.3 (900.9)	429.3 (836.0)	410.5 (829.7)	400.4 (1058.2)	445.9 (615.9)
	0.25	1	168.6 (429.5)	181.5 (413.9)	154.2 (482.1)	165.1 (408.4)	159.2 (425.7)	133.6 (551.4)	257.3 (400.7)
	0.5	1	19.3 (42.5)	26.1 (51.4)	14.3 (30.8)	26.8 (48.0)	18.4 (42.6)	8.8 (48.4)	68.4 (105.9)
	1	1	2.4 (2.1)	4.4 (2.7)	1.9 (1.8)	7.9 (2.5)	2.6 (2.1)	2.1 (1.0)	7.7 (8.8)
	1.5	1	1.2 (0.6)	2.1 (1.0)	1.1 (0.4)	4.9 (1.0)	1.3 (0.8)	1.5 (0.6)	2.2 (1.7)
	2	1	1.0 (0.2)	1.4 (0.5)	1.0 (0.1)	3.7 (0.6)	1.0 (0.3)	1.2 (0.4)	1.2 (0.6)
Pure Shift in δ	0	1.25	37.3 (72.4)	47.1 (67.3)	30.3 (64.1)	45.6 (57.4)	35.9 (65.0)	17.2 (58.7)	102.1 (125.3)
	0	1.5	9.3 (12.4)	14.7 (12.9)	7.7 (11.0)	17.8 (10.8)	9.4 (12.3)	4.7 (7.0)	37.3 (41.9)
	0	1.75	4.7 (5.1)	8.3 (5.7)	4.0 (4.8)	12.0 (4.9)	4.9 (5.1)	3.1 (2.7)	19.0 (20.2)
	0	2	3.2 (3.0)	5.9 (3.6)	2.7 (2.8)	9.6 (3.2)	3.4 (3.1)	2.5 (1.5)	11.6 (11.8)
Mixed Shift in θ and δ	0.1	1.25	34.3 (71.8)	43.8 (60.3)	28.2 (62.8)	42.8 (54.7)	32.8 (59.2)	16.6 (65.9)	95.2 (117.1)
	0.1	1.5	9.1 (12.1)	14.2 (12.2)	7.5 (10.7)	17.4 (10.4)	9.2 (11.8)	4.5 (6.6)	36.2 (41.0)
	0.1	1.75	4.7 (5.0)	8.2 (5.6)	3.9 (4.7)	11.9 (4.9)	4.9 (5.0)	3.0 (2.5)	18.6 (19.8)
	0.1	2	3.2 (3.0)	5.9 (3.6)	2.6 (2.8)	9.6 (3.2)	3.4 (3.1)	2.5 (1.5)	11.5 (11.7)
	0.25	1.25	23.4 (46.1)	31.3 (43.8)	18.8 (36.0)	32.0 (37.2)	22.4 (41.5)	10.7 (45.9)	70.2 (89.9)
	0.25	1.5	7.8 (9.6)	12.6 (10.4)	6.5 (9.1)	16.0 (8.9)	7.9 (9.7)	4.1 (5.5)	30.0 (33.6)
	0.25	1.75	4.4 (4.6)	7.8 (5.3)	3.7 (4.3)	11.5 (4.6)	4.6 (4.6)	2.9 (2.3)	16.6 (17.4)
	0.25	2	3.1 (2.9)	5.6 (3.4)	2.6 (2.7)	9.4 (3.0)	3.3 (2.9)	2.5 (1.5)	10.8 (10.9)
	0.5	1.25	9.0 (12.6)	13.9 (13.3)	7.4 (11.1)	17.2 (11.5)	9.1 (12.1)	4.6 (7.8)	30.9 (38.4)
	0.5	1.5	5.2 (5.8)	8.9 (6.7)	4.4 (5.6)	12.5 (5.7)	5.4 (5.8)	3.2 (3.1)	18.1 (19.9)
	0.5	1.75	3.6 (3.5)	6.4 (4.3)	3.0 (3.4)	10.1 (3.7)	3.8 (3.6)	2.7 (1.8)	12.0 (12.3)
	0.5	2	2.8 (2.5)	5.1 (3.1)	2.3 (2.3)	8.7 (2.8)	3.0 (2.5)	2.4 (1.3)	8.8 (8.6)
	1	1.25	2.5 (2.1)	4.5 (2.8)	2.0 (1.9)	7.9 (2.6)	2.7 (2.2)	2.2 (1.1)	6.8 (7.1)
	1	1.5	2.4 (2.0)	4.2 (2.6)	2.0 (1.8)	7.7 (2.4)	2.6 (2.1)	2.2 (1.1)	6.1 (6.0)
	1	1.75	2.2 (1.8)	3.9 (2.3)	1.9 (1.6)	7.4 (2.2)	2.4 (2.0)	2.1 (1.0)	5.5 (5.2)
	1	2	2.0 (1.6)	3.7 (2.1)	1.7 (1.4)	7.1 (2.0)	2.2 (1.7)	2.1 (0.9)	4.9 (4.6)
	1.5	1.25	1.4 (0.7)	2.3 (1.2)	1.2 (0.6)	5.2 (1.2)	1.5 (1.0)	1.6 (0.6)	2.5 (2.1)
	1.5	1.5	1.5 (0.8)	2.5 (1.3)	1.3 (0.7)	5.5 (1.3)	1.6 (1.1)	1.7 (0.7)	2.7 (2.2)
	1.5	1.75	1.5 (0.9)	2.6 (1.4)	1.3 (0.8)	5.6 (1.4)	1.7 (1.2)	1.7 (0.7)	2.8 (2.3)
	1.5	2	1.5 (0.9)	2.6 (1.4)	1.3 (0.8)	5.6 (1.4)	1.7 (1.2)	1.7 (0.7)	2.9 (2.4)
	2	1.25	1.1 (0.3)	1.6 (0.7)	1.0 (0.2)	4.0 (0.7)	1.1 (0.4)	1.3 (0.5)	1.4 (0.8)
	2	1.5	1.1 (0.4)	1.7 (0.8)	1.1 (0.3)	4.3 (0.9)	1.2 (0.6)	1.4 (0.5)	1.6 (1.0)
	2	1.75	1.2 (0.5)	1.9 (0.9)	1.1 (0.4)	4.5 (0.9)	1.3 (0.7)	1.4 (0.6)	1.8 (1.2)
	2	2	1.2 (0.6)	2.0 (1.0)	1.1 (0.4)	4.7 (1.0)	1.3 (0.8)	1.5 (0.6)	1.9 (1.3)

Note: The HL scheme with the SS UCL is not considered for comparison due to its extraordinary high early FAR.

Table 4.12: The OOC Performance of Various Schemes when $(m, n) = (100, 5)$ and $\lambda = 0.10$ for the Memory-Type Schemes when $ARL_0 \approx 500$ under the Normal Distribution

Case	θ	δ	Memory-Type Schemes ($\lambda = 0.10$)						SL (SS UCL)
			EL		DL		HL		
			TV UCL	SS UCL	TV UCL	SS UCL	TV UCL	SS UCL	
Pure Shift in θ	0.1	1	428.9 (726.0)	419.5 (693.7)	421.2 (800.6)	414.8 (734.2)	422.5 (645.9)	432.8 (925.4)	445.9 (615.9)
	0.25	1	191.0 (402.4)	196.9 (396.0)	170.6 (429.3)	177.4 (390.8)	196.7 (350.7)	167.3 (505.7)	257.3 (400.7)
	0.5	1	27.0 (58.7)	30.4 (57.6)	20.2 (40.4)	28.2 (62.2)	33.9 (50.9)	14.6 (52.1)	68.4 (105.9)
	1	1	2.9 (2.6)	4.3 (2.8)	2.4 (2.2)	6.4 (2.4)	3.9 (3.2)	2.2 (1.2)	7.7 (8.8)
	1.5	1	1.3 (0.7)	2.0 (1.0)	1.2 (0.5)	3.8 (0.9)	1.6 (1.1)	1.5 (0.6)	2.2 (1.7)
	2	1	1.1 (0.2)	1.3 (0.5)	1.0 (0.2)	2.9 (0.6)	1.1 (0.4)	1.2 (0.4)	1.2 (0.6)
Pure Shift in δ	0	1.25	49.7 (81.7)	54.5 (80.9)	40.3 (71.8)	49.8 (67.7)	62.2 (77.5)	30.8 (86.4)	102.1 (125.3)
	0	1.5	12.6 (15.3)	15.9 (15.3)	10.3 (13.2)	16.7 (12.4)	18.0 (18.0)	6.8 (11.3)	37.3 (41.9)
	0	1.75	6.2 (6.4)	8.5 (6.4)	5.1 (5.7)	10.4 (5.3)	8.7 (8.1)	3.7 (3.9)	19.0 (20.2)
	0	2	4.0 (3.7)	5.9 (4.0)	3.4 (3.4)	8.0 (3.3)	5.6 (4.8)	2.8 (2.1)	11.6 (11.8)
Mixed Shift in θ and δ	0.1	1.25	46.1 (78.8)	50.8 (74.4)	37.3 (65.6)	46.5 (63.7)	57.9 (73.1)	27.2 (65.8)	95.2 (117.1)
	0.1	1.5	12.2 (14.8)	15.2 (14.5)	10.0 (12.6)	16.3 (12.3)	17.4 (17.6)	6.5 (10.6)	36.2 (41.0)
	0.1	1.75	6.0 (6.2)	8.4 (6.3)	5.1 (5.7)	10.3 (5.3)	8.6 (7.9)	3.7 (3.9)	18.6 (19.8)
	0.1	2	4.0 (3.7)	5.8 (3.9)	3.4 (3.4)	7.9 (3.2)	5.6 (4.7)	2.8 (2.1)	11.5 (11.7)
	0.25	1.25	31.5 (55.5)	35.2 (49.7)	25.3 (42.3)	33.5 (39.4)	40.3 (48.7)	17.8 (44.4)	70.2 (89.9)
	0.25	1.5	10.4 (12.3)	13.2 (12.2)	8.7 (10.7)	14.7 (10.4)	14.9 (14.9)	5.8 (8.7)	30.0 (33.6)
	0.25	1.75	5.6 (5.7)	7.9 (5.9)	4.7 (5.2)	9.8 (4.9)	7.9 (7.2)	3.5 (3.5)	16.6 (17.4)
	0.25	2	3.9 (3.5)	5.7 (3.7)	3.2 (3.2)	7.7 (3.2)	5.3 (4.5)	2.7 (2.0)	10.8 (10.9)
	0.5	1.25	12.1 (16.6)	15.0 (16.9)	9.9 (13.4)	16.1 (13.6)	16.9 (18.9)	6.6 (12.1)	30.9 (38.4)
	0.5	1.5	6.7 (7.3)	9.0 (7.3)	5.7 (6.6)	10.9 (6.2)	9.6 (9.2)	4.0 (4.8)	18.1 (19.9)
	0.5	1.75	4.5 (4.3)	6.4 (4.6)	3.8 (4.0)	8.5 (3.9)	6.3 (5.5)	3.1 (2.6)	12.0 (12.3)
	0.5	2	3.4 (3.0)	5.0 (3.2)	2.9 (2.8)	7.1 (2.8)	4.6 (3.8)	2.6 (1.7)	8.8 (8.6)
	1	1.25	3.0 (2.6)	4.4 (2.9)	2.5 (2.4)	6.4 (2.5)	4.0 (3.3)	2.3 (1.4)	6.8 (7.1)
	1	1.5	2.8 (2.4)	4.2 (2.7)	2.4 (2.2)	6.3 (2.4)	3.8 (3.1)	2.3 (1.4)	6.1 (6.0)
	1	1.75	2.6 (2.1)	3.9 (2.4)	2.2 (2.0)	6.0 (2.2)	3.5 (2.7)	2.2 (1.2)	5.5 (5.2)
	1	2	2.4 (1.9)	3.5 (2.1)	2.0 (1.7)	5.6 (1.9)	3.2 (2.4)	2.1 (1.1)	4.9 (4.6)
	1.5	1.25	1.5 (0.9)	2.2 (1.1)	1.3 (0.7)	4.1 (1.1)	1.9 (1.3)	1.6 (0.6)	2.5 (2.1)
	1.5	1.5	1.6 (1.0)	2.4 (1.3)	1.4 (0.9)	4.3 (1.2)	2.1 (1.4)	1.7 (0.7)	2.7 (2.2)
	1.5	1.75	1.7 (1.1)	2.5 (1.4)	1.5 (1.0)	4.4 (1.3)	2.2 (1.5)	1.8 (0.7)	2.8 (2.3)
	1.5	2	1.7 (1.1)	2.5 (1.4)	1.5 (1.0)	4.4 (1.3)	2.2 (1.5)	1.8 (0.8)	2.9 (2.4)
	2	1.25	1.1 (0.4)	1.5 (0.6)	1.1 (0.3)	3.1 (0.7)	1.3 (0.7)	1.3 (0.5)	1.4 (0.8)
	2	1.5	1.2 (0.5)	1.7 (0.8)	1.1 (0.4)	3.3 (0.8)	1.4 (0.8)	1.4 (0.5)	1.6 (1.0)
	2	1.75	1.3 (0.6)	1.8 (0.9)	1.2 (0.5)	3.5 (0.9)	1.5 (1.0)	1.5 (0.6)	1.8 (1.2)
	2	2	1.3 (0.7)	1.9 (0.9)	1.2 (0.6)	3.6 (0.9)	1.6 (1.0)	1.5 (0.6)	1.9 (1.3)

Note: The HL scheme with the SS UCL is not considered for comparison due to its extraordinary high early FAR.

Table 4.13: The OOC Performance of Various Schemes when $(m, n) = (100, 5)$ and $\lambda = 0.20$ for the Memory-Type Schemes when $ARL_0 \approx 500$ under the Normal Distribution

Case	θ	δ	Memory-Type Schemes ($\lambda = 0.20$)						SL (SS UCL)
			EL		DL		HL		
			TV UCL	SS UCL	TV UCL	SS UCL	TV UCL	SS UCL	
Pure Shift in θ	0.1	1	435.9 (677.2)	435.9 (666.8)	430.2 (724.6)	429.1 (686.9)	431.5 (604.9)	434.8 (739.9)	445.9 (615.9)
	0.25	1	215.6 (398.2)	216.9 (391.6)	194.4 (408.1)	198.2 (388)	220.0 (350.4)	204.1 (439.4)	257.3 (400.7)
	0.5	1	37.0 (74.3)	38.9 (73.7)	27.7 (51.8)	31.8 (61.9)	45.1 (65.6)	27.8 (65.4)	68.4 (105.9)
	1	1	3.6 (3.2)	4.4 (3.3)	2.9 (2.6)	5.0 (2.5)	5.1 (4.1)	2.7 (2.3)	7.7 (8.8)
	1.5	1	1.5 (0.8)	1.9 (1.0)	1.3 (0.7)	2.8 (0.8)	1.9 (1.2)	1.5 (0.6)	2.2 (1.7)
	2	1	1.1 (0.3)	1.3 (0.5)	1.0 (0.2)	2.1 (0.4)	1.2 (0.5)	1.2 (0.4)	1.2 (0.6)
Pure Shift in δ	0	1.25	63.9 (92.8)	66.6 (92.3)	51.7 (82.2)	58.1 (83.0)	78.0 (93.0)	51.2 (90.0)	102.1 (125.3)
	0	1.5	17.0 (20.4)	18.7 (20.4)	13.3 (16.4)	16.8 (15.8)	23.9 (22.0)	11.9 (18.2)	37.3 (41.9)
	0	1.75	8.0 (8.2)	9.3 (8.2)	6.4 (6.7)	9.2 (6.4)	11.8 (9.8)	5.4 (6.4)	19.0 (20.2)
	0	2	5.1 (4.6)	6.1 (4.6)	4.2 (3.9)	6.6 (3.6)	7.5 (5.9)	3.6 (3.5)	11.6 (11.8)
Mixed Shift in θ and δ	0.1	1.25	58.9 (85.4)	61.5 (84.9)	47.5 (75.1)	54.4 (82.2)	72.2 (84.7)	47.2 (84.8)	95.2 (117.1)
	0.1	1.5	16.3 (19.5)	18.1 (19.5)	12.9 (15.4)	16.3 (15.3)	23.1 (21.3)	11.6 (17.2)	36.2 (41.0)
	0.1	1.75	7.8 (7.9)	9.1 (7.9)	6.4 (6.6)	9.1 (6.2)	11.6 (9.7)	5.3 (6.3)	18.6 (19.8)
	0.1	2	5.0 (4.5)	6.1 (4.6)	4.1 (3.9)	6.6 (3.6)	7.4 (5.8)	3.6 (3.3)	11.5 (11.7)
	0.25	1.25	41.1 (63.9)	43.4 (63.4)	32.9 (50.2)	38.4 (57.0)	51.3 (59.8)	31.5 (58.7)	70.2 (89.9)
	0.25	1.5	13.8 (16.2)	15.4 (16.1)	11.0 (12.9)	14.2 (12.7)	19.8 (18.5)	9.5 (13.5)	30.0 (33.6)
	0.25	1.75	7.2 (7.1)	8.4 (7.1)	5.9 (6.0)	8.6 (5.6)	10.7 (8.8)	4.9 (5.5)	16.6 (17.4)
	0.25	2	4.8 (4.4)	5.8 (4.4)	4.0 (3.7)	6.4 (3.4)	7.1 (5.5)	3.5 (3.2)	10.8 (10.9)
	0.5	1.25	15.9 (21.8)	17.4 (21.7)	12.6 (16.4)	16.2 (18.0)	22.1 (23.7)	11.2 (17.9)	30.9 (38.4)
	0.5	1.5	8.7 (9.3)	10.0 (9.3)	7.1 (7.9)	9.9 (7.5)	12.6 (11.1)	6.0 (7.5)	18.1 (19.9)
	0.5	1.75	5.6 (5.3)	6.7 (5.4)	4.7 (4.6)	7.2 (4.3)	8.3 (6.8)	4.0 (4.1)	12.0 (12.3)
	0.5	2	4.2 (3.6)	5.1 (3.7)	3.5 (3.2)	5.8 (3.0)	6.1 (4.7)	3.1 (2.7)	8.8 (8.6)
	1	1.25	3.6 (3.2)	4.4 (3.2)	3.0 (2.7)	5.1 (2.6)	5.1 (4.1)	2.7 (2.3)	6.8 (7.1)
	1	1.5	3.4 (2.9)	4.1 (3.0)	2.9 (2.6)	5.0 (2.4)	4.8 (3.7)	2.7 (2.1)	6.1 (6.0)
	1	1.75	3.1 (2.5)	3.8 (2.6)	2.6 (2.3)	4.7 (2.2)	4.4 (3.3)	2.5 (1.8)	5.5 (5.2)
	1	2	2.8 (2.2)	3.5 (2.3)	2.4 (2.0)	4.4 (1.9)	3.9 (2.9)	2.3 (1.5)	4.9 (4.6)
	1.5	1.25	1.7 (1.0)	2.1 (1.2)	1.5 (0.9)	3.0 (1.0)	2.2 (1.5)	1.7 (0.7)	2.5 (2.1)
	1.5	1.5	1.8 (1.2)	2.3 (1.3)	1.6 (1.1)	3.2 (1.2)	2.4 (1.7)	1.8 (0.8)	2.7 (2.2)
	1.5	1.75	1.9 (1.3)	2.4 (1.4)	1.7 (1.1)	3.3 (1.2)	2.5 (1.8)	1.8 (0.9)	2.8 (2.3)
	1.5	2	1.9 (1.3)	2.4 (1.4)	1.7 (1.2)	3.3 (1.2)	2.6 (1.8)	1.8 (0.9)	2.9 (2.4)
	2	1.25	1.2 (0.5)	1.4 (0.6)	1.1 (0.4)	2.3 (0.5)	1.4 (0.7)	1.3 (0.5)	1.4 (0.8)
	2	1.5	1.3 (0.6)	1.6 (0.8)	1.2 (0.5)	2.5 (0.7)	1.5 (0.9)	1.4 (0.5)	1.6 (1.0)
	2	1.75	1.4 (0.7)	1.7 (0.9)	1.3 (0.6)	2.6 (0.8)	1.7 (1.0)	1.5 (0.6)	1.8 (1.2)
	2	2	1.5 (0.8)	1.8 (0.9)	1.3 (0.7)	2.7 (0.8)	1.8 (1.1)	1.5 (0.6)	1.9 (1.3)

4.3.2 OOC Performance of the Schemes under the Laplace Distribution

When the process follows the Laplace distribution, the OOC RL properties of various schemes are juxtaposed in Tables 4.14 – 4.16. As such, Tables 4.14, 4.15, and 4.16, are respectively, for the setting of the memory-type schemes when $\lambda = 0.05$, $\lambda = 0.10$, and $\lambda = 0.20$. If the underlying distribution of a process follows the Laplace distribution, from Tables 4.14 – 4.16, almost the same patterns as the Normal distribution are observed. The details are as below:

1. Similarly, there is no shift size that the SL scheme is superior. Further, compared to the time-varying UCL, the HL scheme appears to be better with its steady-state UCL. However, one is not encouraged to use the HL scheme with the steady-state UCL even though it has a lower ARL_1 due to its high early FAR when $\lambda < 0.20$. The opposite pattern is observed for the EL and DL schemes.

2. Again, excluding the DL scheme with the steady-state UCL, the performance of the memory-type schemes worsens as λ value increases. However, their performance is deteriorating in a wider range if compared to that of the Normal distribution. For instance, the EL and DL schemes with time-varying UCLs perform significantly worse in detecting the shift with $\theta < 2$, which is wider compared to $\theta < 1.5$ for the Normal distribution.

3. When $\lambda < 0.20$, in general, if one ignores the HL scheme with the steady-state UCL, the DL scheme with the time-varying UCL seems to outperform other schemes, with some remarks as following.
    a. The EL and HL schemes with time-varying UCLs are also equally good in detecting large pure or mixed shifts with $\theta \geq 2$ when $\lambda = 0.05$.
    b. The proposed HL scheme with the time-varying UCL also appears to perform well in detecting a small pure or mixed shift with $\theta \leq 0.5$ or $\delta \leq 1.5$ when $\lambda = 0.05$.
    c. In detecting a small and pure shift in the location, i.e., $(\theta, \delta) = (0.1, 1)$, the DL scheme with the steady-state UCL is apparently better when $\lambda < 0.20$.

4. Similarly, when $\lambda = 0.20$, the DL scheme with the time-varying UCL appears to be the best in detecting a pure location shift and large mixed shifts, except $(\theta, \delta) = (1, 1)$. Then, the HL scheme with the steady-state UCL appears to be the best for the remaining OOC cases.

Table 4.14: The OOC Performance of Various Schemes when $(m,n) = (100,5)$ and $\lambda = 0.05$ for the Memory-Type Schemes when $ARL_0 \approx 500$ under the Laplace Distribution

Case	θ	δ	Memory-Type Schemes ($\lambda = 0.05$)						SL (SS UCL)
			EL		DL		HL		
			TV UCL	SS UCL	TV UCL	SS UCL	TV UCL	SS UCL	
Pure Shift in θ	0.1	1	462.8 (866.4)	457.0 (806.2)	452.8 (952.9)	446.7 (835.8)	458.6 (893.2)	453.5 (1145.0)	478.5 (653.0)
	0.25	1	269.8 (612.3)	277.6 (575.0)	248.1 (670.1)	261.0 (593.9)	263.6 (633.3)	246.6 (822.6)	365.7 (549.4)
	0.5	1	51.2 (175.9)	58.5 (163.4)	38.0 (155.9)	50.4 (125.1)	47.0 (168.5)	29.8 (212.8)	161.0 (301.4)
	1	1	3.4 (4.2)	6.3 (5.0)	2.6 (3.4)	9.8 (4.3)	3.6 (4.0)	2.5 (2.0)	20.1 (41.1)
	1.5	1	1.5 (0.9)	2.8 (1.4)	1.3 (0.7)	5.9 (1.5)	1.6 (1.1)	1.7 (0.6)	4.1 (5.2)
	2	1	1.1 (0.4)	1.8 (0.8)	1.1 (0.3)	4.5 (0.9)	1.2 (0.6)	1.4 (0.5)	1.8 (1.4)
Pure Shift in δ	0	1.25	73.3 (159.2)	85.3 (170.1)	66.5 (201.0)	80.3 (148.6)	70.8 (161.6)	48.5 (247.1)	152.9 (197.8)
	0	1.5	18.8 (36.3)	25.6 (30.5)	14.9 (27.9)	27.2 (25.8)	18.6 (33.2)	8.2 (20.5)	67.0 (80.8)
	0	1.75	8.5 (11.0)	13.7 (12.3)	6.9 (10.3)	16.6 (9.5)	8.5 (11.0)	4.4 (6.2)	36.6 (41.9)
	0	2	5.2 (6.1)	9.1 (6.6)	4.3 (5.4)	12.7 (5.6)	5.3 (6.0)	3.2 (3.3)	23.0 (25.3)
Mixed Shift in θ and δ	0.1	1.25	68.9 (154.4)	79.2 (152.4)	60.1 (172.1)	75.3 (149.1)	65.7 (150.3)	41.7 (197.7)	147.0 (191.2)
	0.1	1.5	18.1 (38.1)	25.0 (31.7)	14.4 (26.7)	26.7 (26.8)	17.9 (31.2)	8.1 (22.1)	64.8 (78.2)
	0.1	1.75	8.3 (10.8)	13.1 (11.2)	6.7 (9.8)	16.4 (9.5)	8.4 (10.9)	4.2 (5.8)	35.7 (41.3)
	0.1	2	5.2 (5.9)	9.0 (6.5)	4.2 (5.4)	12.5 (5.4)	5.3 (5.9)	3.2 (3.1)	22.7 (25.0)
	0.25	1.25	48.1 (114.6)	59.0 (111.9)	41.3 (126.7)	54.7 (111.1)	46.3 (114.6)	27.4 (147.2)	120.9 (165.1)
	0.25	1.5	14.8 (28.7)	21.1 (24.6)	11.8 (20.6)	23.3 (21.8)	14.7 (22.9)	6.9 (19.2)	56.5 (70.1)
	0.25	1.75	7.5 (9.7)	12.0 (10.1)	6.1 (8.9)	15.4 (8.5)	7.6 (9.6)	3.9 (5.2)	32.2 (37.1)
	0.25	2	4.9 (5.4)	8.4 (6.0)	3.9 (5.0)	12.1 (5.2)	5.0 (5.4)	3.0 (2.7)	21.0 (23.1)
	0.5	1.25	17.5 (40.6)	24.4 (41.7)	13.8 (33.8)	25.5 (34.4)	17.2 (36.9)	8.3 (41.1)	66.4 (101.1)
	0.5	1.5	8.6 (12.8)	13.5 (13.8)	6.9 (11.5)	16.6 (11.8)	8.6 (12.2)	4.4 (8.7)	36.4 (47.1)
	0.5	1.75	5.5 (6.7)	9.2 (7.4)	4.4 (6.1)	12.8 (6.1)	5.6 (6.6)	3.2 (3.4)	23.3 (27.8)
	0.5	2	3.9 (4.2)	7.1 (4.9)	3.2 (3.8)	10.7 (4.1)	4.1 (4.2)	2.7 (2.1)	16.4 (18.4)
	1	1.25	3.3 (3.6)	5.9 (4.4)	2.6 (3.4)	9.5 (3.8)	3.4 (3.5)	2.4 (1.7)	14.1 (20.4)
	1	1.5	3.0 (3.0)	5.4 (3.7)	2.4 (2.7)	9.0 (3.3)	3.2 (3.0)	2.4 (1.4)	11.2 (13.9)
	1	1.75	2.7 (2.5)	4.9 (3.1)	2.2 (2.2)	8.5 (2.8)	2.9 (2.5)	2.3 (1.3)	9.3 (10.7)
	1	2	2.4 (2.1)	4.4 (2.7)	2.0 (1.9)	8.0 (2.5)	2.6 (2.2)	2.2 (1.1)	7.9 (8.6)
	1.5	1.25	1.6 (1.0)	2.9 (1.6)	1.3 (0.8)	6.1 (1.6)	1.7 (1.3)	1.8 (0.7)	4.1 (4.6)
	1.5	1.5	1.6 (1.1)	3.0 (1.6)	1.4 (0.9)	6.2 (1.6)	1.8 (1.3)	1.8 (0.7)	4.1 (4.3)
	1.5	1.75	1.6 (1.1)	3.0 (1.6)	1.4 (0.9)	6.2 (1.6)	1.8 (1.3)	1.8 (0.7)	4.0 (4.0)
	1.5	2	1.6 (1.1)	3.0 (1.6)	1.4 (0.9)	6.2 (1.6)	1.8 (1.3)	1.8 (0.7)	3.9 (3.8)
	2	1.25	1.2 (0.5)	2.0 (0.9)	1.1 (0.4)	4.7 (1.0)	1.3 (0.7)	1.5 (0.6)	2.0 (1.6)
	2	1.5	1.2 (0.6)	2.1 (1.0)	1.1 (0.4)	4.9 (1.0)	1.3 (0.8)	1.5 (0.6)	2.2 (1.8)
	2	1.75	1.3 (0.6)	2.2 (1.0)	1.1 (0.5)	5.0 (1.1)	1.4 (0.9)	1.6 (0.6)	2.3 (1.9)
	2	2	1.3 (0.6)	2.2 (1.0)	1.2 (0.5)	5.1 (1.1)	1.4 (0.9)	1.6 (0.6)	2.4 (1.9)

Note: The HL scheme with the SS UCL is not considered for comparison due to its extraordinary high early FAR.

Table 4.15: The OOC Performance of Various Schemes when $(m, n) = (100, 5)$ and $\lambda = 0.10$ for the Memory-Type Schemes when $ARL_0 \approx 500$ under the Laplace Distribution

Case	θ	δ	Memory-Type Schemes ($\lambda = 0.10$)						SL (SS UCL)
			EL		DL		HL		
			TV UCL	SS UCL	TV UCL	SS UCL	TV UCL	SS UCL	
Pure Shift in θ	0.1	1	467.0 (774.4)	455.2 (730.4)	454.0 (837.9)	451.9 (785.3)	466.2 (708.7)	450.0 (946.6)	478.5 (653.0)
	0.25	1	297.5 (580.0)	292.4 (549.5)	265.4 (589.4)	270.2 (560.2)	305.2 (532.2)	267.5 (701.1)	365.7 (549.4)
	0.5	1	70.1 (197.5)	72.9 (185.8)	50.6 (157.8)	58.9 (153.8)	79.3 (179.9)	50.9 (235.2)	161.0 (301.4)
	1	1	4.6 (6.4)	6.4 (6.3)	3.5 (4.7)	8.2 (5.0)	6.4 (7.5)	2.8 (3.5)	20.1 (41.1)
	1.5	1	1.7 (1.2)	2.7 (1.5)	1.4 (0.9)	4.7 (1.4)	2.2 (1.6)	1.8 (0.7)	4.1 (5.2)
	2	1	1.2 (0.5)	1.7 (0.8)	1.1 (0.4)	3.5 (0.7)	1.4 (0.8)	1.4 (0.5)	1.8 (1.4)
Pure Shift in δ	0	1.25	92.4 (178.9)	97.4 (165.6)	82.1 (188.1)	91.6 (168.2)	106.7 (156.3)	64.6 (191.4)	152.9 (197.8)
	0	1.5	25.7 (42.5)	29.4 (35.9)	20.4 (32.6)	28.4 (31.5)	34.7 (41.3)	14.4 (41.0)	67.0 (80.8)
	0	1.75	11.3 (13.5)	14.5 (14.2)	9.2 (12.2)	15.7 (11.8)	16.4 (17.0)	6.2 (10.3)	36.6 (41.9)
	0	2	6.9 (7.6)	9.4 (7.7)	5.6 (6.5)	11.1 (6.2)	9.9 (9.5)	4.0 (4.6)	23.0 (25.3)
Mixed Shift in θ and δ	0.1	1.25	85.9 (158.4)	91.7 (157.9)	75.1 (168.5)	85.2 (158.8)	101.0 (149.3)	63.0 (195.5)	147.0 (191.2)
	0.1	1.5	24.7 (42.0)	28.5 (37.2)	19.7 (31.8)	27.4 (30.7)	33.5 (40.2)	13.5 (32.4)	64.8 (78.2)
	0.1	1.75	11.1 (13.3)	14.3 (13.9)	9.0 (12.0)	15.2 (10.7)	16.0 (16.4)	6.0 (9.6)	35.7 (41.3)
	0.1	2	6.8 (7.5)	9.3 (7.6)	5.5 (6.4)	10.9 (6.0)	9.7 (9.3)	3.9 (4.6)	22.7 (25.0)
	0.25	1.25	63.1 (127.0)	68.0 (122.6)	53.3 (131.4)	62.4 (117.7)	76.3 (122.1)	42.1 (128.6)	120.9 (165.1)
	0.25	1.5	20.1 (33.4)	24.1 (29.8)	16.1 (26.2)	23.3 (23.8)	27.9 (33.3)	10.9 (25.5)	56.5 (70.1)
	0.25	1.75	10.0 (12.1)	12.9 (12.0)	8.1 (10.6)	14.1 (10.4)	14.2 (14.5)	5.5 (8.4)	32.2 (37.1)
	0.25	2	6.4 (6.8)	8.7 (7.0)	5.2 (6.1)	10.5 (5.7)	9.0 (8.6)	3.7 (4.1)	21.0 (23.1)
	0.5	1.25	24.2 (51.8)	27.8 (45.7)	19.1 (44.9)	26.7 (42.4)	31.9 (50.5)	13.8 (53.3)	66.4 (101.1)
	0.5	1.5	11.6 (16.5)	14.7 (17.9)	9.3 (13.7)	15.4 (13.0)	16.4 (19.1)	6.3 (12.3)	36.4 (47.1)
	0.5	1.75	7.2 (8.3)	9.6 (8.4)	5.9 (7.5)	11.2 (7.0)	10.2 (10.4)	4.1 (5.3)	23.3 (27.8)
	0.5	2	5.1 (5.3)	7.2 (5.3)	4.2 (4.6)	9.1 (4.5)	7.2 (6.7)	3.2 (3.0)	16.4 (18.4)
	1	1.25	4.2 (4.7)	6.0 (5.2)	3.3 (4.2)	7.9 (4.1)	5.8 (6.1)	2.8 (2.5)	14.1 (20.4)
	1	1.5	3.7 (3.8)	5.4 (4.0)	3.0 (3.3)	7.4 (3.4)	5.1 (4.9)	2.6 (2.1)	11.2 (13.9)
	1	1.75	3.3 (3.1)	4.8 (3.3)	2.7 (2.8)	6.9 (2.8)	4.5 (4.0)	2.5 (1.6)	9.3 (10.7)
	1	2	2.9 (2.6)	4.4 (2.9)	2.4 (2.3)	6.5 (2.4)	4.0 (3.3)	2.3 (1.4)	7.9 (8.6)
	1.5	1.25	1.8 (1.3)	2.8 (1.6)	1.5 (1.1)	4.8 (1.5)	2.4 (1.8)	1.8 (0.7)	4.1 (4.6)
	1.5	1.5	1.9 (1.4)	2.9 (1.6)	1.6 (1.2)	4.9 (1.5)	2.5 (1.8)	1.9 (0.8)	4.1 (4.3)
	1.5	1.75	1.9 (1.4)	2.9 (1.6)	1.6 (1.2)	4.9 (1.5)	2.5 (1.8)	1.9 (0.8)	4.0 (4.0)
	1.5	2	1.9 (1.3)	2.9 (1.6)	1.6 (1.2)	4.9 (1.5)	2.5 (1.8)	1.9 (0.8)	3.9 (3.8)
	2	1.25	1.3 (0.6)	1.9 (0.9)	1.2 (0.5)	3.7 (0.9)	1.5 (1.0)	1.5 (0.6)	2.0 (1.6)
	2	1.5	1.3 (0.7)	2.0 (1.0)	1.2 (0.5)	3.8 (0.9)	1.6 (1.1)	1.5 (0.6)	2.2 (1.8)
	2	1.75	1.4 (0.7)	2.1 (1.0)	1.2 (0.6)	3.9 (1.0)	1.7 (1.1)	1.6 (0.6)	2.3 (1.9)
	2	2	1.4 (0.8)	2.1 (1.1)	1.2 (0.6)	4.0 (1.0)	1.8 (1.2)	1.6 (0.6)	2.4 (1.9)

Note: The HL scheme with the SS UCL is not considered for comparison due to its extraordinary high early FAR.

Table 4.16: The OOC Performance of Various Schemes when $(m, n) = (100, 5)$ and $\lambda = 0.20$ for the Memory-Type Schemes when $ARL_0 \approx 500$ under the Laplace Distribution

Case	θ	δ	Memory-Type Schemes ($\lambda = 0.20$)						SL (SS UCL)
			EL		DL		HL		
			TV UCL	SS UCL	TV UCL	SS UCL	TV UCL	SS UCL	
Pure Shift in θ	0.1	1	471.1 (710.9)	473.4 (706.1)	468.2 (772.4)	462.2 (724.9)	472.0 (665.2)	468.7 (784.3)	478.5 (653.0)
	0.25	1	322.4 (567.0)	325.0 (560.3)	294.4 (569.3)	298.0 (543.4)	331.7 (524.0)	307.9 (603.8)	365.7 (549.4)
	0.5	1	94.5 (230.6)	97.0 (229.3)	69.0 (184.6)	74.3 (188.0)	106.6 (218.9)	85.2 (258.7)	161.0 (301.4)
	1	1	6.2 (9.5)	7.3 (9.6)	4.6 (6.5)	7.0 (5.8)	9.0 (11.1)	4.2 (7.7)	20.1 (41.1)
	1.5	1	2.0 (1.5)	2.6 (1.6)	1.6 (1.2)	3.5 (1.3)	2.7 (2.0)	1.8 (0.9)	4.1 (5.2)
	2	1	1.3 (0.6)	1.6 (0.8)	1.2 (0.5)	2.5 (0.7)	1.6 (0.9)	1.4 (0.5)	1.8 (1.4)
Pure Shift in δ	0	1.25	110.8 (181.1)	113.8 (179)	97.5 (182.8)	102.2 (170.7)	125.7 (164.7)	96.0 (183.7)	152.9 (197.8)
	0	1.5	34.2 (48.6)	36.5 (49.4)	26.6 (40.0)	31.8 (47.3)	45.1 (49.9)	25.7 (45.2)	67.0 (80.8)
	0	1.75	15.5 (18.7)	17.2 (18.7)	11.9 (14.6)	15.4 (14.3)	22.1 (20.8)	10.6 (15.8)	36.6 (41.9)
	0	2	9.1 (9.6)	10.5 (9.6)	7.2 (7.9)	10.1 (7.6)	13.5 (11.6)	6.2 (7.9)	23.0 (25.3)
Mixed Shift in θ and δ	0.1	1.25	104.6 (173.8)	107.2 (171.4)	92.2 (177.9)	95.8 (155.5)	119.9 (159.8)	88.6 (177.9)	147.0 (191.2)
	0.1	1.5	33.1 (48.6)	35.4 (48.0)	25.6 (37.8)	30.8 (46.5)	43.6 (48.4)	24.3 (43.7)	64.8 (78.2)
	0.1	1.75	15.1 (18.2)	16.9 (18.4)	11.7 (14.4)	15.1 (14.3)	21.8 (20.8)	10.6 (16.4)	35.7 (41.3)
	0.1	2	8.9 (9.5)	10.3 (9.5)	7.0 (7.8)	10.0 (7.4)	13.3 (11.4)	6.0 (7.5)	22.7 (25.0)
	0.25	1.25	78.6 (136.7)	81.3 (136.1)	65.7 (127.5)	71.4 (122.7)	92.8 (134.0)	65.8 (140.3)	120.9 (165.1)
	0.25	1.5	27.5 (42.6)	29.7 (42.8)	21.2 (31.2)	25.6 (35.2)	36.9 (40.9)	20.2 (35.6)	56.5 (70.1)
	0.25	1.75	13.3 (15.6)	15.0 (15.7)	10.4 (13.0)	13.8 (12.6)	19.5 (18.5)	9.2 (14.4)	32.2 (37.1)
	0.25	2	8.3 (8.8)	9.7 (8.8)	6.5 (7.1)	9.4 (6.8)	12.4 (10.7)	5.6 (7.1)	21.0 (23.1)
	0.5	1.25	33.0 (64.3)	35.0 (63.7)	25.3 (56.0)	29.4 (52.6)	42.7 (63.8)	25.9 (62.7)	66.4 (101.1)
	0.5	1.5	15.7 (21.5)	17.3 (21.6)	12.1 (17.6)	15.5 (17.2)	22.1 (23.9)	11.0 (19.9)	36.4 (47.1)
	0.5	1.75	9.5 (11.0)	10.9 (11.2)	7.4 (8.9)	10.3 (8.5)	13.9 (13.2)	6.4 (9.2)	23.3 (27.8)
	0.5	2	6.6 (6.7)	7.8 (6.8)	5.2 (5.6)	7.9 (5.2)	9.7 (8.4)	4.5 (5.2)	16.4 (18.4)
	1	1.25	5.4 (7.0)	6.5 (7.0)	4.2 (5.5)	6.7 (4.7)	7.9 (8.2)	3.7 (4.9)	14.1 (20.4)
	1	1.5	4.7 (4.9)	5.7 (4.9)	3.7 (4.1)	6.1 (3.8)	6.8 (6.3)	3.3 (3.6)	11.2 (13.9)
	1	1.75	4.1 (4.0)	5.0 (4.0)	3.3 (3.2)	5.6 (3.0)	5.9 (5.1)	3.0 (2.7)	9.3 (10.7)
	1	2	3.6 (3.2)	4.5 (3.3)	2.9 (2.7)	5.1 (2.5)	5.2 (4.1)	2.7 (2.2)	7.9 (8.6)
	1.5	1.25	2.1 (1.6)	2.8 (1.7)	1.8 (1.3)	3.6 (1.4)	2.9 (2.2)	1.9 (1.0)	4.1 (4.6)
	1.5	1.5	2.2 (1.7)	2.8 (1.8)	1.8 (1.4)	3.7 (1.5)	3.0 (2.3)	2.0 (1.0)	4.1 (4.3)
	1.5	1.75	2.2 (1.7)	2.8 (1.8)	1.9 (1.4)	3.7 (1.5)	3.1 (2.2)	2.0 (1.0)	4.0 (4.0)
	1.5	2	2.2 (1.6)	2.8 (1.7)	1.8 (1.4)	3.7 (1.4)	3.0 (2.2)	2.0 (1.0)	3.9 (3.8)
	2	1.25	1.4 (0.7)	1.8 (0.9)	1.2 (0.6)	2.7 (0.8)	1.7 (1.1)	1.5 (0.6)	2.0 (1.6)
	2	1.5	1.5 (0.8)	1.9 (1.0)	1.3 (0.7)	2.8 (0.9)	1.9 (1.2)	1.6 (0.6)	2.2 (1.8)
	2	1.75	1.5 (0.9)	2.0 (1.0)	1.3 (0.7)	2.9 (0.9)	2.0 (1.3)	1.6 (0.7)	2.3 (1.9)
	2	2	1.6 (0.9)	2.0 (1.1)	1.4 (0.8)	2.9 (1.0)	2.0 (1.3)	1.6 (0.7)	2.4 (1.9)

4.3.3 OOC Performance of the Schemes under the Shifted Exponential Distribution

The $OOC\ RL$ properties of various schemes are presented in Tables 4.17 – 4.19 by assuming that the process follows a Shifted Exponential distribution. Precisely, when the smoothing parameter for the memory-type NSPM Lepage-type schemes are $\lambda = 0.05$, $\lambda = 0.10$, and $\lambda = 0.20$, the results are, respectively, tabulated in Tables 4.17, 4.18, and 4.19. From Tables 4.17 – 4.19, considers a process that follows the Shifted Exponential distribution, most of the observations are similar to that of the Normal and Laplace distributions, with some exceptions. To be precise,

1. Surprisingly, for the small and pure shift in the location parameter, i.e., $(\theta, \delta) = (0.1, 1)$, the SL scheme appears to outperform all the other memory-type schemes.

2. As expected, generally, both EL and DL schemes seem to perform better with their time-varying UCLs if compared with their respective steady-state UCLs. The opposite pattern is observed for the HL scheme.

3. Also, when λ value is increasing, excluding the DL scheme with the steady-state UCL, the performance of other schemes appears to deteriorate, in terms of detecting a small to moderate shift. However, particularly, the performance in detecting $(\theta, \delta) = (0.1, 1)$ of the memory-type schemes appears to significantly improve when λ value increases, except the HL scheme with the steady-state UCL.

4. Particularly, in terms of detecting a mixed shift that involves $\theta \geq 2$, all the schemes, except the DL scheme with the steady-state UCL, are performing equally well.

5. In general, the DL scheme with the time-varying UCL seems to be superior when $\lambda \in \{0.05, 0.10\}$. In addition, the other two memory-type schemes with time-varying UCLs also appear to perform well, in terms of detecting a large disturbance in the process.

6. Generally, the HL scheme with the steady-state UCL seems to be superior in detecting a pure scale shift and small to moderate mixed shift when $\lambda = 0.20$. Then, in terms of detecting a pure location shift, the DL scheme with the time-varying UCL appears to be the best.

Table 4.17: The OOC Performance of Various Schemes when $(m, n) = (100, 5)$ and $\lambda = 0.05$ for the Memory-Type Schemes when $ARL_0 \approx 500$ under the Shifted Exponential Distribution

Case	θ	δ	Memory-Type Schemes ($\lambda = 0.05$)						SL (SS UCL)
			EL		DL		HL		
			TV UCL	SS UCL	TV UCL	SS UCL	TV UCL	SS UCL	
Pure Shift in θ	0.1	1	1029.9 (1532.4)	993.2 (1456.1)	1025.3 (1643.1)	1032.3 (1550.9)	1061.3 (1597.7)	912.5 (1719.7)	879.9 (1144.6)
	0.25	1	128.1 (469.2)	136.5 (458.5)	100.1 (463.6)	113.7 (433.3)	119.3 (472.9)	96.7 (540.5)	510.1 (787.2)
	0.5	1	5.8 (7.0)	9.9 (6.9)	3.2 (4.0)	12.5 (4.2)	5.4 (5.7)	2.5 (26.9)	161.8 (298.2)
	1	1	1.7 (1.1)	3.6 (1.6)	1.2 (0.5)	7.0 (1.7)	1.8 (1.2)	1.8 (0.4)	16.7 (38.5)
	1.5	1	1.0 (0.2)	1.8 (0.6)	1.0 (0.1)	4.6 (0.8)	1.0 (0.2)	1.3 (0.5)	2.2 (3.4)
	2	1	1.0 (0.0)	1.2 (0.4)	1.0 (0.0)	3.7 (0.5)	1.0 (0.0)	1.0 (0.2)	1.1 (0.4)
Pure Shift in δ	0	1.25	122.0 (303.5)	133.4 (275.0)	107.3 (323.6)	126.9 (283.1)	113.0 (288.0)	89.2 (398.9)	195.3 (278.6)
	0	1.5	24.3 (48.5)	32.1 (48.7)	19.5 (42.9)	32.7 (41.4)	23.4 (44.0)	11.3 (56.3)	68.5 (93.2)
	0	1.75	9.2 (13.1)	14.2 (15.5)	7.5 (11.5)	17.1 (12.0)	9.2 (12.6)	4.6 (8.3)	30.5 (38.0)
	0	2	5.2 (6.0)	8.6 (6.8)	4.3 (5.7)	12.2 (5.8)	5.3 (5.9)	3.2 (3.5)	16.8 (19.6)
Mixed Shift in θ and δ	0.1	1.25	121.4 (354.4)	127.0 (325.1)	113.1 (411.7)	125.4 (360.5)	111.6 (343.3)	86.8 (432.4)	182.0 (294.8)
	0.1	1.5	19.3 (37.6)	26.4 (42.8)	15.5 (36.4)	27.5 (38.5)	18.4 (32.6)	9.5 (58.0)	56.9 (79.5)
	0.1	1.75	7.5 (10.2)	12.0 (11.4)	6.2 (9.7)	15.3 (9.5)	7.6 (9.8)	4.1 (6.5)	25.7 (32.3)
	0.1	2	4.5 (4.9)	7.7 (5.8)	3.7 (4.7)	11.2 (5.0)	4.7 (4.9)	2.9 (2.5)	14.5 (16.9)
	0.25	1.25	22.6 (67.3)	29.3 (78.1)	16.1 (75.6)	27.9 (68.4)	20.1 (54.1)	9.7 (71.7)	110.5 (184.8)
	0.25	1.5	8.1 (11.6)	12.8 (13.2)	6.0 (10.1)	15.3 (9.7)	7.8 (10.5)	3.8 (7.1)	38.0 (52.8)
	0.25	1.75	4.6 (5.0)	7.9 (6.0)	3.5 (4.4)	11.3 (5.0)	4.7 (4.8)	2.8 (2.3)	18.3 (22.7)
	0.25	2	3.2 (3.0)	5.7 (3.7)	2.5 (2.7)	9.3 (3.3)	3.4 (3.0)	2.4 (1.5)	10.9 (12.5)
	0.5	1.25	4.1 (3.9)	7.4 (4.5)	2.5 (2.5)	10.7 (3.3)	4.0 (3.4)	2.2 (1.7)	43.2 (71.3)
	0.5	1.5	3.0 (2.5)	5.5 (3.2)	2.0 (1.7)	9.0 (2.7)	3.1 (2.4)	2.1 (0.7)	17.8 (24.7)
	0.5	1.75	2.3 (1.8)	4.4 (2.4)	1.7 (1.2)	7.8 (2.2)	2.5 (1.8)	1.9 (0.6)	9.8 (11.9)
	0.5	2	1.9 (1.4)	3.6 (1.9)	1.5 (0.9)	7.0 (1.8)	2.1 (1.5)	1.9 (0.5)	6.4 (7.0)
	1	1.25	1.4 (0.8)	2.9 (1.3)	1.1 (0.4)	6.1 (1.4)	1.5 (0.9)	1.7 (0.4)	6.5 (10.0)
	1	1.5	1.3 (0.6)	2.4 (1.0)	1.1 (0.3)	5.5 (1.2)	1.3 (0.7)	1.6 (0.5)	3.8 (4.7)
	1	1.75	1.2 (0.4)	2.2 (0.9)	1.0 (0.2)	5.1 (1.0)	1.2 (0.6)	1.5 (0.5)	2.7 (2.8)
	1	2	1.1 (0.4)	2.0 (0.8)	1.0 (0.2)	4.8 (0.9)	1.1 (0.5)	1.4 (0.5)	2.2 (2.0)
	1.5	1.25	1.0 (0.1)	1.7 (0.6)	1.0 (0.0)	4.3 (0.7)	1.0 (0.1)	1.2 (0.4)	1.6 (1.5)
	1.5	1.5	1.0 (0.1)	1.5 (0.6)	1.0 (0.0)	4.1 (0.6)	1.0 (0.1)	1.2 (0.4)	1.3 (0.9)
	1.5	1.75	1.0 (0.1)	1.4 (0.5)	1.0 (0.0)	3.9 (0.6)	1.0 (0.1)	1.1 (0.3)	1.2 (0.6)
	1.5	2	1.0 (0.1)	1.3 (0.5)	1.0 (0.0)	3.8 (0.6)	1.0 (0.1)	1.1 (0.3)	1.1 (0.5)
	2	1.25	1.0 (0.0)	1.2 (0.4)	1.0 (0.0)	3.6 (0.5)	1.0 (0.0)	1.0 (0.1)	1.0 (0.2)
	2	1.5	1.0 (0.0)	1.1 (0.3)	1.0 (0.0)	3.4 (0.5)	1.0 (0.0)	1.0 (0.1)	1.0 (0.1)
	2	1.75	1.0 (0.0)	1.1 (0.3)	1.0 (0.0)	3.3 (0.5)	1.0 (0.0)	1.0 (0.1)	1.0 (0.1)
	2	2	1.0 (0.0)	1.1 (0.2)	1.0 (0.0)	3.3 (0.4)	1.0 (0.0)	1.0 (0.1)	1.0 (0.1)

Note: The HL scheme with the SS UCL is not considered for comparison due to its extraordinary high early FAR.

Table 4.18: The OOC Performance of Various Schemes when $(m, n) = (100, 5)$ and $\lambda = 0.10$ for the Memory-Type Schemes when $ARL_0 \approx 500$ under the Shifted Exponential Distribution

Case	θ	δ	Memory-Type Schemes ($\lambda = 0.10$)						SL (SS UCL)
			EL		DL		HL		
			TV UCL	SS UCL	TV UCL	SS UCL	TV UCL	SS UCL	
Pure Shift in θ	0.1	1	967.4 (1377.8)	944.7 (1332.5)	982.4 (1485.2)	972.2 (1424.9)	952.1 (1310.3)	951.6 (1556.8)	879.9 (1144.6)
	0.25	1	165.9 (467.3)	161.9 (440.7)	118.7 (436.7)	125.2 (416.2)	166.5 (427.2)	137.1 (543.4)	510.1 (787.2)
	0.5	1	9.3 (11.5)	11.6 (10.9)	5.2 (6.4)	10.9 (5.6)	12.2 (11.8)	3.1 (4.8)	161.8 (298.2)
	1	1	2.2 (1.6)	3.5 (1.8)	1.5 (0.9)	5.5 (1.5)	3.0 (2.1)	1.9 (0.3)	16.7 (38.5)
	1.5	1	1.1 (0.3)	1.7 (0.7)	1.0 (0.1)	3.5 (0.7)	1.2 (0.6)	1.4 (0.5)	2.2 (3.4)
	2	1	1.0 (0.0)	1.1 (0.4)	1.0 (0.0)	2.9 (0.4)	1.0 (0.1)	1.0 (0.2)	1.1 (0.4)
Pure Shift in δ	0	1.25	140.2 (280.5)	145.1 (273.1)	127.1 (299.9)	137.9 (291.8)	152.7 (253.4)	115.3 (344.4)	195.3 (278.6)
	0	1.5	32.2 (58.0)	37.3 (57.9)	26.4 (51.3)	34.7 (51.4)	41.7 (57.2)	19.3 (58.8)	68.5 (93.2)
	0	1.75	12.1 (16.0)	15.3 (17.7)	10.0 (14.1)	16.2 (14.8)	16.9 (18.6)	6.5 (11.3)	30.5 (38.0)
	0	2	6.6 (7.5)	8.8 (7.7)	5.6 (6.7)	10.7 (6.4)	9.3 (9.4)	3.9 (4.8)	16.8 (19.6)
Mixed Shift in θ and δ	0.1	1.25	137.4 (326.8)	139.2 (302.9)	124.8 (354.9)	133.7 (343.0)	139.7 (274.0)	106.6 (368.1)	182.0 (294.8)
	0.1	1.5	26.0 (45.8)	29.7 (48.4)	20.9 (41.8)	28.5 (44.4)	33.4 (43.7)	14.5 (41.9)	56.9 (79.5)
	0.1	1.75	10.0 (13.1)	12.7 (14.1)	8.2 (11.5)	13.9 (10.8)	14.0 (15.2)	5.5 (9.7)	25.7 (32.3)
	0.1	2	5.7 (6.2)	7.7 (6.4)	4.8 (5.6)	9.7 (5.5)	8.0 (7.8)	3.6 (3.9)	14.5 (16.9)
	0.25	1.25	32.9 (82.3)	35.8 (80.6)	23.1 (78.5)	30.2 (62.6)	38.9 (64.1)	17.3 (72.3)	110.5 (184.8)
	0.25	1.5	11.2 (15.7)	14.1 (16.3)	8.4 (12.4)	14.2 (12.8)	15.4 (17.1)	5.5 (10.6)	38.0 (52.8)
	0.25	1.75	6.0 (6.7)	8.1 (7.0)	4.8 (5.6)	9.7 (5.4)	8.3 (8.2)	3.4 (3.7)	18.3 (22.7)
	0.25	2	4.0 (3.8)	5.7 (4.2)	3.3 (3.4)	7.7 (3.3)	5.5 (4.9)	2.7 (2.0)	10.9 (12.5)
	0.5	1.25	6.0 (5.9)	8.1 (6.0)	3.8 (3.6)	8.9 (3.6)	8.0 (7.1)	2.6 (2.2)	43.2 (71.3)
	0.5	1.5	4.0 (3.5)	5.7 (3.7)	2.8 (2.5)	7.4 (2.6)	5.4 (4.3)	2.3 (1.3)	17.8 (24.7)
	0.5	1.75	2.9 (2.4)	4.4 (2.6)	2.2 (1.8)	6.3 (2.1)	3.9 (3.0)	2.1 (0.9)	9.8 (11.9)
	0.5	2	2.4 (1.8)	3.6 (2.0)	1.8 (1.3)	5.6 (1.7)	3.1 (2.3)	1.9 (0.7)	6.4 (7.0)
	1	1.25	1.7 (1.1)	2.8 (1.4)	1.3 (0.6)	4.8 (1.2)	2.2 (1.5)	1.7 (0.4)	6.5 (10.0)
	1	1.5	1.4 (0.8)	2.3 (1.1)	1.2 (0.5)	4.3 (1.0)	1.8 (1.2)	1.6 (0.5)	3.8 (4.7)
	1	1.75	1.3 (0.6)	2.1 (0.9)	1.1 (0.4)	3.9 (0.9)	1.6 (1.0)	1.6 (0.5)	2.7 (2.8)
	1	2	1.2 (0.5)	1.9 (0.8)	1.1 (0.3)	3.7 (0.8)	1.4 (0.9)	1.5 (0.5)	2.2 (2.0)
	1.5	1.25	1.0 (0.2)	1.5 (0.6)	1.0 (0.1)	3.3 (0.6)	1.1 (0.4)	1.2 (0.4)	1.6 (1.5)
	1.5	1.5	1.0 (0.2)	1.4 (0.5)	1.0 (0.1)	3.2 (0.5)	1.1 (0.3)	1.2 (0.4)	1.3 (0.9)
	1.5	1.75	1.0 (0.1)	1.3 (0.5)	1.0 (0.0)	3.1 (0.4)	1.0 (0.2)	1.1 (0.3)	1.2 (0.6)
	1.5	2	1.0 (0.1)	1.3 (0.4)	1.0 (0.0)	3.0 (0.4)	1.0 (0.2)	1.1 (0.3)	1.1 (0.5)
	2	1.25	1.0 (0.0)	1.1 (0.3)	1.0 (0.0)	2.8 (0.4)	1.0 (0.0)	1.0 (0.1)	1.0 (0.2)
	2	1.5	1.0 (0.0)	1.1 (0.2)	1.0 (0.0)	2.7 (0.5)	1.0 (0.0)	1.0 (0.1)	1.0 (0.1)
	2	1.75	1.0 (0.0)	1.0 (0.2)	1.0 (0.0)	2.6 (0.5)	1.0 (0.0)	1.0 (0.1)	1.0 (0.1)
	2	2	1.0 (0.0)	1.0 (0.2)	1.0 (0.0)	2.6 (0.5)	1.0 (0.0)	1.0 (0.1)	1.0 (0.1)

Note: The HL scheme with the SS UCL is not considered for comparison due to its extraordinary high early FAR.

Table 4.19: The OOC Performance of Various Schemes when $(m, n) = (100, 5)$ and $\lambda = 0.20$ for the Memory-Type Schemes when $ARL_0 \approx 500$ under the Shifted Exponential Distribution

Case	θ	δ	Memory-Type Schemes ($\lambda = 0.20$)						SL (SS UCL)
			EL		DL		HL		
			TV UCL	SS UCL	TV UCL	SS UCL	TV UCL	SS UCL	
Pure Shift in θ	0.1	1	917.3 (1247.7)	914.7 (1234.7)	929.6 (1332.1)	947.2 (1328.5)	909.0 (1203.8)	930.8 (1345.8)	879.9 (1144.6)
	0.25	1	231.2 (504.3)	231.2 (496.5)	153.6 (441.1)	155.7 (432.0)	238.3 (480.2)	209.1 (537.4)	510.1 (787.2)
	0.5	1	17.6 (25.9)	18.9 (25.8)	8.1 (11.0)	10.8 (11.5)	22.7 (25.3)	8.8 (19.2)	161.8 (298.2)
	1	1	2.9 (2.6)	3.7 (2.6)	2.0 (1.4)	4.2 (1.4)	4.2 (3.3)	2.0 (1.0)	16.7 (38.5)
	1.5	1	1.2 (0.4)	1.6 (0.7)	1.0 (0.2)	2.5 (0.6)	1.4 (0.8)	1.4 (0.5)	2.2 (3.4)
	2	1	1.0 (0.1)	1.1 (0.3)	1.0 (0.0)	2.0 (0.2)	1.0 (0.2)	1.0 (0.2)	1.1 (0.4)
Pure Shift in δ	0	1.25	160.9 (275.5)	163.9 (271.7)	147.1 (294.1)	150.1 (273.1)	172.5 (255.7)	139.0 (284.8)	195.3 (278.6)
	0	1.5	42.0 (67.7)	44.2 (67.1)	34.2 (60.0)	38.6 (58.3)	51.8 (65.6)	32.9 (69.0)	68.5 (93.2)
	0	1.75	15.8 (20.4)	17.5 (20.7)	12.8 (17.6)	16.1 (18.7)	22.1 (23.0)	11.4 (18.3)	30.5 (38.0)
	0	2	8.4 (9.7)	9.7 (9.7)	7.0 (7.9)	9.7 (8.0)	12.2 (11.3)	5.8 (7.8)	16.8 (19.6)
Mixed Shift in θ and δ	0.1	1.25	151.0 (297.1)	153.5 (293.4)	140.5 (329.1)	144.0 (316.7)	156.7 (266.7)	131.4 (314.3)	182.0 (294.8)
	0.1	1.5	33.8 (54.3)	35.9 (54.1)	27.0 (47.6)	31.4 (49.3)	42.0 (52.2)	26.0 (59.0)	56.9 (79.5)
	0.1	1.75	13.1 (16.9)	14.6 (17.2)	10.5 (13.9)	13.6 (14.5)	18.3 (18.7)	9.3 (16.7)	25.7 (32.3)
	0.1	2	7.2 (8.0)	8.4 (8.1)	6.0 (6.6)	8.5 (6.4)	10.4 (9.5)	5.1 (6.4)	14.5 (16.9)
	0.25	1.25	49.1 (97.2)	51.1 (96.3)	32.7 (83.4)	36.4 (80.3)	56.2 (85.2)	35.2 (86.7)	110.5 (184.8)
	0.25	1.5	16.1 (23.7)	17.7 (24.0)	11.4 (16.7)	14.4 (16.1)	21.6 (24.0)	10.6 (18.6)	38.0 (52.8)
	0.25	1.75	8.0 (9.4)	9.2 (9.5)	6.1 (6.9)	8.7 (6.6)	11.3 (10.6)	5.3 (7.4)	18.3 (22.7)
	0.25	2	5.1 (5.0)	6.0 (5.0)	4.1 (4.0)	6.4 (3.8)	7.3 (6.3)	3.5 (3.6)	10.9 (12.5)
	0.5	1.25	9.2 (11.0)	10.4 (11.0)	5.4 (5.5)	7.9 (4.9)	12.8 (11.9)	5.1 (8.1)	43.2 (71.3)
	0.5	1.5	5.5 (5.5)	6.5 (5.5)	3.8 (3.4)	6.1 (3.3)	7.7 (6.5)	3.3 (3.7)	17.8 (24.7)
	0.5	1.75	3.8 (3.3)	4.6 (3.3)	2.8 (2.4)	5.0 (2.2)	5.3 (4.2)	2.6 (2.0)	9.8 (11.9)
	0.5	2	2.9 (2.3)	3.6 (2.4)	2.3 (1.8)	4.3 (1.7)	4.0 (3.0)	2.2 (1.3)	6.4 (7.0)
	1	1.25	2.1 (1.5)	2.8 (1.6)	1.5 (1.0)	3.6 (1.1)	2.9 (2.0)	1.8 (0.6)	6.5 (10.0)
	1	1.5	1.7 (1.1)	2.3 (1.2)	1.3 (0.7)	3.1 (0.9)	2.3 (1.5)	1.7 (0.5)	3.8 (4.7)
	1	1.75	1.5 (0.8)	2.0 (1.0)	1.2 (0.6)	2.9 (0.8)	1.9 (1.2)	1.6 (0.5)	2.7 (2.8)
	1	2	1.3 (0.7)	1.8 (0.8)	1.2 (0.4)	2.7 (0.7)	1.7 (1.0)	1.5 (0.5)	2.2 (2.0)
	1.5	1.25	1.1 (0.3)	1.4 (0.6)	1.0 (0.2)	2.3 (0.5)	1.2 (0.6)	1.3 (0.4)	1.6 (1.5)
	1.5	1.5	1.1 (0.2)	1.3 (0.5)	1.0 (0.1)	2.2 (0.4)	1.2 (0.5)	1.2 (0.4)	1.3 (0.9)
	1.5	1.75	1.0 (0.2)	1.2 (0.5)	1.0 (0.1)	2.1 (0.4)	1.1 (0.4)	1.1 (0.3)	1.2 (0.6)
	1.5	2	1.0 (0.2)	1.2 (0.4)	1.0 (0.1)	2.1 (0.3)	1.1 (0.3)	1.1 (0.3)	1.1 (0.5)
	2	1.25	1.0 (0.0)	1.1 (0.2)	1.0 (0.0)	2.0 (0.1)	1.0 (0.1)	1.0 (0.1)	1.0 (0.2)
	2	1.5	1.0 (0.0)	1.0 (0.2)	1.0 (0.0)	2.0 (0.1)	1.0 (0.1)	1.0 (0.1)	1.0 (0.1)
	2	1.75	1.0 (0.0)	1.0 (0.1)	1.0 (0.0)	2.0 (0.1)	1.0 (0.1)	1.0 (0.1)	1.0 (0.1)
	2	2	1.0 (0.0)	1.0 (0.1)	1.0 (0.0)	2.0 (0.1)	1.0 (0.1)	1.0 (0.1)	1.0 (0.1)

4.4 OOC Performance Analysis of the SL, EL, DL, and HL Schemes at Macro Level

From the OOC performance comparison study in Section 4.3, one might think that, on average, the DL scheme with the time-varying UCL appears to be the best choice to use for process monitoring if $\lambda < 0.20$. Then, if one uses $\lambda = 0.20$, both the DL scheme with the time-varying UCL and the HL scheme with the steady-state UCL seem to be competitively good. To this end, quality practitioners prefer to use a scheme with the best overall performance due to the exact shift size is hardly known in real life. To achieve this objective, the $EARL$ index of various schemes are assessed. Similar to the OOC performance comparison study done in Section 4.3, only the setting of $(m, n) = (100, 5)$ with $ARL_0 \approx 500$ is implemented here.

To compare the OOC performance of various schemes at the macro level, four scenarios will be considered, which are explained in Table 4.20. One may find that the possible downward shift in the scale parameter is not included here. This is because, in many contexts, especially the manufacturing sectors, the reduction of scale is not treated as an issue; instead, it is regarded as a process improvement.

Table 4.20: Four Scenarios of OOC Cases Studied in Macro Level

Scenario	Possible shift		Description on
	Location (L) parameter	Scale (S) parameter	$\boldsymbol{\theta} \times \boldsymbol{\delta}$
I (LUB-SUB)	U in B	U in B	$[0, 3] \times [1, 3]$
II (LDB-SUB)	D in B	U in B	$[-3, 0] \times [1, 3]$
III (LUM-SUM)	U in M	U in M	$[0, 1.5] \times [1,2]$
IV (LDM-SUM)	D in M	U in M	$[-1.5, 0] \times [1,2]$

Note:
(i) U indicates an upward shift, while D indicates a downward shift.
(ii) B indicates a broader region, while M indicates a small to moderate region.

The $EARL$ values of all the schemes under Normal, Laplace, and Shifted Exponential distributions are tabulated in Tables 4.21, 4.22, and 4.23, respectively. Refers to Tables 4.21 – 4.23, one can easily notice that the $EARL$ value of the SL scheme is always the highest among all the schemes. This indicates that the SL scheme performs the worst because it requires more test samples to signal an OOC signal in general. Hence, it is much interesting to study and compare the performance of the memory-type EL, DL, and HL schemes.

Some of the observations regarding the memory-type schemes that can be made by referring to Tables 4.21 – 4.23 are

1. Regardless of the probability distribution and scenarios, the EL and DL schemes seem to perform better with their time-varying UCLs, compared to their respective steady-state UCLs. This is because their $EARL$ values with time-varying UCLs are lower. On the other hand, the HL scheme displays an opposite pattern, i.e., the HL scheme with the steady-state UCL outperforms the HL scheme with the time-varying UCL. These findings are probably related to the IC's performance of the schemes.

Typically, a scheme with a better IC performance will have a wider control band, which makes the detection of any OOC signal to be slower. Hence, the OOC's performance of the scheme appears as the opposite of its IC's performance. Therefore, since the HL scheme with the time-varying UCL has a better IC performance compared to the HL scheme with the steady-state UCL, the latter scheme has a better OOC performance compared to the former scheme.

2. The HL scheme with the steady-state UCL has the lowest $EARL$ value, regardless of the distribution and scenarios. This indicates that this scheme appears to be superior. However, as discussed previously, the HL scheme with the steady-state UCL is not recommended due to its extraordinary high early FAR when $\lambda < 0.20$. To this end,
    a. When $\lambda = 0.05$ and $\lambda = 0.10$, the DL scheme with the time-varying UCL appears to be the better option due to its lowest $EARL$ value.
    b. It is worth mentioning that when $\lambda = 0.05$, both the proposed DL and HL schemes with time-varying UCLs seem to be the two best performers, where the DL scheme with the time-varying UCL is marginally better.
    c. When $\lambda = 0.20$, both the HL scheme with the steady-state UCL and the DL scheme with the time-varying UCL seem to be good choices, where the HL scheme with the steady-state UCL is marginally better, except under the LDB-SUB and LDM-SUM scenarios of the Laplace distribution.

3. When the value of λ value increases, it is noticed that the performance of all the memory-type schemes, except the DL scheme with the steady-state UCL, deteriorates ($EARL$ value increases). For the DL scheme with the steady-state UCL, when λ value increases,
    a. Its performance improves under the LUB-SUB and LDB-SUB scenarios of the Normal and Shifted Exponential distributions.
    b. Its performance deteriorates under the LUM-SUM and LDM-SUM scenarios of the Normal and Laplace distributions.
    c. Its performance improves, but it deteriorates if one keeps on increasing λ value under the LUB-SUB and LDB-SUB scenarios of the Laplace distribution, and under the LUB-SUB and LDB-SUB scenarios of the Shifted Exponential distribution.

4. One can find that the value of the smoothing parameter plays an essential role in determining the performance of a scheme. For instance,
    a. λ value should be small, says 0.05, for all the schemes, except the DL scheme with the steady-state UCL.
    b. For the DL scheme with the steady-state UCL, λ value should be slightly larger, says 0.10.

5. Under a symmetric distribution, the performance of a scheme in detecting an upward shift or a downward shift in the location parameter is almost similar. For instance, under the Normal distribution, from Table 4.21, it is observed that the $EARL$ value of all the schemes in the

LUB-SUB and LDB-SUB scenarios are nearly the same. Similarly, the $EARL$ value in the LUM-SUM and LDM-SUM scenarios are also nearly the same. Note that the same deduction can be made for the symmetric Laplace distribution (refers to Table 4.22).

6. On the flip side, for the asymmetric Shifted Exponential distribution (Table 4.23), one may see that all the schemes appear to be better in detecting a downward location shift (lower $EARL$ value). For instance, the $EARL$ values of all the schemes in the LDB-SUB scenario are relatively lower than their corresponding $EARL$ value in the LUB-SUB scenario. The same findings are obtained by comparing the LDM-SUM and LUM-SUM scenarios.

Table 4.21: $EARL$ Values of Various Schemes when $(m, n) = (100, 5)$ and $ARL_0 \approx 500$ under the Normal Distribution

	λ	EL		DL		HL		SL
		TV UCL	SS UCL	TV UCL	SS UCL	TV UCL	SS UCL	(SS UCL)
(I) LUB-SUB	0.05	10.050	11.933	9.244	14.510	9.814	8.308	
	0.10	11.382	12.464	10.309	13.759	12.669	9.629	17.374
	0.20	12.791	13.463	11.605	13.612	14.459	11.450	
	λ	EL		DL		HL		SL
		TV UCL	SS UCL	TV UCL	SS UCL	TV UCL	SS UCL	(SS UCL)
(II) LDB-SUB	0.05	10.048	11.982	9.294	14.433	9.868	8.378	
	0.10	11.368	12.506	10.380	13.823	12.759	9.542	17.329
	0.20	12.782	13.475	11.688	13.625	14.602	11.417	
	λ	EL		DL		HL		SL
		TV UCL	SS UCL	TV UCL	SS UCL	TV UCL	SS UCL	(SS UCL)
(III) LUM-SUM	0.05	29.807	33.558	27.586	35.588	28.783	24.024	
	0.10	33.631	35.469	30.640	35.684	36.699	28.191	49.247
	0.20	37.573	38.756	34.358	37.332	41.443	33.728	
	λ	EL		DL		HL		SL
		TV UCL	SS UCL	TV UCL	SS UCL	TV UCL	SS UCL	(SS UCL)
(IV) LDM-SUM	0.05	29.813	33.731	27.760	35.331	28.974	24.265	
	0.10	33.597	35.625	30.880	35.904	37.011	27.900	49.148
	0.20	37.552	38.807	34.638	37.389	41.927	33.624	

Table 4.22: $EARL$ Values of Various Schemes when $(m, n) = (100, 5)$ and $ARL_0 \approx 500$ under the Laplace Distribution

	λ	EL		DL		HL		SL
		TV UCL	SS UCL	TV UCL	SS UCL	TV UCL	SS UCL	(SS UCL)
(I) LUB-SUB	0.05	14.222	16.565	13.036	18.902	13.944	12.005	
	0.10	16.150	17.464	14.595	18.417	18.037	13.511	26.189
	0.20	18.373	19.250	16.478	18.638	20.814	16.466	
	λ	EL		DL		HL		SL
		TV UCL	SS UCL	TV UCL	SS UCL	TV UCL	SS UCL	(SS UCL)
(II) LDB-SUB	0.05	14.211	16.548	13.031	18.862	13.938	11.862	
	0.10	16.156	17.439	14.596	18.439	18.026	13.567	26.251
	0.20	18.389	19.238	16.447	18.624	20.823	16.492	
	λ	EL		DL		HL		SL
		TV UCL	SS UCL	TV UCL	SS UCL	TV UCL	SS UCL	(SS UCL)
(III) LUM-SUM	0.05	42.518	46.963	39.316	47.809	41.370	35.641	
	0.10	47.883	49.909	43.660	48.902	52.327	40.128	72.496
	0.20	53.905	55.402	48.920	51.889	59.412	48.821	
	λ	EL		DL		HL		SL
		TV UCL	SS UCL	TV UCL	SS UCL	TV UCL	SS UCL	(SS UCL)
(IV) LDM-SUM	0.05	42.499	46.906	39.299	47.680	41.367	35.173	
	0.10	47.922	49.837	43.660	48.990	52.331	40.323	72.675
	0.20	54.001	55.407	48.823	51.883	59.495	48.913	

Table 4.23: $EARL$ Values of Various Schemes when $(m, n) = (100, 5)$ and $ARL_0 \approx 500$ under the Shifted Exponential Distribution

	λ	EL		DL		HL		SL
		TV UCL	SS UCL	TV UCL	SS UCL	TV UCL	SS UCL	(SS UCL)
(I) LUB-SUB	0.05	16.907	18.048	16.131	20.351	16.687	14.623	
	0.10	17.786	18.285	16.699	19.396	18.279	15.796	27.139
	0.20	19.090	19.545	17.590	19.263	20.008	17.570	
	λ	EL		DL		HL		SL
		TV UCL	SS UCL	TV UCL	SS UCL	TV UCL	SS UCL	(SS UCL)
(II) LDB-SUB	0.05	7.833	9.439	7.308	12.111	7.834	6.775	
	0.10	8.771	9.714	8.057	11.246	9.901	7.560	13.048
	0.20	9.733	10.325	8.920	10.729	11.200	8.641	
	λ	EL		DL		HL		SL
		TV UCL	SS UCL	TV UCL	SS UCL	TV UCL	SS UCL	(SS UCL)
(III) LUM-SUM	0.05	53.003	55.347	50.769	57.248	52.264	45.647	
	0.10	55.467	56.125	52.296	56.255	56.452	49.315	82.394
	0.20	59.192	60.087	54.806	57.308	61.292	54.688	
	λ	EL		DL		HL		SL
		TV UCL	SS UCL	TV UCL	SS UCL	TV UCL	SS UCL	(SS UCL)
(IV) LDM-SUM	0.05	22.088	24.895	20.798	27.331	21.859	18.675	
	0.10	24.556	25.978	22.762	27.025	27.020	21.007	34.170
	0.20	26.927	27.889	25.003	27.345	30.034	24.007	

4.5 Implementation in e-Commerce

In this era of globalisation, the internet and mobile data are no longer exclusive to the rich; instead, they are now important for everybody. This indirectly encourages the development of e-commerce, where it is convenient to both sellers and buyers since everything is done online. The development of e-commerce also causes this sector to become more and more competitive. Hence, as e-commerce sellers, they need to understand, and even better, if they can predict the purchasing intention of online shoppers. To this end, an online seller can benefit from some assistants provided by the Google company. This is because Google Analytics introduces various indicators or metrics to help an e-commerce seller to understand their customers more, such as bounce rate, exit rate, page value, among others.

Sakar et al. (2019) employed a few selection methods to classify and predict the purchasing intention of online shoppers in real-time. The techniques they used are minimum redundancy maximum relevance, mutual information, and correlation, which can improve the performance of the system's classification. From the results, they found that the exit rate metric plays an important role in the classification, i.e., it is ranked in the Top 3 among all the variables they studied. The exit rate is defined as the frequency that visitors left a site from a single page, where this metric can help e-commerce sellers to understand their page's performance.

In this dissertation, the dataset used by Sakar et al. (2019), which is available on the Kaggle website, is used as an illustrative example for implementing the schemes. In the dataset, all the behaviours of customers in an e-commerce website from February to December of a given year are recorded. There are 12330 observations for each variable in this dataset. However, only the exit rate is monitored with SL, EL, DL, and HL schemes in this dissertation. Note that there is no data recorded for April; hence April is treated as a break. To this end, the observations before the break, i.e., 184 and 1907 observations from February and March, respectively, are treated as the Phase-I dataset. The stability of this Phase-I dataset is examined in Section 4.5.1. Next, the observations after the break is used for Phase-II monitoring. Since there are many data available for Phase-II monitoring, instead of using all, only the observations straight after the break, i.e., 3364 observations in May are regarded as the Phase-II dataset.

4.5.1 Phase-I Retrospective Analysis of Exit Rate

As discussed in Chapter 1, in SPM, one should first ensure that the Phase-I reference sample is statistically IC. Then, it is suitable to be used as a reference or benchmark in the Phase-II monitoring. Therefore, in this dissertation, a total of three Phase-I analysis methods are used to check the stability and suitability of the Phase-I sample, i.e.,

1. The conventional recursive segmentation and permutation (RS/P) method, which was proposed by Capizzi and Masarotto (2013).

2. The nonparametric Phase-I scheme based on the multi-sample Lepage statistic, which was proposed by Li et al. (2019).
3. The nonparametric Phase-I scheme based on the multi-sample Cucconi statistic, which was proposed by Li et al. (2020).

There are 2091 (i.e., $184 + 2091$) data points available in the Phase-I dataset. In this case study, the subgroup size of a sample is chosen as $n = 20$, which yields 104 samples ($104 \times 20 = 2080$ data points) and 11 redundant data points that have to be omitted. Since it is online monitoring, dropping older data points is better than omitting more recent data points. Consequently, the 11 observations from the beginning are omitted. Note that anyone can randomly skip 11 points, and this will hardly affect the result. Further, the FAR of the Phase-I analysis is set as 0.10 so that a fair comparison among the three aforementioned methods can be made.

The results for Phase-I analysis with the RS/P method, multi-sample Lepage statistic, and multi-sample Cucconi statistic, are depicted in Figures 4.1, 4.2, and 4.3, respectively. The Phase-I sample is deemed statistically IC if one uses multi-sample Lepage statistic (Figure 4.2) and multi-sample Cucconi statistic (Figure 4.3). This is because none of the plotting statistics falls beyond their respective UCLs. However, the RS/P approach suggests that the Phase-I sample is not statistically IC in both the location and scale parameters. From Figure 4.1, both the p-values for testing the location parameter (less than 0.001) and the scale parameter (0.052), are smaller than the FAR chosen. Precisely, it is observed that the plotting statistics of the first ten samples are relatively higher than the rest, as shown in Figure 4.1. This incident is known as a step shift, where it is not surprising that the RS/P approach performs better than the other two Phase-I approaches to detect this kind of shift.

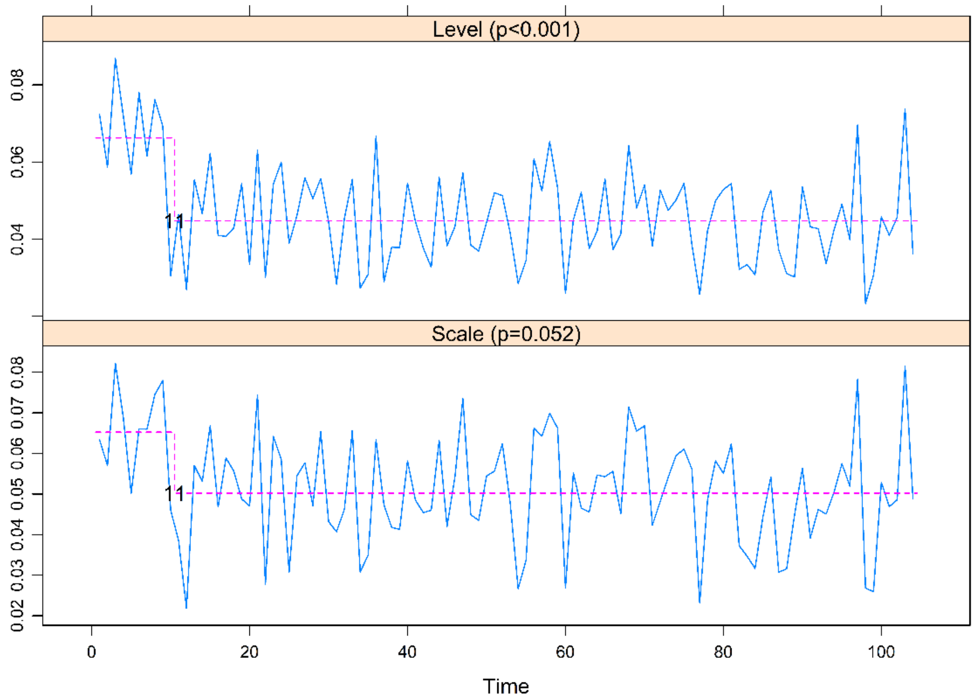

Figure 4.1: Phase-I Analysis of Exit Rate with the RS/P Approach

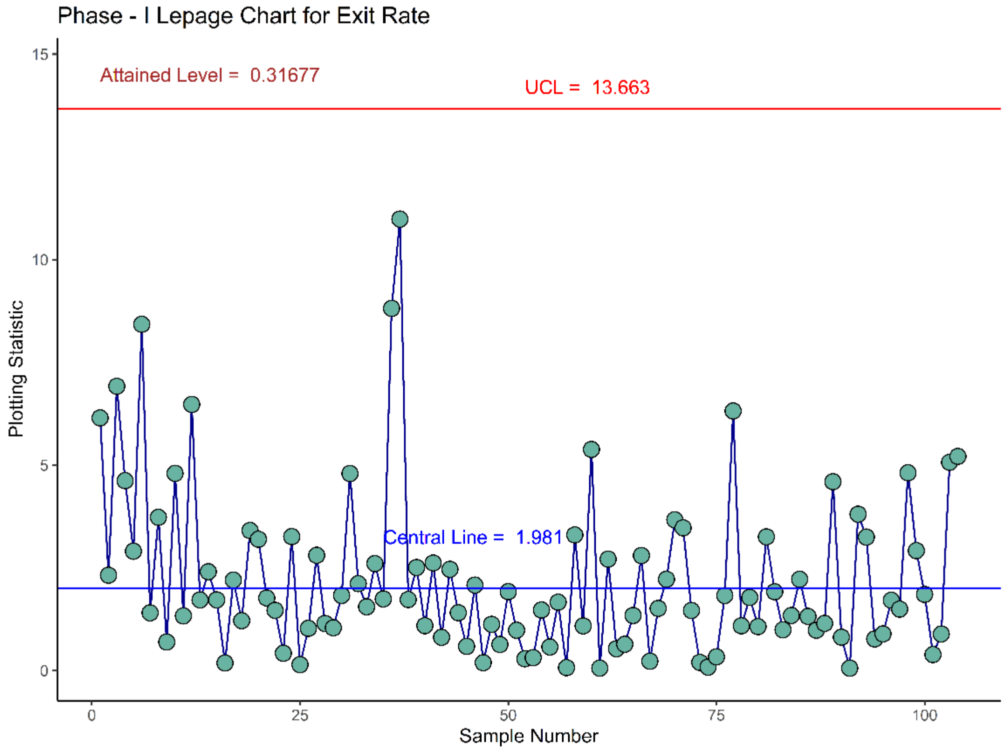

Figure 4.2: Phase-I Analysis of Exit Rate with the Multi-Sample Lepage Statistic

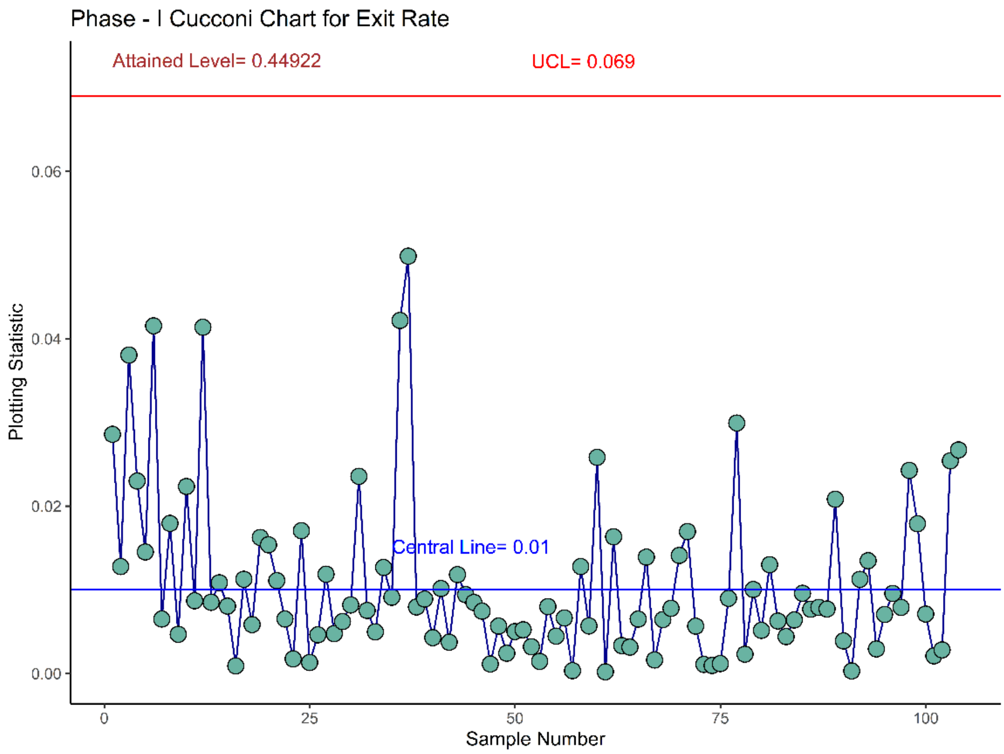

Figure 4.3: Phase-I Analysis of Exit Rate with the Multi-Sample Cucconi Statistic

Then, suppose that the assignable cause(s) of variation in the first ten samples ($10 \times 20 = 200$ observations) is detected, and all these observations are removed. To this end, the revised Phase-I sample is only left with 94 samples, or equivalent to 1880 observations. Again, the three approaches are employed to test the stability of this revised Phase-I sample. The results are then displayed in Figures 4.4, 4.5, and 4.6, respectively, for the RS/P approach, multi-sample Lepage statistic, and multi-sample Cucconi statistic.

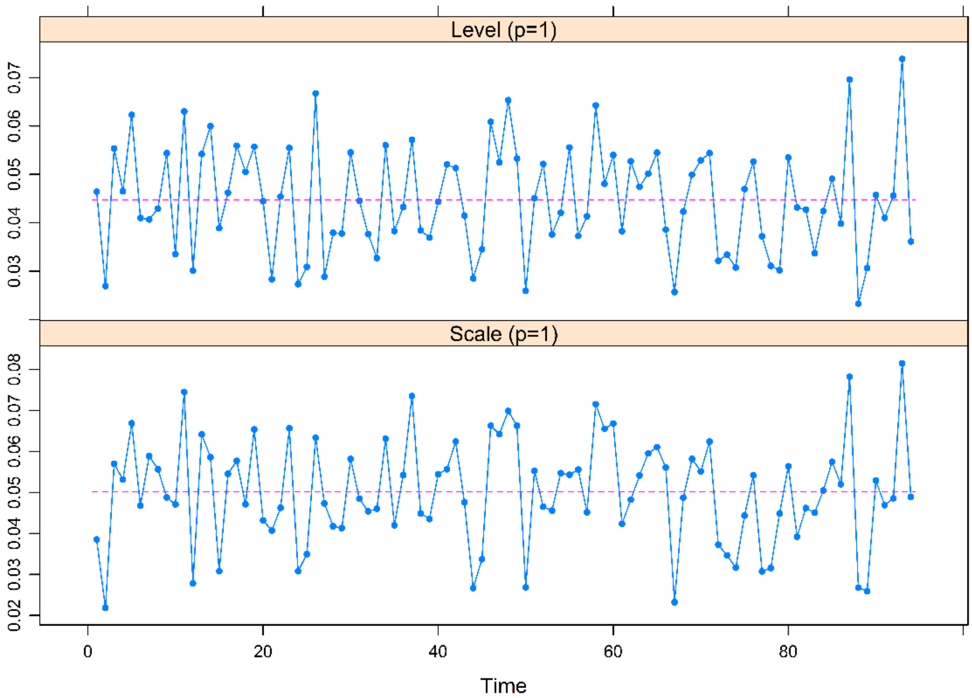

Figure 4.4: Revised Phase-I Analysis of Exit Rate with the RS/P Approach

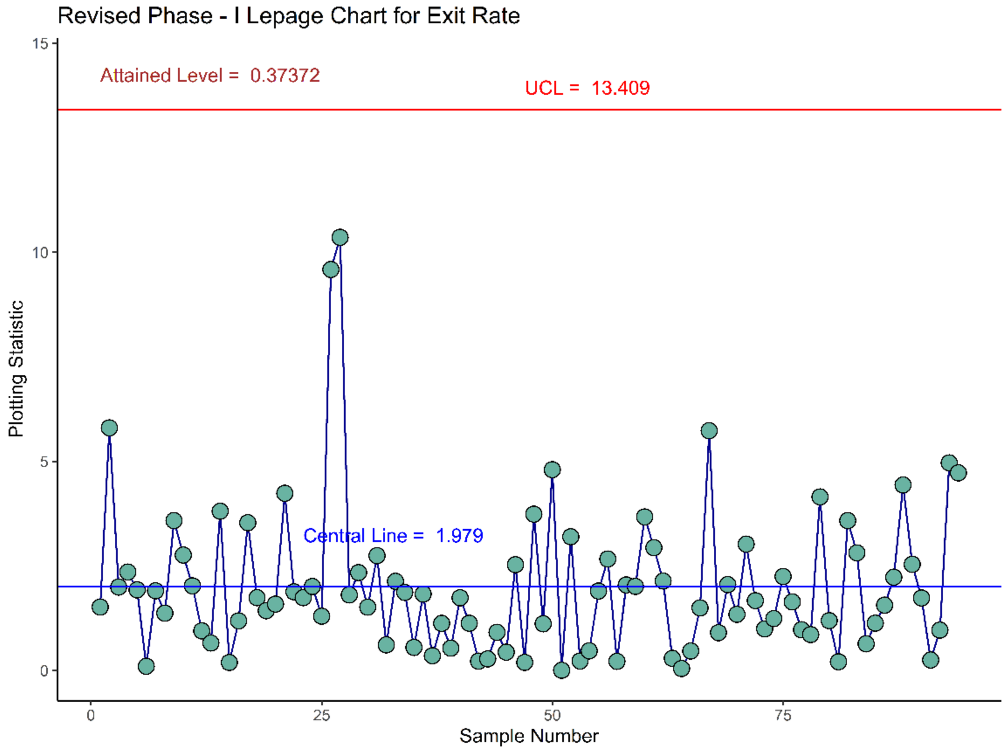

Figure 4.5: Revised Phase-I Analysis of Exit Rate with the Multi-Sample Lepage Statistic

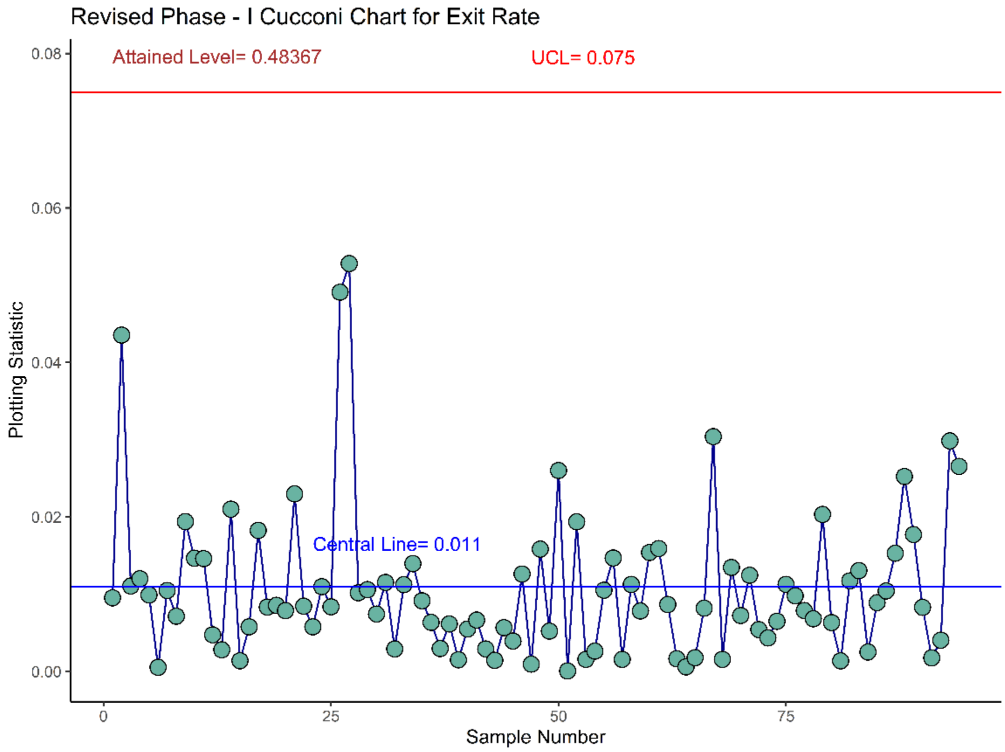

Figure 4.6: Revised Phase-I Analysis of Exit Rate with the Multi-Sample Cucconi Statistic

In conclusion, the revised Phase-I sample is said to be statistically IC based on all three approaches. This is because, with the RS/P method, the p-values for testing the location and scale parameters depicted in Figure 4.4, are all more than FAR, i.e., both are 1. Moreover, from the multi-sample Lepage and Cucconi statistics, none of the 94 plotting statistics is above the UCLs as illustrated in Figures 4.5 and 4.6.

In order to justify the necessity of removing the first ten samples, the estimated kernel densities of the removed 200 data points (10 samples) and the remaining 1880 data points (94 samples) are plotted in Figure 4.7.

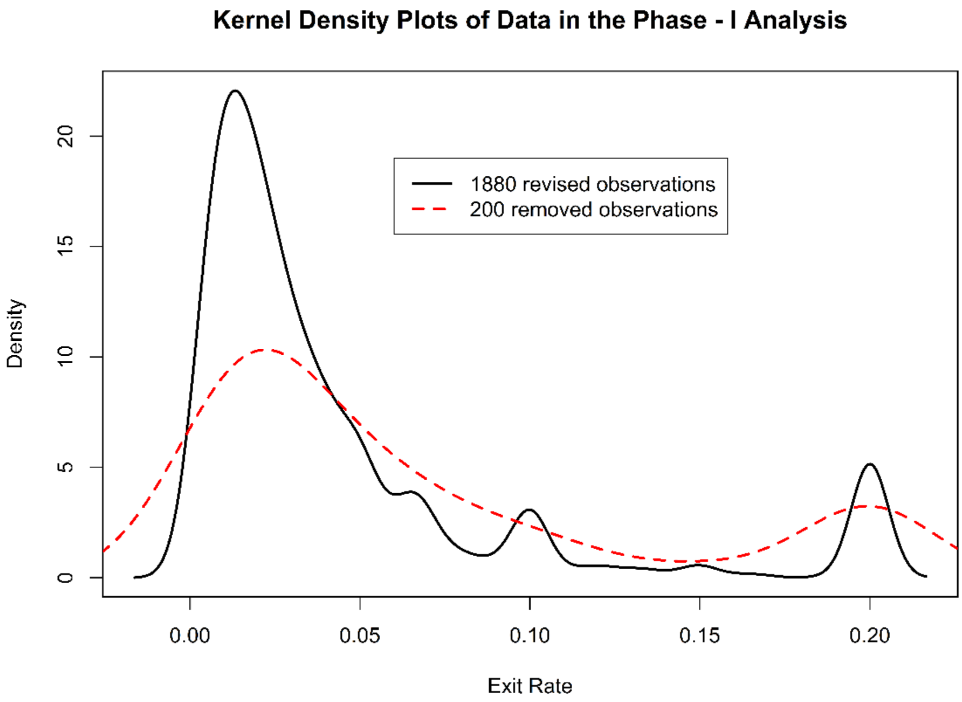

Figure 4.7: Kernel Density Plots of the Removed and Revised Samples

Obviously, from Figure 4.7, the 200 removed observations appear significantly different from the 1880 revised observations. Further, it is found that the density plot of the 1880 revised observations does not follow any statistical probability distribution. To this end, the parametric SPM-type schemes cannot be used to monitor the exit rate in this dataset. Thus, the nonparametric NSPM-type schemes will be the ideal alternatives. This includes the SL, EL, DL, and HL schemes, to be studied in this case study.

Table 4.24: The Ljung-Box Test for the Revised Phase-I Sample

lag	5	7	10	20	29	52	75	100	150	200
p-value	0.320	0.179	0.313	0.565	0.562	0.824	0.811	0.941	0.631	0.725

Further, it is appropriate to assume that all the observations in the revised Phase-I sample are independent. This is because each of the sessions available in the dataset belongs to a distinct online shopper. Besides, the 1880 observations are statistically independent with the Ljung-Box test, which is tabulated in Table 4.24. Hassani and Yeganegi (2020) suggested some suitable lags be used in the Ljung-Box test. For instance, when there are 1000 observations, the selected lags could be 5, 7, 10, 20, 29, and 52. Since the number of observations here is more than 1000, some extra lags, such as 75, 100, 150, and 200, are also considered. From Table 4.11, it is observed that all the p-values at every lag are more than 0.10, which suggests that the 1880 observations available in the revised Phase-I sample are independent.

4.5.2 Phase-II Monitoring of Exit Rate

There are 3364 observations available in the Phase-II sample. Similar to Phase-I analysis, the subgroup size of a test sample in Phase-II monitoring is also fixed as $n = 20$. Therefore, there are 168 test samples ($168 \times 20 = 3360$ observations) available and four redundant observations. Since Phase-II monitoring is done straight after the April break, the first 3360 observations are considered as the Phase-II sample by omitting the last four observations.

In this case study, the targeted ARL_0 is set as 500, and the smoothing parameter of the memory-type schemes is $\lambda = 0.05$. Then, when $m = 1880$ and $n = 20$, the estimated values of ξ_1 and ξ_2 are 0.00166 and 3.8981, respectively. Hence, with the standard searching algorithm, the charting constants of various schemes are tabulated in Table 4.25. Next, the 168 plotting statistics of various schemes are calculated and plotted against their respective UCLs.

Table 4.25: Charting Constants of Various Schemes when $(\boldsymbol{m}, \boldsymbol{n}) = (\mathbf{1880}, \mathbf{20})$ and $\boldsymbol{\lambda} = \mathbf{0.05}$ for the Memory-Type Schemes when $\boldsymbol{ARL_0} \approx \mathbf{500}$

Memory-Type Schemes ($\boldsymbol{\lambda} = \mathbf{0.05}$)						**$\boldsymbol{SL}$ (SS $\boldsymbol{UCL}$)**
$\boldsymbol{EL}$		**$\boldsymbol{DL}$**		**$\boldsymbol{HL}$**		
TV $\boldsymbol{UCL}$	**SS $\boldsymbol{UCL}$**	**TV $\boldsymbol{UCL}$**	**SS $\boldsymbol{UCL}$**	**TV $\boldsymbol{UCL}$**	**SS $\boldsymbol{UCL}$**	
$\boldsymbol{L_{EL}}$	$\boldsymbol{\Psi_{EL}}$	$\boldsymbol{L_{DL}}$	$\boldsymbol{\Psi_{DL}}$	$\boldsymbol{L_{HL}}$	$\boldsymbol{\Psi_{HL}}$	$\boldsymbol{\Psi_{SL}}$
2.595	2.812	1.693	2.362	3.257	2.574	12.277

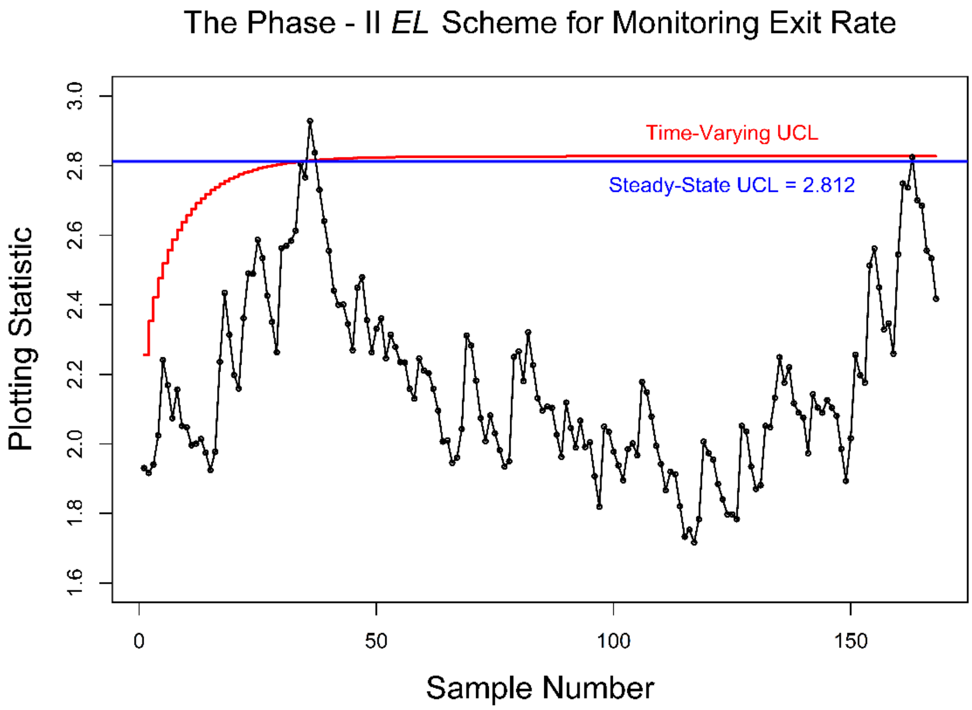

Figure 4.8: Phase-II *EL* Scheme for Monitoring Exit Rate

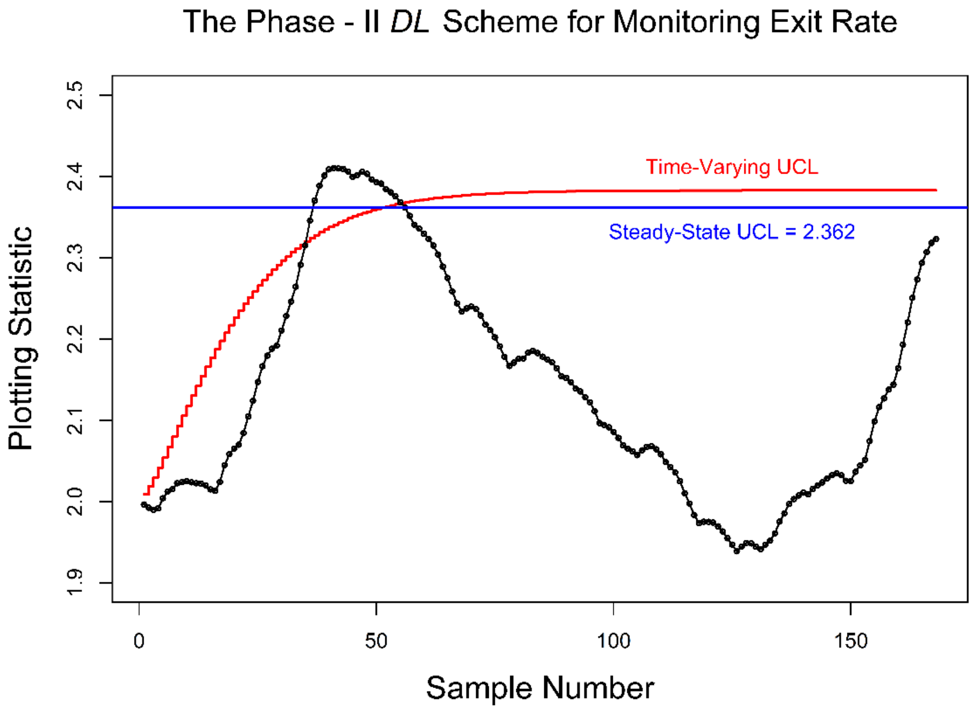

Figure 4.9: Phase-II *DL* Scheme for Monitoring Exit Rate

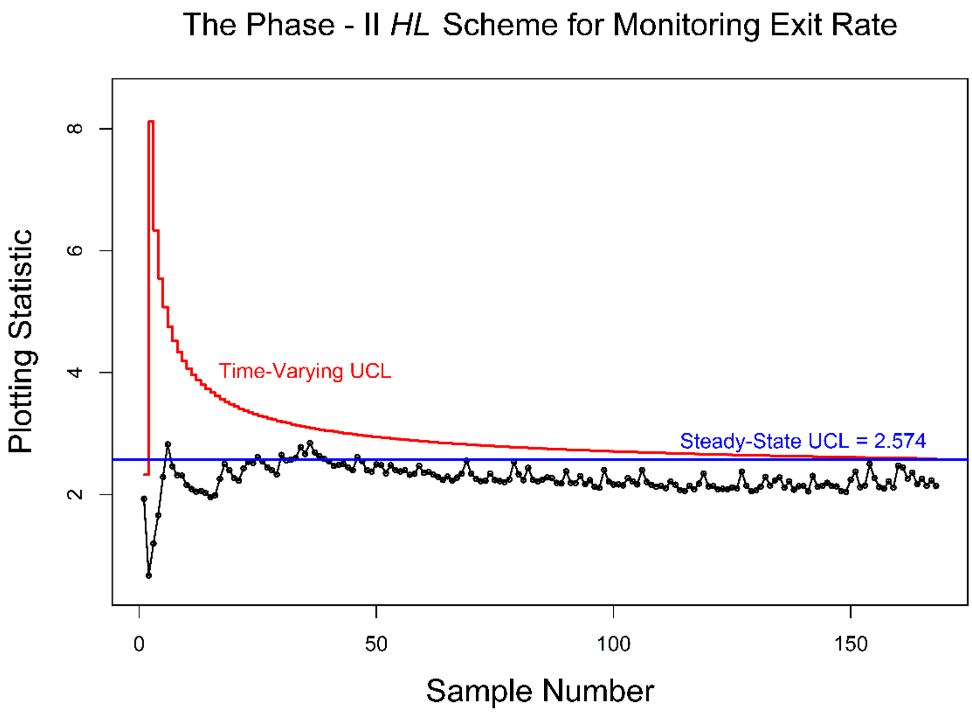

Figure 4.10: Phase-II *HL* Scheme for Monitoring Exit Rate

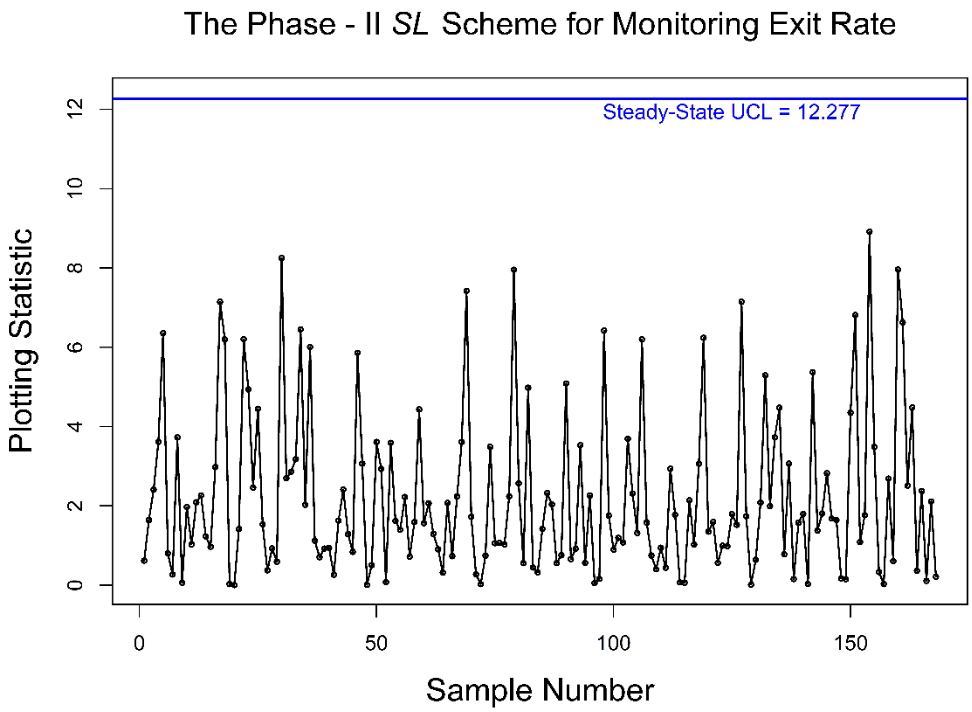

Figure 4.11: Phase-II *SL* Scheme for Monitoring Exit Rate

The exit rate is monitored with EL, DL, HL, and SL schemes, and respectively, plotted in Figures 4.8, 4.9, 4.10, and 4.11. Out of the 168 test samples, the OOC signals that are detected by the schemes are juxtaposed in Table 4.26. From Table 4.26, note that the HL scheme with the time-varying UCL and SL scheme with the steady-state UCL are not identifying any OOC signals, while the remaining schemes are signalling some OOC signals.

Table 4.26: OOC Signals Detected by Various Schemes in Monitoring Exit Rate

Scheme	Type of UCL	OOC Signals (i^{th} Test Sample)
EL	TV UCL	36^{th} and 37^{th}
	SS UCL	36^{th}, 37^{th}, and 163^{rd}
DL	TV UCL	36^{th} continuously until 55^{th}
	SS UCL	37^{th} continuously until 55^{th}
HL	TV UCL	None
	SS UCL	6^{th}, 25^{th}, 30^{th}, 33^{rd} continuously until 39^{th}, and 46^{th}
SL	SS UCL	None

Comparatively, the HL scheme with the steady-state UCL detects an OOC signal the fastest, i.e., at the 6^{th} test sample. However, it is known that the early FAR of this scheme is very high, and the OOC signals detected might be false alarms. Besides, the DL scheme, regardless of the types of UCL, is able to signal a vast number of OOC signals. Even though the first OOC indication signalled by the DL scheme is the same as the EL scheme, i.e., at the 36^{th} test sample, suggests that these two schemes are apparently equally good. Nevertheless, if one sees Figure 4.9 carefully, an upward trend is observed starting from the 16^{th} test sample. Montgomery (2019) mentioned that if there are six consecutive plotting statistics that display an increasing trend, it is an OOC signal too. To this end, the DL scheme has signalled an OOC indication as early as the 21^{st} test sample.

In order to check the nature of the shifts detected by the EL, DL, and HL schemes, a follow-up procedure with p_W^* and p_A^* are computed and tabulated in Table 4.27. From Table 4.27, only the p_W^* and p_A^* of the 6th test sample detected by the HL scheme with the steady-state UCL are insignificant. Noting the results obtained from the simulation study, it is highly suspected that this is an early false alarm. Then, the remaining test samples detected are all facing a pure location shift due to $p_W^* \leq 0.0001$ and p_A^* is insignificant. Further, the increasing trend observed in the DL scheme, which is signalled at the 21^{st} test sample is also facing a pure location shift.

Table 4.27: Follow-Up Procedure of the OOC Signals Detected

Sample	p_W^*	p_A^*	Sample	p_W^*	p_A^*
6	0.0122	0.1943	43	<0.0001	0.7068
21	0.0001	0.9563	44	<0.0001	0.6336
25	<0.0001	0.5278	45	<0.0001	0.6695
30	<0.0001	0.6362	46	<0.0001	0.5386
33	<0.0001	0.6012	47	<0.0001	0.6431
34	<0.0001	0.6588	48	<0.0001	0.6407
35	<0.0001	0.5229	49	<0.0001	0.5821
36	<0.0001	0.5898	50	<0.0001	0.4738
37	<0.0001	0.5865	51	<0.0001	0.3701
38	<0.0001	0.5879	52	<0.0001	0.372
39	<0.0001	0.5055	53	<0.0001	0.3963
40	<0.0001	0.5007	54	<0.0001	0.4838
41	<0.0001	0.5421	55	<0.0001	0.5811
42	<0.0001	0.5927	163	<0.0001	0.04271

In this case study, even though the HL scheme with the steady-state UCL is found to be the most sensitive scheme, i.e., detect a shift the fastest, this scheme is still not recommended due to its high early FAR. Further, it is not surprising that the memoryless SL scheme is the worst because it cannot detect any OOC signal. To this end, the DL scheme, regardless of the types of UCL, outperforms other schemes in monitoring the exit rate.

CHAPTER 5

CONCLUSIONS AND FUTURE RESEARCH

5.1 Introduction

SPM or NSPM plays a contributing role in ensuring the quality of a product or service can meet or even exceed the customer's expectation. Among the SPM or NSPM tools, the control scheme is the most significant tool for achieving this goal. Following the current trend of big data and IR4.0, a control scheme is not only limited to monitor the manufacturing process; instead, it can be one of the vital contributors in accelerating the pace of IR4.0. In this dissertation, a case study is conducted using a few NSPM-type control schemes, precisely the popular Lepage-type schemes, in monitoring e-commerce activity. The results showed that if an online shopping platform seller knows how to employ a control scheme, he or she will be able to identify the customer's purchasing intention easily. Besides, he or she can rectify an issue immediately if something wrong is detected with the help of a control scheme.

To this end, in this chapter, the findings and contribution of this dissertation is firstly revealed in Section 5.2. Then, Section 5.3 discusses some of the research limitations, precisely, the limitations of the NSPM-type schemes proposed here. Lastly, a few propositions for future research are suggested in Section 5.4.

5.2 Findings and Contributions of this Dissertation

The NSPM-type schemes are generally preferred and act as a good complement to the parametric SPM-type schemes, especially when there is a lack of prior knowledge and details regarding the underlying process distribution. Further, the stability of a process is more reliable and convincible if both the location and scale parameters of the process are statistically IC, rather than only the location parameter being stable. Accordingly, two novel memory-type Lepage-type schemes, which can monitor the location-scale of a process jointly, namely the DL and HL schemes, are presented in this dissertation. Two types of UCLs of the proposed schemes, i.e., the time-varying UCLs and steady-state UCLs are also derived and explained in-depth in this dissertation (see Chapter 3). In addition, the charting procedures of the proposed schemes are also described step-by-step. This eases quality practitioners in implementing the proposed schemes in monitoring any process.

In the simulation study and the illustrative example, it is obvious that the performance of the two novel memory-type schemes outshines the existing memoryless SL scheme, even in terms of detecting a large shift in the process. For instance, the SL scheme has the worst performance, as displayed in the simulation study, because this scheme takes more samples to detect an OOC signal. Further, in the case study of monitoring the exit rate, both the proposed schemes, especially the DL scheme, detect OOC signals hastily so that remedial action can be taken quickly. On the flip side, the SL scheme is unable to identify any OOC situation, which gives a wrong perception, as the exit rate appears to be IC even though it is OOC. Even though the Shewhart-type scheme is shown to be less effective in detecting a small disturbance of a process, the significance of the Shewhart-type scheme cannot be neglected. This is because, in a real application, one will never know the exact shift level of a process, and there is a tendency that the process is facing a large disturbance, which is the situation where the Shewhart-type scheme performs well.

Besides, the supremacy of the two proposed schemes over the traditional EL scheme can also be spotted in the simulation and case studies. By assessing the $EARL$ value, the proposed DL scheme with the time-varying UCL seems to have the best performance when $\lambda < 0.20$, while the HL scheme with the steady-state UCL appears to have the best performance when $\lambda = 0.20$. Note that the HL scheme with the steady-state UCL is not considered when $\lambda < 0.20$ due to its high early FAR, and it is recommended to select $\lambda \geq 0.20$ when employing this scheme in process monitoring. Note that Montgomery (2019) mentioned that typically for detecting a large shift in the process, the selection of λ is large, says, 0.20. However, the statement claimed is based on the EWMA-type scheme, and it is not necessarily held for the HWMA-type scheme. In addition, based on the simulation study, one can easily notice that the HL scheme with the steady-state UCL is able to detect small shifts in the process well even though one uses $\lambda = 0.20$. Further, in terms of detecting the small to moderate disturbances of a process, one can easily find that the proposed schemes also appear to outperform the EL scheme. For instance, the DL and HL schemes with time-varying UCLs are regarded as the two best performers when $\lambda = 0.05$. In addition, it is worth emphasising that in the case study, the DL scheme, regardless of the types of UCL, surpasses all the schemes because it can detect the OOC signal the fastest without giving any false alarms.

To this end, this dissertation provides some better alternatives to quality practitioners so that they are not limited only to the CUSUM- or EWMA-type schemes when they want to employ a memory-type scheme. Precisely, the DL scheme with the time-varying UCL appears as a better option due to its superior performance, or one may also choose the HL scheme with the steady-state UCL when $\lambda \geq 0.20$.

5.3 Limitations of Research

Some of the limitations of this research are:

1. Unlike the parametric SPM-type schemes, the expression of all the RL metrics of the NSPM-type schemes, which includes the proposed DL and HL schemes, are hard to obtain. To this end, one has to use the Monte-Carlo simulation with a sufficient amount of replicates to obtain all the RL metrics.

2. By comparing the IC performance of various schemes, it is noticed that the performance of the EL and DL schemes with their steady-state UCLs are relatively better than their time-varying UCLs. However, it is still acceptable to use any type of UCLs for these two schemes. On the other hand, the performance of the HL scheme with the steady-state UCL, especially when $\lambda < 0.20$, is definitely unacceptable due to its

extraordinary high early FAR. To this end, the best performer in detecting OOC signals, i.e., the HL scheme with the steady-state UCL when $\lambda < 0.20$, is not recommended in practical situations.

3. The design of the schemes follow the standard-setting, such that the scheme is designed so that the targeted ARL_0 is achieved. However, one knows that the RL distribution of any control scheme is asymmetric, i.e., they are right-skewed. To this end, it seems unsatisfied to compare the performance of the schemes by evaluating the mean values, i.e., ARL_0 and ARL_1.

4. Besides, the schemes are designed without considering the inertial effect. To this end, the schemes naturally have a weaker performance if the inertial effect exists.

5.4 Propositions for Future Research

Following the current trend in the research field of statistical quality control and some limitations of the schemes proposed, all the following research ideas are precious to investigate.

1. From the simulation study, especially by referring to the $EARL$ value, it is found that the value of the smoothing parameter chosen should be small, says $\lambda = 0.05$. However, this is not true for the DL scheme with the steady-state UCL. The results show that the value of λ value should be slightly larger, says, $\lambda = 0.10$. Therefore, effectively optimising the

value of λ not only for the DL scheme with the steady-state UCL, but for all the control schemes is an interesting topic.

2. It is found that the early FAR for some of the schemes, especially the HL scheme with the steady-state UCL, is unacceptable. Further, the RL distributions for all the control schemes are not symmetrical. Therefore, rather than fixing the ARL_0, a better design of the schemes is worth studying. For instance, one can design the schemes by fixing the IC-MRL or employ the percentile-based approach as in Faraz et al. (2019) so that the percentile of RL meets some nominal value. In order to reduce the early FAR, one may fix the 5^{th} percentile of RL, says, equal to 25.

3. Another design of the schemes, which have a better performance if the inertial effect has occurred, can be considered. For instance, one may follow the charting design proposed by Mukherjee (2017), i.e., employs the max-approach in getting the plotting statistic, or one may include the adaptive feature in the schemes.

4. In this dissertation, the extension of the EWMA-type scheme, i.e., the DEWMA-type scheme, is studied. Another inspiring idea is to further extend the DEWMA-type scheme to a triple EWMA (TEWMA)-type scheme. To be precise, a distribution-free TEWMA-type, such as the TEWMA-Lepage scheme, can be explored.

5. The literature shows that the Lepage-type scheme is currently the most popular location-scale monitoring scheme. However, one should not forget that the Cucconi-type scheme is also another important location-scale monitoring scheme. To this end, developing new Cucconi-type schemes, such as the DEWMA-Cucconi and HWMA-Cucconi schemes, are also worth studying.

REFERENCES

Abbas, N., 2018. Homogeneously Weighted Moving Average control chart with an application in substrate manufacturing process. *Computers & Industrial Engineering,* 120, pp. 460 – 470.

Abid, M., Shabbir, A., Nazir, H.Z., Sherwani, R.A. and Riaz, M., 2020. A Double Homogeneously Weighted Moving Average control chart for monitoring of the process mean. *Quality and Reliability Engineering International*, 36(5), pp. 1513 – 1527.

Adegoke, N.A., Smith, A.N., Anderson, M.J., Sanusi, R.A. and Pawley, M.D., 2019. Efficient Homogeneously Weighted Moving Average chart for monitoring process mean using an auxiliary variable. *IEEE Access,* 7, pp. 94021 – 94032.

Adeoti, O.A. and Koleoso, S.O., 2020. A hybrid Homogeneously Weighted Moving Average control chart for process monitoring. *Quality and Reliability Engineering International,* 36(6), pp. 2170 – 2186.

Alevizakos, V. and Koukouvinos, C., 2020. Monitoring of zero-inflated Poisson processes with EWMA and DEWMA control charts. *Quality and Reliability Engineering International,* 36(1), pp. 88 – 111.

Alkahtani, S.S., 2013. Robustness of DEWMA versus EWMA control charts to non-normal processes. *Journal of Modern Applied Statistical Methods,* 12(1), pp. 148 – 163.

Amin, R.W., Reynolds, M.R. and Saad, B., 1995. Nonparametric quality control charts based on the sign statistic. *Communications in Statistics – Theory and Methods*, 24(6), pp. 1597 – 1623.

Amin, R.W. and Searcy, A.J., 1991. A nonparametric exponentially weighted moving average control scheme. *Communications in Statistics – Simulation and Computation*, 20(4), pp. 1049 – 1072.

Amiri, A., Nedaie, A. and Alikhani, M., 2014. A new adaptive variable sample size approach in EWMA control chart. *Communications in Statistics – Simulation and Computation*, 43(4), pp. 804 – 812.

Bakir, S.T., 2004. A Distribution-Free Shewhart Quality Control Chart Based on Signed-Ranks. *Quality Engineering*, 16(4), pp. 613 – 623.

Bakir, S.T. and Reynolds, M.R., 1979. A Nonparametric Procedure for Process Control Based on Within-Group Ranking. *Technometrics*, 21(2), pp. 175 – 183.

Basu, A.P., 1971. On a Sequential Rule for Estimating the Location Parameter of an Exponential Distribution. *Naval Research Logistics Quarterly*, 18(3), pp. 329 – 337.

Bersimis, S., Degiannakis, S. and Georgakellos, D., 2017. Real-time monitoring of carbon monoxide using value-at-risk measure and control charting. *Journal of Applied Statistics*, 44(1), pp. 89 – 108.

Borror, C.M., Montgomery, D.C. and Runger, G.C., 1999. Robustness of the EWMA control chart to non-normality. *Journal of Quality Technology*, 10, pp. 139 – 149.

Capizzi, G. and Masarotto, G., 2003. An adaptive exponentially weighted moving average chart. *Technometrics*, 45(3), pp. 199 – 207.

Capizzi, G. and Masarotto, G., 2013. Phase I distribution-free analysis of univariate data. *Journal of Quality Technology*, 45(3), pp. 273 – 284.

Castagliola, P., Celano, G., Fichera, S. and Nunnari, V., 2008. A variable sample size S^2-EWMA control chart for monitoring the process variance. *International Journal of Reliability, Quality and Safety Engineering*, 15(3), pp. 181 – 201.

Chakraborti, S. and Graham, M.A., 2019. Nonparametric (Distribution-free) control charts: An updated overview and some results. *Quality Engineering*, 31(4), pp. 1 – 22.

Chakraborti, S., Human, S.W. and Graham, M.A., 2009. Phase I Statistical Process Control Charts: An Overview and Some Results. *Quality Engineering*, 21(1), pp. 52 – 62.

Chakraborti, S., Human, S.W. and Graham, M.A., 2011. Nonparametric (distribution-free) quality control charts. In: Balakrishnan N. (eds). *Handbook of methods and applications of statistics: Engineering, Quality control, and physical sciences*. New York: John Wiley & Sons, pp. 298 – 329.

Chakraborti, S., Van Der Laan, P. and Bakir, S.T., 2001. Nonparametric Control Charts: An Overview and Some Results. *Journal of Quality Technology*, 33(3), pp. 304 – 315.

Chen, G. and Cheng, S.W., 1998. Max Chart: Combining X-bar chart and S chart. *Statistica Sinica*, 8(1), pp. 263 – 271.

Cheng, S.W. and Thaga, K., 2006. Single Variables Control Charts: An Overview. *Quality and Reliability Engineering International*, 22(7), pp. 811 – 820.

Chong, Z.L., Mukherjee, A. and Khoo, M.B.C., 2017. Distribution-free Shewhart-Lepage type Premier control schemes for simultaneous monitoring of location and scale. *Computers & Industrial Engineering*, 104, pp. 201 – 215.

Chong, Z.L., Mukherjee, A. and Khoo, M.B.C., 2020. Some simplified Shewhart-type distribution-free joint monitoring schemes and its application in monitoring drinking water turbidity. *Quality Engineering*, 32(1), pp. 91 – 110.

Chong, Z.L., Mukherjee, A. and Marozzi, M., 2021. Simultaneous monitoring of origin and scale of a shifted exponential process with unknown and estimated parameters. *Quality and Reliability Engineering International*, 37(1), pp. 242 – 261.

Chowdhury, S., Mukherjee, A. and Chakraborti, S., 2014. A New Distribution-free Control Chart for Joint Monitoring of Unknown Location and Scale Parameters of Continuous Distributions. *Quality and Reliability Engineering International*, 30(2), pp. 191 – 204.

Chowdhury, S., Mukherjee, A. and Chakraborti, S., 2015. Distribution-free Phase II CUSUM control chart for joint monitoring of location and scale. *Quality and Reliability Engineering International*, 31(1), pp. 135 – 151.

Crowder, S.V., 1987. A simple method for studying run-length distributions of exponentially weighted moving average charts. *Technometrics*, 29(4), pp. 401 – 407.

Cucconi O., 1968. Un nuovo test non parametrico per il confronto tra due gruppi campionari. *Giornale degli Economisti*, 27, pp. 225 – 248.

Faraz, A., Saniga, E. and Montgomery, D., 2019. Percentile-based control chart design with an application to Shewhart $\bar{X}$ and S^2 control charts. *Quality and Reliability Engineering International*, 35(1), pp. 116 – 126.

Garvin, D.A., 1987. Competing in the Eight Dimensions of Quality. *Harvard Business Review*, 87(6), pp. 101 – 109.

Gitlow, H., Oppenheim, A. and Oppenheim, R., 1995. *Quality Management: Tools and Methods for Improvement*, 2nd ed. Chicago: Irwin.

Haq, A., Ejaz, S. and Khoo, M.B.C., 2020. A new double EWMA-t chart for process mean. *Communications in Statistics – Simulation and Computation*, pp. 1 – 16. doi: 10.1080/03610918.2020.1805630.

Hassani, H. and Yeganegi, M.R., 2020. Selecting optimal lag order in Ljung–Box test. *Physica A: Statistical Mechanics and Its Applications*, 541. doi: 10.1016/j.physa.2019.123700.

Hawkins, D.M. and Deng, Q., 2009. Combined Charts for Mean and Variance Information. *Journal of Quality Technology*, 41(4), pp. 415 – 425.

Hawkins, D.M. and Deng, Q., 2010. A Nonparametric Change-Point Control Chart. *Journal of Quality Technology*, 42(2), pp. 165 – 173.

Jensen, W.A., Jones-Farmer, L.A., Champ, C.W. and Woodall, W.H., 2006. Effects of parameter estimation on control chart properties: A literature review. *Journal of Quality Technology*, 38, pp. 349 – 364.

Jones, L.A., Champ, C.W. and Rigdon, S.E., 2001. The Performance of Exponentially Weighted Moving Average Charts With Estimated Parameters. *Technometrics*, 43(2), pp. 156 – 167.

Jones-Farmer, L.A., Woodall, W.H., Steiner, S.H. and Champ, C.W., 2014. An Overview of Phase I Analysis for Process Improvement and Monitoring. *Journal of Quality Technology*, 46(3), pp. 265 – 280.

Khoo, M.B.C., Teh, S.Y. and Wu, Z., 2010. Monitoring process mean and variability with one Double EWMA chart. *Communications in Statistics - Theory and Methods,* 39(20), pp. 3678 – 3694.

Lashley, R., 1995. Using SAS/QC To Automate The “Magnificent Seven” Tools of Quality. *SAS Conference Proceedings: Midwest SAS Users Group*, 1995 Cleveland. Ohio: SAS Institute Inc, pp. 166 – 173.

Lepage, Y., 1971. A combination of Wilcoxon’s and Ansari-Bradley’s statistics. *Biometrika*, 58(1), pp. 213 – 217.

Li, C., Mukherjee, A. and Marozzi, M., 2020. A new distribution-free Phase-I procedure for bi-aspect monitoring based on the multi-sample Cucconi statistic. *Computers & Industrial Engineering*, 149. doi: 10.1016/j.cie.2020.106760.

Li, C., Mukherjee, A. and Su, Q., 2019. A distribution-free Phase I monitoring scheme for subgroup location and scale based on the multi-sample Lepage statistic. *Computers & Industrial Engineering*, 129, pp. 259 – 273.

Li, S.-Y., Tang, L.-C. and Ng, S.-H., 2010. Nonparametric CUSUM and EWMA Control Charts for Detecting Mean Shifts. *Journal of Quality Technology*, 42(2), pp. 209 – 226.

Lucas, J.M. and Saccucci, M.S., 1990. Exponentially weighted moving average control schemes: properties and enhancements. *Technometrics*, 32(1), pp. 1 – 12.

Madanhire, I. and Mbohwa, C., 2016. Application of statistical process control (SPC) in manufacturing industry in a developing country. *Procedia CIRP*, 40, pp. 580 – 583.

Magnier, M., 1999, *Rebuilding Japan With the Help of 2 Americans* [Online]. Available at: https://www.latimes.com/archives/la-xpm-1999-oct-25-ss-26184-story.html [Accessed: 23 April 2021].

Malela-Majika, J.-C., 2020. New distribution-free memory-type control charts based on the Wilcoxon rank-sum statistic. *Quality Technology & Quantitative Management*, pp. 1 – 21. doi: 10.1080/16843703.2020.1753295.

McCracken, A.K., Chakraborti, S. and Mukherjee, A., 2013. Control charts for simultaneous monitoring of unknown mean and variance of normally distributed processes. *Journal of Quality Technology*, 45(4), pp. 360 – 376.

Montgomery, D.C., 2019. *Introduction to Statistical Quality Control*, 8th ed. New York: John Wiley & Sons, Inc.

Mukherjee, A., 2017. Distribution-free Phase-II Exponentially Weighted Moving Average schemes for joint monitoring of location and scale based on subgroup samples. *The International Journal of Advanced Manufacturing Technology*, 92(1 – 4), pp. 101 – 116.

Mukherjee, A. and Chakraborti, S., 2012. A distribution-free control chart for the joint monitoring of location and scale. *Quality and Reliability Engineering International*, 28(3), pp. 335 – 352.

Mukherjee, A., Graham, M.A. and Chakraborti, S., 2013. Distribution-Free Exceedance CUSUM Control Charts for Location. *Communications in Statistics – Simulation and Computation*, 42(5), pp. 1153 – 1187.

Mukherjee, A. and Marozzi, M., 2017a. A distribution-free Phase-II CUSUM procedure for monitoring service quality. *Total Quality Management & Business Excellence*, 28(11 – 12), pp. 1227 – 1263.

Mukherjee, A. and Marozzi, M., 2017b. Distribution-free Lepage type Circular-grid charts for joint monitoring of location and scale parameters of a process. *Quality and Reliability Engineering International,* 33(2), pp. 241 – 274.

Mukherjee, A., McCracken, A.K. and Chakraborti, S., 2015. Control charts for simultaneous monitoring of parameters of a shifted exponential distribution. *Journal of Quality Technology*, 47(2), pp. 176 – 192.

Mukherjee, A. and Sen, R., 2018. Optimal design of Shewhart–Lepage type schemes and its application in monitoring service quality. *European Journal of Operational Research*, 266(1), pp. 147 – 167.

Page, E.S., 1954. Continuous Inspection Schemes. *Biometrika*, 41(1/2), pp. 100 – 115.

Parasuraman, A., Zeitharnl, V.A. and Berry, L.L., 1985. A Conceptual Model of Service Quality and Its Implications for Future Research. *Journal of Marketing*, 49, pp. 41 – 50.

Qiu, P., 2014. *Introduction to Statistical Process Control*, 1st ed. Boca Raton, FL: Chapman & Hall/CRC.CRC Press.

Qiu, P., 2018. Some perspectives on nonparametric statistical process control. *Journal of Quality Technology*, 50(1), pp. 49 – 65.

Qiu, P. and Li, Z., 2011. Distribution-free monitoring of univariate processes. *Statistics & Probability Letters*, 81(12), pp. 1833 – 1840.

Quesenberry, C.P., 1991. SPC Q Charts for Start-Up Processes and Short or Long Runs. *Journal of Quality Technology*, 23(3), pp. 213 – 224.

Quesenberry, C.P., 1993. The Effect of Sample Size on Estimated Limits for $\bar{X}$ and X Control Charts. *Journal of Quality Technology*, 25(4), pp. 237 – 247.

Ramzy, A., 2005. *Schemes for Joint Monitoring of Process Mean and Process Variance.* Master's Thesis, National University of Singapore, Singapore.

Raza, M.A., Nawaz, T., Aslam, M., Bhatti, S.H. and Sherwani, R.A., 2020a. A new nonparametric Double Exponentially Weighted Moving Average control chart. *Quality and Reliability Engineering International*, 36(1), pp. 68 – 87.

Raza, M.A., Nawaz, T. and Han, D., 2020b. On designing distribution-free Homogeneously Weighted Moving Average control charts. *Journal of Testing and Evaluation*, 48(4), pp. 3154 – 3171.

Riaz, M. and Abbasi, S.A., 2016. Nonparametric Double EWMA control chart for process monitoring. *Revista Colombiana de Estadística*, 39(2), pp. 167 – 184.

Riaz, M., Abbasi, S.A., Abid, M. and Hamzat, A.K., 2020. A New HWMA dispersion control chart with an application to wind farm data. *Mathematics*, 8(12). doi: 10.3390/math8122136.

Roberts, S.W., 1959. Control Chart Tests Based on Geometric Moving Averages. *Technometrics*, 1(3), pp. 239 – 250.

Ryu, J.-H., Wan, H.G. and Kim, S., 2010. Optimal design of a CUSUM chart for a mean shift of unknown size. *Journal of Quality Technology*, 42(3), pp. 311 – 326.

Saccucci, M.S., Amin, R.W. and Lucas, J.M., 1992. Exponentially weighted moving average control schemes with variable sampling intervals. *Communications in Statistics – Simulation and Computation*, 21(3), pp. 627 – 657.

Sakar, C.O., Polat, S.O., Katircioglu, M. and Kastro, Y., 2019. Real-time prediction of online shoppers' purchasing intention using multilayer perceptron and LSTM Recurrent Neural Networks. *Neural Computing and Applications,* 31, pp. 6893 – 6908.

Sanusi, R.A., Chong, Z.L., Mukherjee, A. and Xie, M., 2020. Distribution-free hybrid schemes for process surveillance with application in monitoring chlorine content of water. *Chemometrics and Intelligent Laboratory Systems*, 206. doi: 10.1016/j.chemolab.2020.104099.

Scagliarini, M., Boccaforno, N. and Vandi, M., 2021. Comparison of control charts for Poisson count data in healthcare monitoring. *Applied Stochastic Models in Business and Industry,* 37(1), pp. 139 – 154.

Shamma, S.E. and Shamma, A.K., 1992. Development and evaluation of control charts using Double Exponentially Weighted Moving averages. *International Journal of Quality & Reliability Management*, 9(6), pp. 18 – 25.

Shewhart, W.A., 1926. Quality Control Charts. *The Bell System Technical Journal*, 5(4), pp. 593 – 603.

Shu, L., Jiang, W. and Wu, S., 2007. A one-sided EWMA control chart for monitoring process means. *Communications in Statistics – Simulation and Computation*, 36(4), pp. 901 – 920.

Smith, G.M., 1998. *Statistical Process Control and Quality Improvement*, 3rd ed. Upper Saddle River, New Jersey: Prentice Hall.

Song, Z., Mukherjee, A., Marozzi, M. and Zhang, J., 2020a. A Class of Distribution-Free Exponentially Weighted Moving Average Schemes for Joint Monitoring of Location and Scale Parameters. In: Koutras, M.V., and. Triantafyllou, I.S. (eds.). *Distribution-Free Methods for Statistical Process Monitoring and Control*. Switzerland: Springer, pp. 183 – 217.

Song, Z., Mukherjee, A. and Tao, G., 2020b. A class of distribution-free one-sided Cucconi schemes for joint surveillance of location and scale parameters and their application in monitoring cab services. *Computers & Industrial Engineering*, 148. doi: 10.1016/j.cie.2020.106625.

Woodall, W.H. and Mahmoud, M.A., 2005. The inertial properties of quality control charts. *Technometrics*, 47(4), pp. 425 – 436.

Xiang, D., Gao, S., Li, W., Pu, X. and Dou, W., 2019. A new nonparametric monitoring of data streams for changes in location and scale via Cucconi statistic, *Journal of Nonparametric Statistics*, 31(3), pp. 743 – 760.

Xie, M., Goh, T.N. and Kuralmani, V., 2002. *Statistical Models and Control Charts for High-Quality Processes*. Boston: Kluwer Academic Publishers.

Yang, M., Wu, Z., Lee, K.M. and Khoo, M.B.C., 2012. The X control chart for monitoring process shifts in mean and variance. *International Journal of Production Research*, 50, pp. 893 – 907.

Yeh, A.B., Lin, D.K.J. and Venkataramani, C., 2004. Unified CUSUM Charts for Monitoring Process Mean and Variability. *Quality Technology & Quantitative Management*, 1(1), pp. 65 – 86.

Zhang, L. and Chen, G., 2005. An extended EWMA mean chart. *Quality Technology & Quantitative Management*, 2(1), pp. 39 – 52.

Zhang, L., Govindaraju, K., Lai, C.D. and Bebbington, M.S., 2003. Poisson DEWMA Control Chart. *Communications in Statistics – Simulation and Computation*, 32(4), pp. 1265 – 1283.

Zhang, J., Li, E. and Li, Z., 2017. A Cramér-von Mises test-based distribution-free control chart for joint monitoring of location and scale. *Computers & Industrial Engineering*, 110, pp. 484 – 497.

Zou, C. and Tsung, F., 2010. Likelihood Ratio-based Distribution-free EWMA Control Charts. *Journal of Quality Technology*, 42(2), pp. 174 – 196.

APPENDIX A

LEMMA FOR THE DERIVATION OF THE TIME-VARYING UCL FOR THE DL SCHEME

A.1 Lemma 1

It is defined as

$$1 + 2r + 3r^2 + \cdots + (i-1)r^{i-2} + ir^{i-1} = \frac{1-r^i}{(1-r)^2} - \frac{ir^i}{1-r}. \tag{A.1}$$

Proof of Lemma 1

Firstly, let the summation be S, i.e.,

$S = 1 + 2r + 3r^2 + \cdots + (i-1)r^{i-2} + ir^{i-1}$.

Then, multiply the equation above by r, and it is obtained that

$rS = r + 2r^2 + 3r^3 + \cdots + (i-1)r^{i-1} + ir^i$,

and thus,

$S - rS = 1 + r + r^2 + \cdots + r^{i-1} - ir^i$

$(1-r)S = \frac{1-r^i}{1-r} - ir^i$.

Finally, the summation is expressed as

$S = \frac{1-r^i}{(1-r)^2} - \frac{ir^i}{1-r}$.

A.2 Lemma 2

It is defined as

$$1 + 2^2r^2 + 3^2r^4 + \cdots + i^2r^{2(i-1)}$$
$$= \frac{2\left(1-r^{2i}\right)}{(1-r^2)^3} + \frac{i^2r^{2(i+1)}+\left(1-2i-i^2\right)r^{2i}-1}{(1-r^2)^2}. \tag{A.2}$$

Proof of Lemma 2

Firstly, let the summation be S, i.e.,

$S = 1 + 2^2r^2 + 3^2r^4 + \cdots + i^2r^{2(i-1)}$.

Then, multiply the equation above by r^2, and it is obtained that

$r^2S = r^2 + 2^2r^4 + 3^2r^6 + \cdots + (i-2)^2r^{2(i-2)} + (i-1)^2r^{2(i-1)} + i^2r^{2i}$,

and thus,

$S - r^2S = 1 + 3r^2 + 5r^4 + \cdots + (2i-3)r^{2(i-2)} + (2i-1)r^{2(i-1)} - i^2r^{2i}$

$(1-r^2)S = 1 + 3r^2 + \cdots + (2i-3)r^{2(i-2)} + (2i-1)r^{2(i-1)} - i^2r^{2i}$.

Next, multiply the equation above by r^2, and it is obtained that

$r^2(1-r^2)S = r^2 + 3r^4 + \cdots + (2i-3)r^{2(i-1)} + (2i-1)r^{2i} - i^2r^{2(i+1)}$,

and thus,

$(1-r^2)S - r^2(1-r^2)S = 1 + 2r^2 + 2r^4 + \cdots + 2r^{2(i-1)} + (1 - 2i -$

$i^2)r^{2i} + i^2r^{2(i+1)}$,

which can be simplified as

$(1-r^2)^2S = \frac{2\left(1-r^{2i}\right)}{1-r^2} + \left[i^2r^{2(i+1)} + (1-2i-i^2)r^{2i} - 1\right]$.

Finally, the summation is expressed as

$S = \frac{2\left(1-r^{2i}\right)}{(1-r^2)^3} + \frac{i^2r^{2(i+1)}+\left(1-2i-i^2\right)r^{2i}-1}{(1-r^2)^2}$.

APPENDIX B

COMPUTER PROGRAMS FOR MONTE-CARLO SIMULATION

B.1 R Program Code for ξ_1 and ξ_2 Estimation

The program below is used to estimate the values of ξ_1 and ξ_2, which are the two important components in the time-varying UCL.

```
rm(list=ls(all=TRUE))

const=function(m,n,sim_num=25000,win_lim=25000)
{
  N=m+n
  x=rep(0,m)
  y=rep(0,n)
  z=rep(0,n)
  lep=rep(0,win_lim)
  Ex_Lj=rep(0,sim_num)
  Var_Lj=rep(0,sim_num)

  for (i in 1:sim_num)
  {
    x=rnorm(m,0,1)

    for (j in 1:win_lim)
    {
      y=rnorm(n,0,1)
      R=rank(c(x,y))
      WRS=((sum(R[(m+1):N]))-
(0.5*n*(N+1)))/sqrt((m*n*(N+1)/12))

      for(k in 1:n) {z[k]=abs(R[m+k]-(0.5*(N+1)))}
      if((N%%2)==0)                          {AB=((sum(z[1:n]))-
(0.25*n*N))/sqrt(((m*n*((N*N)-4)/(48*(N-1)))))}
      else                    {AB=((sum(z[1:n]))-(0.25*n*((N*N)-
1))/N)/sqrt(((m*n*(N+1)*((N*N)+3)/(48*N*N))))}

      lep[j]=(WRS*WRS)+(AB*AB)
    }

    Ex_Lj[i]=mean(lep) #It is E(Lj|Xm, IC)
    Var_Lj[i]=var(lep) #It is Var(Lj|Xm, IC)
  }

  Var_Ex_Lj=var(Ex_Lj) #It is Var[E(Lj|Xm, IC)]
  Ex_Var_Lj=mean(Var_Lj) #It is E[Var(Lj|Xm, IC)]
  print(c(Var_Ex_Lj,Ex_Var_Lj))
}
```

```
#Example
const(m=100, n=5)
```

B.2 R Program Code for the EL Scheme

The program below is used to obtain the IC and OOC performances of the EL scheme with the time-varying UCL.

```
library(doParallel)
library(foreach)

rm(list=ls(all=TRUE))

el_tv=function(case,m,n,C,win_lim=5000,sim_num=50000,loc,sca,la
m)
{
  N=m+n
  x=rep(0,m)
  y=rep(0,n)
  z=rep(0,n)
  lep=rep(0,win_lim)
  comp=rep(0,win_lim)
  ewma=rep(0,win_lim)

evl=c(3.52572525,3.69092682,3.72876761,3.575762399,3.76727793,3
.83059074,3.586651011,3.781145634,3.848191288)     #E[Var(Lj|Xm,
IC)]

vel=c(0.02665154,0.04685424,0.07874633,0.007554594,0.01052258,0
.01474126,0.004471669,0.005533597,0.007193758)     #Var[E(Lj|Xm,
IC)]

  grp=makeCluster(7)
  registerDoParallel(grp)

  rl=rep(0,sim_num)
  rl=foreach(i=1:sim_num,.combine=c)%dopar%
    {
      x=rnorm(m,0,1)
      j=0

      repeat
      {
        j=j+1
        y=rnorm(n,loc,sca)
        R=rank(c(x,y))

        WRS=((sum(R[(m+1):N]))-
(0.5*n*(N+1)))/sqrt((m*n*(N+1)/12))

        for(k in 1:n) {z[k]=abs(R[m+k]-(0.5*(N+1)))}
        if((N%%2)==0)                       {AB=((sum(z[1:n]))-
(0.25*n*N))/sqrt(((m*n*((N*N)-4)/(48*(N-1)))))}
```

```
        else                    {AB=((sum(z[1:n]))-(0.25*n*((N*N)-
1))/N)/sqrt(((m*n*(N+1)*((N*N)+3)/(48*N*N))))}

        lep[j]=(WRS*WRS)+(AB*AB)
        for (a in 1:j) {comp[a]=lam*((1-lam)^(j-a))*lep[a]}
        value=sum(comp[1:j])+((1-lam)^j)*2
        ewma[j]=value

        part_one=((lam)/(2-lam))*(1-((1-lam)^(2*j)))
        part_two=(1-((1-lam)^j))^2

var_elj=((part_one)*(evl[case]))+((part_two)*(vel[case]))
        H=2+(C*(sqrt(var_elj)))
        if((ewma[j]>=H)||(j==win_lim)) break
      }
      rl[i]=j
    }
  stopCluster(grp)

  print(c(m,n,lam,C,loc,sca,
mean(rl),sqrt(var(rl)/sim_num),sd(rl),min(rl),quantile(rl,c(0.0
5,0.25,0.50,0.75,0.95)),max(rl)))
}

#Example
el_tv(case=1, m=100, n=5, C=1.945, loc=0, sca=1, lam=0.05)
```

The program below is used to obtain the IC and OOC performances of the EL scheme with the steady-state UCL.

```
library(doParallel)
library(foreach)

rm(list=ls(all=TRUE))

el_ss=function(m,n,H,win_lim=5000,sim_num=50000,loc,sca,lam)
{
  N=m+n
  x=rep(0,m)
  y=rep(0,n)
  z=rep(0,n)
  lep=rep(0,win_lim)
  comp=rep(0,win_lim)
  ewma=rep(0,win_lim)

  grp=makeCluster(7)
  registerDoParallel(grp)

  rl=rep(0,sim_num)
  rl=foreach(i=1:sim_num,.combine=c)%dopar%
    {
      x=rnorm(m,0,1)
      j=0

      repeat
      {
        j=j+1
        y=rnorm(n,loc,sca)
```

```
        R=rank(c(x,y))

        WRS=((sum(R[(m+1):N]))-
(0.5*n*(N+1)))/sqrt((m*n*(N+1)/12))

        for(k in 1:n) {z[k]=abs(R[m+k]-(0.5*(N+1)))}
        if((N%%2)==0)                          {AB=((sum(z[1:n]))-
(0.25*n*N))/sqrt(((m*n*((N*N)-4)/(48*(N-1)))))}
        else                  {AB=((sum(z[1:n]))-(0.25*n*((N*N)-
1))/N)/sqrt(((m*n*(N+1)*((N*N)+3)/(48*N*N))))}

        lep[j]=(WRS*WRS)+(AB*AB)
        for (a in 1:j) {comp[a]=lam*((1-lam)^(j-a))*lep[a]}
        value=sum(comp[1:j])+((1-lam)^j)*2
        ewma[j]=value


        if((ewma[j]>=H)||(j==win_lim)) break
      }
      rl[i]=j
    }
  stopCluster(grp)

  print(c(m,n,lam,H,loc,sca,
mean(rl),sqrt(var(rl)/sim_num),sd(rl),min(rl),quantile(rl,c(0.0
5,0.25,0.50,0.75,0.95)),max(rl)))
}

#Example
el_ss(m=100, n=5, H=2.642, loc=0, sca=1, lam=0.05)
```

B.3 R Program Code for the DL Scheme

The program below is used to obtain the IC and OOC performances of the DL scheme with the time-varying UCL.

```
library(doParallel)
library(foreach)

rm(list=ls(all=TRUE))

dl_tv=function(case,m,n,C,win_lim=5000,sim_num=50000,loc,sca,la
m)
{
  N=m+n
  x=rep(0,m)
  y=rep(0,n)
  z=rep(0,n)
  lep=rep(0,win_lim)
  comp=rep(0,win_lim)
  dewma=rep(0,win_lim)

evl=c(3.52572525,3.69092682,3.72876761,3.575762399,3.76727793,3
```

```
.83059074,3.586651011,3.781145634,3.848191288)     #E[Var(Lj|Xm,
IC)]

vel=c(0.02665154,0.04685424,0.07874633,0.007554594,0.01052258,0
.01474126,0.004471669,0.005533597,0.007193758)     #Var[E(Lj|Xm,
IC)]

  grp=makeCluster(7)
  registerDoParallel(grp)

  rl=rep(0,sim_num)
  rl=foreach(i=1:sim_num,.combine=c)%dopar%
    {
      x=rnorm(m,0,1)
      j=0

      repeat
      {
        j=j+1
        y=rnorm(n,loc,sca)
        R=rank(c(x,y))

        WRS=((sum(R[(m+1):N]))-
(0.5*n*(N+1)))/sqrt((m*n*(N+1)/12))

        for(k in 1:n) {z[k]=abs(R[m+k]-(0.5*(N+1)))}
        if((N%%2)==0)                          {AB=((sum(z[1:n]))-
(0.25*n*N))/sqrt(((m*n*((N*N)-4)/(48*(N-1)))))}
        else                    {AB=((sum(z[1:n]))-(0.25*n*((N*N)-
1))/N)/sqrt(((m*n*(N+1)*((N*N)+3)/(48*N*N))))}

        lep[j]=(WRS*WRS)+(AB*AB)
        for  (a  in  1:j)  {comp[a]=((j-a+1)*(lam^2))*((1-lam)^(j-
a))*lep[a]}
        value=sum(comp[1:j])+(1+j*lam)*((1-lam)^j)*2
        dewma[j]=value

        part_one_a=((2*lam)/((2-lam)^3))*(1-((1-lam)^(2*j)))
        part_one_b=((lam^2)/((2-lam)^2))*((j*j*((1-
lam)^(2*(j+1))))+((1-(2*j)-(j*j))*((1-lam)^(2*j)))-1)
        part_one=part_one_a+part_one_b
        part_two=1-((1+(j*lam))*((1-lam)^j))

var_dlj=((part_one)*(evl[case]))+((part_two)*(part_two)*(vel[ca
se]))
        H=2+(C*(sqrt(var_dlj)))
        if((dewma[j]>=H)||(j==win_lim)) break
      }
      rl[i]=j
    }
  stopCluster(grp)

  print(c(m,n,lam,C,loc,sca,
mean(rl),sqrt(var(rl)/sim_num),sd(rl),min(rl),quantile(rl,c(0.0
5,0.25,0.50,0.75,0.95)),max(rl)))
}

#Example
dl_tv(case=1, m=100, n=5, C=1.011, loc=0, sca=1, lam=0.05)
```

The program below is used to obtain the IC and OOC performances of the DL scheme with the steady-state UCL.

```
library(doParallel)
library(foreach)

rm(list=ls(all=TRUE))

dl_ss=function(m,n,H,win_lim=5000,sim_num=50000,loc,sca,lam)
{
  N=m+n
  x=rep(0,m)
  y=rep(0,n)
  z=rep(0,n)
  lep=rep(0,win_lim)
  comp=rep(0,win_lim)
  dewma=rep(0,win_lim)

  grp=makeCluster(7)
  registerDoParallel(grp)

  rl=rep(0,sim_num)
  rl=foreach(i=1:sim_num,.combine=c)%dopar%
    {
      x=rnorm(m,0,1)
      j=0

      repeat
      {
        j=j+1
        y=rnorm(n,loc,sca)
        R=rank(c(x,y))

        WRS=((sum(R[(m+1):N]))-
(0.5*n*(N+1)))/sqrt((m*n*(N+1)/12))

        for(k in 1:n) {z[k]=abs(R[m+k]-(0.5*(N+1)))}
        if((N%%2)==0)                        {AB=((sum(z[1:n]))-
(0.25*n*N))/sqrt(((m*n*((N*N)-4)/(48*(N-1))))))}
        else                  {AB=((sum(z[1:n]))-(0.25*n*((N*N)-
1))/N)/sqrt(((m*n*(N+1)*((N*N)+3)/(48*N*N))))}

        lep[j]=(WRS*WRS)+(AB*AB)
        for (a in 1:j) {comp[a]=((j-a+1)*(lam^2))*((1-lam)^(j-
a))*lep[a]}
        value=sum(comp[1:j])+(1+j*lam)*((1-lam)^j)*2
        dewma[j]=value

        if((dewma[j]>=H)||(j==win_lim)) break
      }
      rl[i]=j
    }
  stopCluster(grp)

  print(c(m,n,lam,H,loc,sca,
mean(rl),sqrt(var(rl)/sim_num),sd(rl),min(rl),quantile(rl,c(0.0
5,0.25,0.50,0.75,0.95)),max(rl)))
}
```

```
#Example
dl_ss(m=100, n=5, H=2.234, loc=0,sca=1, lam=0.05)
```

B.4 R Program Code for the HL Scheme

The program below is used to obtain the IC and OOC performances of the HL scheme with the time-varying UCL.

```
library(doParallel)
library(foreach)

rm(list=ls(all=TRUE))

hl_tv=function(case,m,n,C,win_lim=5000,sim_num=50000,loc,sca,om
e)
{
  N=m+n
  x=rep(0,m)
  y=rep(0,n)
  z=rep(0,n)
  lep=rep(0,win_lim)
  hwma=rep(0,win_lim)

evl=c(3.52572525,3.69092682,3.72876761,3.575762399,3.76727793,3
.83059074,3.586651011,3.781145634,3.848191288)    #E[Var(Lj|Xm,
IC)]

vel=c(0.02665154,0.04685424,0.07874633,0.007554594,0.01052258,0
.01474126,0.004471669,0.005533597,0.007193758)    #Var[E(Lj|Xm,
IC)]

  grp=makeCluster(7)
  registerDoParallel(grp)

  rl=rep(0,sim_num)
  rl=foreach(i=1:sim_num,.combine=c)%dopar%
    {
      x=rnorm(m,0,1)
      j=0

      repeat
      {
        j=j+1
        y=rnorm(n,loc,sca)

        R=rank(c(x,y))
        WRS=((sum(R[(m+1):N]))-
(0.5*n*(N+1)))/sqrt((m*n*(N+1)/12))

        for(k in 1:n) {z[k]=abs(R[m+k]-(0.5*(N+1)))}
        if((N%%2)==0)                          {AB=((sum(z[1:n]))-
(0.25*n*N))/sqrt(((m*n*((N*N)-4)/(48*(N-1)))))}
        else                 {AB=((sum(z[1:n]))-(0.25*n*((N*N)-
1))/N)/sqrt(((m*n*(N+1)*((N*N)+3)/(48*N*N))))}
```

```
        lep[j]=(WRS*WRS)+(AB*AB)

        if (j==1) {value=ome*lep[j]+(1-ome)*2}
        else {value=ome*lep[j]+((1-ome)/(j-1))*sum(lep[1:j-1])}
        hwma[j]=value

        if (j==1) {H=2+(C*sqrt(ome*ome*(vel[case]+evl[case])))}
        else     {H=2+(C*sqrt((evl[case]*((ome*ome)+((1-ome)*(1-
ome)/(j-1))))+vel[case]))}
        if((hwma[j]>=H)||(j==win_lim)) break
      }
      rl[i]=j
    }
  stopCluster(grp)

  print(c(m,n,ome,C,loc,sca,
mean(rl),sqrt(var(rl)/sim_num),sd(rl),min(rl),quantile(rl,c(0.0
5,0.25,0.50,0.75,0.95)),max(rl)))
}

#Example
hl_tv(case=1, m=100, n=5, C=1.652, loc=0, sca=1, ome=0.05)
```

The program below is used to obtain the IC and OOC performances of the HL scheme with the steady-state UCL.

```
library(doParallel)
library(foreach)

rm(list=ls(all=TRUE))

hl_ss=function(m,n,H,win_lim=5000,sim_num=50000,loc,sca,ome)
{
  N=m+n
  x=rep(0,m)
  y=rep(0,n)
  z=rep(0,n)
  lep=rep(0,win_lim)
  hwma=rep(0,win_lim)

  grp=makeCluster(7)
  registerDoParallel(grp)

  rl=rep(0,sim_num)
  rl=foreach(i=1:sim_num,.combine=c)%dopar%
    {
      x=rnorm(m,0,1)
      j=0

      repeat
      {
        j=j+1
        y=rnorm(n,loc,sca)

        R=rank(c(x,y))
        WRS=((sum(R[(m+1):N]))-
(0.5*n*(N+1)))/sqrt((m*n*(N+1)/12))
```

```
        for(k in 1:n) {z[k]=abs(R[m+k]-(0.5*(N+1)))}
        if((N%%2)==0)                        {AB=((sum(z[1:n]))-
(0.25*n*N))/sqrt(((m*n*((N*N)-4)/(48*(N-1)))))}
        else                 {AB=((sum(z[1:n]))-(0.25*n*((N*N)-
1))/N)/sqrt(((m*n*(N+1)*((N*N)+3)/(48*N*N))))}

        lep[j]=(WRS*WRS)+(AB*AB)

        if (j==1) {value=ome*lep[j]+(1-ome)*2}
        else {value=ome*lep[j]+((1-ome)/(j-1))*sum(lep[1:j-1])}
        hwma[j]=value

        if((hwma[j]>=H)||(j==win_lim)) break
      }
      rl[i]=j
    }
  stopCluster(grp)

  print(c(m,n,ome,H,loc,sca,
mean(rl),sqrt(var(rl)/sim_num),sd(rl),min(rl),quantile(rl,c(0.0
5,0.25,0.50,0.75,0.95)),max(rl)))
}

#Example
hl(m=100, n=5, H=2.436, loc=0, sca=1, ome=0.05)
```

B.5 R Program Code for the SL Scheme

The program below is used to obtain the IC and OOC performances of the SL scheme with the steady-state UCL.

```
library(doParallel)
library(foreach)

rm(list=ls(all=TRUE))

sl=function(m,n,H,win_lim=5000,sim_num=50000,loc,sca)
{
  N=m+n
  x=rep(0,m)
  y=rep(0,n)
  z=rep(0,n)
  lep=rep(0,win_lim)
  shew=rep(0,win_lim)

  grp=makeCluster(7)
  registerDoParallel(grp)

  rl=rep(0,sim_num)
  rl=foreach(i=1:sim_num,.combine=c)%dopar%
    {
      x=rnorm(m,0,1)
      j=0
```

```
      repeat
      {
        j=j+1
        y=rnorm(n,loc,sca)
        R=rank(c(x,y))

        WRS=((sum(R[(m+1):N]))-
(0.5*n*(N+1)))/sqrt((m*n*(N+1)/12))

        for(k in 1:n) {z[k]=abs(R[m+k]-(0.5*(N+1)))}
        if((N%%2)==0)                        {AB=((sum(z[1:n]))-
(0.25*n*N))/sqrt(((m*n*((N*N)-4)/(48*(N-1)))))}
        else                {AB=((sum(z[1:n]))-(0.25*n*((N*N)-
1))/N)/sqrt(((m*n*(N+1)*((N*N)+3)/(48*N*N))))}

        lep[j]=(WRS*WRS)+(AB*AB)
        shew[j]=lep[j]
        if((shew[j]>=H)||(j==win_lim)) break
      }
      rl[i]=j
    }
  stopCluster(grp)

  print(c(m,n,H,loc,sca,
mean(rl),sqrt(var(rl)/sim_num),sd(rl),min(rl),quantile(rl,c(0.0
5,0.25,0.50,0.75,0.95)),max(rl)))
}

#Example
sl(m=100, n=5, H=11.247)
```

APPENDIX C

PUBLICATION

Chan, K.M., Mukherjee, A., Chong, Z.L., Lee, H.C., 2021. Distribution-free Double Exponentially and Homogeneously Weighted Moving Average Lepage Schemes with An Application in Monitoring Exit Rate. *Computers & Industrial Engineering*, 161. doi: 10.1016/j.cie.2021.107370 [Published online]

Chan, K.M., Chong, Z.L., Khoo, M.B.C., Khaw, K.W., Teoh, W.L., 2021. A comparative study of the EWMA and double EWMA control schemes. *IOP Journal of Physics: Conference Series*, 7th International Conference on Applications & Design in Mechanical Engineering (ICADME 2021). 23 August 2021, Virtual Conference. https://iopscience.iop.org/issue/1742-6596/2051/1 [Published online]